2011

Differential regulation of MLC20 phosphorylation in tonic and phasic smooth muscles of the stomach

Othman Al-Shboul
Virginia Commonwealth University

VCU Graduate School

Approval form for thesis/dissertation and final oral examination

Student name: Al-Shboul (Last) Othman (First) A (Middle initial) **V number:** V00278324

Document type: (check one) ☐ Master's thesis ☐ ■ Doctoral dissertation

Department: Physiology and Biophysics

Thesis/dissertation title: Differential regulation of MLC20 phosphorylation in tonic and phasic smooth muscles of the stomach

Approval numbers

- ☐ IRB
- ☑ IACUC AM10281 & AM10280
- ☐ Exempt
- ☐ Not applicable

Thesis/dissertation and final oral defense

Date: 04/05/2011

Graduate Advisory Committee (type name and sign)

	Failed	Passed
Karnam, Srinivasa M.		✓
Akbarali, Hamid I.		✓
Grider, John R.		✓
Lyall, Vijay		✓
Ghosh, Siddhartha S.		✓

Graduate program director/department chair: Logothetis, Diomedes E **Date:**

School/college dean: **Date:**

DIFFERENTIAL REGULATION OF MLC20 PHOSPHORYLATION IN TONIC AND PHASIC SMOOTH MUSCLES OF THE STOMACH

A thesis submitted in partial fulfillment of the requirements for the degree of Doctor of Philosophy at Virginia Commonwealth University

by

Othman A Al-Shboul

B.S in Dentistry, Jordan University of Science and Technology, Jordan, 2004

Director: Murthy S Karnam, Ph.D.
Professor, Department of Physiology

Virginia Commonwealth University
Richmond, Virginia
April, 2011

ACKNOWLEDGMENT

(وَمَا بِكُم مِّن نِّعْمَةٍ فَمِنَ اللَّهِ ثُمَّ إِذَا مَسَّكُمُ الضُّرُّ فَإِلَيْهِ تَجْأَرُونَ) -النحل53 -

And whatever you have of favor - it is from Allah. Then when adversity touches you, to Him you cry for help. (Holly Quran, 16: 53)

All the unique praises and thanks are to God ‘Allah’, the creator and the sustainer, who gave me the opportunity to realize a bit of his incredible power and wisdom. If I did well, it is from him, and if I did bad, it is my weakness.

Then it is a pleasure to thank all those who helped me during my study and made this work possible. Firstly, I am heartily thankful to my supervisor, Dr.Murthy Karnam, who didn’t save any effort to guide and support me from the initial to the final level. His personality is supreme and great, indeed, Dr.Murthy is a rare character. He developed my technical skills and enhanced my understanding of science. He was a teacher, a friend, and a brother. Even the best words are less than to thank him.

I would like also to extend my thanks to my committee members; Dr.Grider, Dr.Hamid, Dr.Ghosh, and Dr.Vijay for the time and effort they devoted to be in touch with the progress in my research.

I owe my most sincere gratitude to Dr.Sunila for her unlimited encouragement and help. She opened my eyes to the new techniques being used in science these days. Her suggestions and comments made a big difference in my improvement.

Thanks are due to all my friends and colleagues at the GI group for being a lovely family during the many years. Their collaboration and help made our lab a delightful place to work in.

Special thanks go Jordan University of Science and Technology for the constant financial support provided during the period of my study. It is a good moment here also to acknowledge and thank Dr. Said Khatib for his great and valuable recommendations and advices throughout my study.

My sincere thanks are for the two persons who are behind my presence in this world, my parents. To my father, my best and great example who left this temporary life before seeing this moment, I send a very special prayer. I ask God ‘Allah’ to send peace and blessings to his grave and I ask Allah to gather us again in the best and permanent place.

My deep heartfelt thanks are due to my precious wife, the most beloved partner who occupied a special place inside my heart. I will never forget her great sacrifice of being away from home country and all her relatives for years just to stay beside her husband. Her patience and endless encouragement offered me the success; really she is the beginning and the end of this whole story.

TABLE OF CONTENT

LIST OF TABLES

Page

LIST OF FIGURES

Page

List of Abbreviations

5-HT……...Serotonin

8-Br-cGMP..……...…….……8-bromo cGMP

AC…….Adenylate cyclase

ACh……..Acetylcholine

ADP……..Adenosine diphosphate

AMPK…….Adenosine monophosphate kinase

ATP……..Adenosine triphosphate

BAPTA……1,2-bis(o-aminophenoxy)ethane-N,N,N',N'-tetraacetic acid

bp…….……base pair

BSA…….……...Bovine serum albumin

CaD……..Caldesmon

CaM…….Calmodulin

CaMKII……..Calmodulin-dependent kinase II

CaMKK-β……Calmodulin-dependent kinase kinase β

cAMP……...Cyclic adenosine monophosphate

CaP.....Calponin

cDNA……...Complementary deoxyribonucleic acid

cGMP……...Cyclic guanosine monophosphate

CGRP……...…Calcitonin gene related peptide

cpm.....Count per minute

CPI-17……..PKC Potentiated Inhibitor 17 kDa protein

CT…….……Cycle threshold

DAP……...……Death–associated protein

DMEM…….Dulbecco's Modified Eagle Medium

dNTP……Deoxynucleotide Triphosphate

EGTA……...Ethylene glycol tetraacetic acid

EJP……...Excitatory junctional potentials

F-actin……Filamentous actin

G- actin……Globular actin

GAPDH……...Glyceraldehyde 3-phosphate dehydrogenase

GEF……..Guanine nucleotide exchange factor

GI …….Gastrointestinal

GSNO……..S-Nitrosoglutathione

GTP……..Guanosine triphosphate

h…….Hour

HEPES……...……..N-2-hydroxyethylpiperazine-N’ 2-ethanesulfonic acid

IBMX……...3-isobutyl-1-methylxanthine

ICC……...Interstitila cells of cajal

ICC-DMP……Deep muscular plexus ICC

ICC-IM……Intramuscular ICC

ICC-MY…….Myenteric ICC

IJP…….Inhibitory junctional potentials

ILK……..Integrin-linked kinase

IP3……...Inositol trisphosphate

IP3R……...Inositol trisphosphate receptor

LPA……Lysophosphatidic acid

MBP……..Myelin basic protein

MHC……..Myosin heavy chain

MLC……Myosin light chain

MLCK……...Myosin light chain kinase

MLCP……..Myosin light chain phosphatase

mRNA…….……Messenger Ribonucleic acid

MRP……Multidrug resistant protein

MYPT1……Myosin phosphatase target subunit 1

NKA…….Neurokinin A

NM II…….Non-muscle myosin II

NO……...Nitric oxide

NOS……..Nitric oxide synthase

PACAP……...Pituitary adenylate cyclase-activating polypeptide

PAK1…….p21-activated protein kinase 1

PCR……..Polymerase chain reaction

PDE……..Phosphodiesterase

PI……...Phosphatidylinositol

Pi……Inorganic phosphate

PI3K…….Phosphoinositide 3-kinase

PKA……Protein kinase A

PKC…….Protein kinase C

PKG……Protein kinase G

PLA2……...Phopholipase A2

PLC…….Phospholipase C

PMA……Phorbol 12-myristate 13-acetate

ppicδ……Protein phosphatase delta isoform

qRT-PCR……...……Real time-PCR

S1P……Sphingosine-1-phosphate

SDS-PAGE……..Sodium dodecyl sulfate polyacrylamide gel electrophoresis

SEM……...…….Standard error of the mean

sGC……...…Soluble guanylate cyclase

SIP2……..Sphingosine 1-phosphate receptor 2

TBS-T…….…….Tris-Buffered Saline Tween-20

Tm……Tropomyosin

UTP…….....Uridine 5'-triphosphate

VIP……..……Vasoactive intestinal peptide

VPAC2……..Vasoactive pituitary adenylate cyclase 2

ZIPK……...zipper interacting protein kinase

Abstract

DIFFERENTIAL REGULATION OF MLC20 PHOSPHORYLATION IN TONIC AND PHASIC SMOOTH MUSCLES OF THE STOMACH

By Othman A. Al-Shboul, Ph.D.

A thesis submitted in partial fulfillment of the requirements for the degree of Doctor of Philosophy at Virginia Commonwealth University.

Virginia Commonwealth University, 2011

Major Director: S.Murthy Karnam
Professor, Department of Physiology

Gastrointestinal (GI) smooth muscle possesses distinct regional and functional properties that distinguish it from other types of visceral and vascular smooth muscle. On the basis of electrical properties and contractile phenotype, GI smooth muscles have been classified into phasic (non-sphinteric) and tonic (sphinteric) smooth muscles. The biochemical basis of phasic and tonic phenotypes of smooth muscle is not clear and is the major question of inquiry of the present study. Phosphorylation of Ser^{19} on the 20 kDa myosin light chain (MLC) is essential for acto-myosin interaction and contraction in both phasic and tonic muscles. The levels of MLC_{20}

phosphorylation are regulated by Ca^{2+}/calmodulin-dependent MLC kinase (MLCK) and MLC phosphatase (MLCP), and the activity of these enzymes are in turn regulated by various signaling molecules whose expression and activity are important in determining the strength and duration of their activity. The signaling proteins are AMP kinase (MLCK activity), Rho kinase, zipper-interacting protein kinase (ZIPK), CPI-17 and telokin (MLCP activity), phosphodiesterase 5 (PDE5) and multi-drug resistance protein 5 (MRP5). The overarching goal of the dissertation is to identify the differences in the signaling pathways that regulate MLCK and MLCP activities, and thus MLC_{20} phosphorylation and muscle function. Using biochemical, molecular and functional approaches, and antrum (distal stomach) and fundus (proximal stomach) of rabbit stomach as models of phasic and tonic smooth muscles, respectively, the present study characterized important differences in the signaling pathways that highly correlate with the contractile phenotype. These include: 1) tissue-specific expression of contractile proteins such as myosin heavy chain isoforms, actin, caldesmon, calponin, α- and β-tropomyosin, smoothelin-A and -B; 2) higher expression of AMPK, selective feedback inhibition of MLCK activity via AMPK-mediated phosphorylation, and higher expression of telokin and activation of MLCP correlate with the rapid cyclical contractile function in phasic muscle; 3) higher expression and activation of Rho kinase/ZIPK/MYPT1 and PKC/CPI-17 pathways, preferential inhibition of MLCP activity, and sustained phosphorylation of MLC_{20} correlate with the sustained contraction in tonic muscle; and 4) rapid termination of cGMP signal and muscle relaxation by preferential degradation and efflux of cGMP via higher expression of PDE5 and MRP5, respectively, correlate with the brief relaxation and rapid restoration of contraction in tonic muscle. It is anticipated that these findings could be important in providing the underlying mechanisms involved in the pathophysiology of smooth muscle function and new insights for the development of therapeutic agents that should act on smooth muscle in the gut to treat motility disorders as

well as in other regions such as airways and vascular smooth muscle where similar intracellular mechanisms may prevail.

CHAPTER 1

INTRODUCTION AND BACKGROUND

1.1 Introduction

The gastrointestinal (GI) tract is a complex multi-organ system with tissues that differ structurally and functionally. The dynamic interactions between the neuronal, muscular, immune, and glandular tissues allow the GI tract to perform its main physiological functions, which include digestion, absorption, excretion, and protection. Normal gut motility provides for the mixing and propulsion of intraluminal contents to enable efficient digestion of food, progressive absorption of nutrients, and evacuation of residues. These fine and delicate GI tract movements are generated by a highly-regulated interaction between an intricate network of neurons located within the wall of the alimentary canal (i.e., the enteric nervous system), an intrinsic pacemaker system (i.e., interstitial cells of Cajal or ICC) and the final effector cells (i.e., smooth muscle cells).

1.2 GI tract wall

GI tract wall is composed of four layers that have morphological and functional differences. The four layers, from inside of the gut tube to outside, are the mucosa, the submucosa, the muscularis propia and the serosa. The smooth muscle of muscularis propia of the gut consists of a thin, outer longitudinal layer and a thick, densely innervated circular layer (and another oblique layer in the stomach); the layers derive their names from the orientation of the

long axis of muscle cells in them. The muscle cells are separated by laminar septa into bundles that are embedded in a connective tissue matrix. The muscle layers are separated by neurons, glial cells, fibroblasts, and interstitial cells of Cajal (ICC)[1].

1.3 GI tract smooth muscle

GI tract smooth muscle possesses distinct regional and functional properties that distinguish it from other types of visceral and vascular smooth muscle. Gut smooth muscles contract spontaneously in the absence of neural, humoral, or hormonal stimuli and in response to stretch. They contract as a syncytium (i.e., contract in unison) and therefore classified as unitary-type smooth muscle[2].

In general, smooth muscle cells are spindle-shaped of about 400μm in length and 5 to 15 μm wide. They lack the visible cross-striations seen in other muscle types. Their plasma membranes consist of two specialized structures known as caveolae and dense bands. The caveolae are clusters of basket-shaped invaginations of the membrane, the bases of which are surrounded by the endoplasmic reticulum (called sarcoplasmic reticulum in smooth muscle). Different caveolin proteins bind to a variety of signaling molecules and act as scaffolds to facilitate signaling. Clusters of caveolae are separated from each other by electron-dense structures called dense bands; the site of attachment of thin actin filaments to transmembrane integrins[2].

Two types of coupling connect neighboring smooth muscle cells; mechanical coupling which is provided by the intermediate junctions - formed by the juxtaposed dense bands from adjacent cells, and electrical coupling which is provided by gap junctions (or nexuses). Gap junctions are patches of the closely opposed plasma membranes of adjacent cells, the space of which is bridged by intercellular channels though which intracellular regulatory molecules like Ca^{2+} and cyclic nucleotides are capable of movement between neighboring cells[2].

Dense bodies are Z-lines-like structures, from which actin thin filaments emerge and interdigitate with myosin thick filaments. Most of the interior space of muscle cell is occupied by the contractile filaments and dense bodies while the remainder is occupied by the various organelles[2]. Sarcoplasmic reticulum is located immediately beneath and parallel to plasma membrane, and is the site of Ca^{2+} uptake and release[3].

1.4 Contractile apparatus; thin and thick filaments

Three types of filaments can be distinguished in smooth muscle cells: thin actin filaments, thick myosin filaments, and intermediate desmin filaments. Intermediate filaments link dense bands in the plasma membrane to dense bodies in the cytoplasm[4].

Thin filaments consist of actin; a ubiquitous 42 kDa globular protein (G-actin) that polymerizes to form 2-stranded helical filaments (F-actin). Inserted in the grooves of the actin helix is another protein, tropomyosin. Thin filaments in smooth muscle have a distinct polarity, they insert into and emerge from the dense bodies, and they are arranged in bundles that run parallel to the long axis of the cells, with their free ends surrounding and interdigitating with thick myosin filaments. Actin filaments are organized through attachments to the dense bodies that contain α-actinin, a Z-band protein in skeletal muscle[4].

Thick filaments are aggregates of myosin molecules formed from the association of six different proteins: one pair of myosin heavy chains (MHCs) and two pairs of myosin light chains (MLCs). Myosin II is the molecular motor of muscle cells and the velocity of muscle contraction is determined by the ATPase activity of myosin as it interacts with actin[5]. The heavy chains are coiled around each other to form an α-helical core or tail. Each strand of the core terminates in a globular head surrounded by two MLCs: a 20 kDa regulatory and phosphorylatable chain (MLC_{20}) and a 17 kDa chain. Each globular head contains a binding site for actin and an actin-activated magnesium-adenosine triphosphatase (Mg^{2+}-ATP).

Hydrolysis of ATP is the fundamental reaction whereby chemical energy is converted into mechanical energy in smooth muscle. The reaction generates force or induces shortening as a result of the sliding of the overlapping and interdigitating thin and thick filaments. The force generated by crossbridge cycling depends on the number of crossbridges acting in parallel. The crossbridges do not cycle in unison; thus, in smooth muscle, unlike in striated muscle, both the number and the cycling rate of crossbridges are under regulation[6].

1.5 The actomyosin crossbridge cycle

ATP, bound weakly to myosin, is hydrolyzed to ADP and inorganic phosphate (Pi). The products of hydrolysis remain bound to the myosin head, and the energy released is stored in the myosin molecule, which has a high affinity for actin in this state. The binding of myosin to actin can promote a major change in conformation (the power stroke), consisting of a reorientation of part of the myosin head distal to the actin-binding site which is accompanied by the dissociation of Pi. Upon release of ADP and Pi, ATP binds again to myosin, which then reverts to a state of low affinity for actin. Cross-bridge cycling ceases after the stimulus is withdrawn; the dephosphorylated myosin cross-bridges are arrested in a detached state, which is characteristic of relaxed muscle[7].

A unique pattern of crossbridge cycling is observed during sustained (tonic) contraction of smooth muscle, in which muscle contraction attains a peak and maintains it near steady state. This state has been called the “latch” state which represents a transition from a state of rapidly cycling crossbridges to a state of attached non-cycling or slowly cycling crossbridges. These latch bridges maintain force in sustained contraction[7].

1.6 Neural regulation of smooth muscle contraction

The intrinsic electrical and mechanical properties of smooth muscle are modulated by neurotransmitters released from neurons of the enteric nervous system, especially neurons of the

myenteric plexus. Myenteric plexus contains two main types of neurons: one type contains inhibitory neurotransmitters such as VIP or PACAP together with NO synthase (NOS), the enzyme responsible for synthesis of nitric oxide in the nerve terminals, while the majority of the neurons contain excitatory neurotransmitters, mainly acetylcholine, usually together with tachykinins; substance P and neurokinin A (NKA), which are released at higher frequencies of stimulation[8].

Excitatory neurotransmitters stimulate Ca^{2+} release, increase muscle tone, and depolarize the plasma membrane (i.e., trigger excitatory junctional potentials or EJPs). The depolarization can result from either a direct action of neurotransmitters on muscle cells or may be mediated through intramuscular ICC (ICC-IM) which are coupled electrically to muscle cells. EJPs can induce Ca^{2+} influx and contraction if the depolarization reaches a level at which voltage-gated Ca^{2+} channels open; this is likely to occur in tonic smooth muscle as the membrane potential is close to the Ca^{2+} threshold or in phasic smooth muscle during the peak of slow wave activity[4].

A large variety of receptors and receptor subtypes have been identified as capable of mediating smooth muscle contraction. These include receptors for peptides (e.g., tachykinins, endothelin, motilin), amines (histamine, 5- hydroxytryptamine), pyrimidines/purines (UTP and ATP), and lipids (S1P, LPA)[9].

M2 and m3 receptors are the main muscarinic receptor types expressed in smooth muscle. Acetylcholine (ACh) interaction with m3 receptor couples it to Gαq leading to activation of phospholipase C (PLC) and hydrolysis of phosphatidyl inositol (PI) into inositol 1, 4, 5- trisphosphate (IP3) and DAG. IP3 binds IP3 receptors on SR and stimulates Ca^{2+} release and thus smooth muscle contraction. ACh interacts also with m2 receptor -the predominant (80%) receptor species in smooth muscle- and couples it to Gαi3 leading to inhibition of adenylate cyclase[10,11].

Inhibitory neurotransmitters, on the other hand, inhibit Ca^{2+} release, decrease muscle tone (i.e., relax), and hyperpolarize the plasma membrane directly or indirectly via ICC-IM (i.e., trigger inhibitory junctional potentials or IJPs). IJPs lower the plateau potential of slow waves and inhibit Ca^{2+} influx and phasic contraction[4].

VIP or PACAP induce relaxation by interacting with VPAC2 receptors, which possess equal affinity for VIP and PACAP. These receptors couple to Gs and thereby lead to activation of adenylate cyclase (AC) which increases cAMP generation and thus PKA activation. Nitric oxide activates soluble guanylate cyclase (sGC) which increases cGMP formation, and thus leads to activation of PKG. Both kinases (PKA and PKG) act in conjunction to cause hyperpolarization and relaxation of smooth muscle cells[12].

1.7 Role of ICC in smooth muscle contraction

ICC are mesenchymal cells, interposed between enteric nerves and smooth muscle cells, with small cell bodies and several elongated processes and are classified based on their location and distribution[13]. They express c-kit, the proto-oncogene that encodes the receptor tyrosine kinase, kit[14]. Myenteric ICC (ICC-MY) reside between the longitudinal and circular muscle layers in the myenteric region. These cells are important as pacemakers; they are spontaneously active and generate slow wave depolarization in different parts of the GI tract[15]. Another group of ICC has an intramuscular location (ICC-IM) with individual ICC being distributed in between smooth muscle cells. Other morphologically similar ICC are located in the deep muscular plexus of the small intestine (ICC-DMP). ICC-IM and ICC-DMP are found to be interposed between nerve terminals and smooth muscle cells and closely associated with neuronal processes[16]. In addition, slow waves are modified by other substances such as hormones, paracrine substances,

and inflammatory mediators. It is not clear yet if these substances have sites of action on ICC-IM[17].

The amplitude of the slow wave and the resultant contractile force are regulated by the enteric nervous system. An excitatory neural input (i.e., release of acetylcholine or tachykinins) increases the amplitude and duration of the plateau potential of slow waves, which then increases Ca^{2+} entry and enhances force of contraction. Spike potentials can be superimposed on plateau potential and further augment intracellular Ca^{2+} level (or $[Ca^{2+}]i$) and muscle contraction. On the other hand, an inhibitory neural input (i.e., release of NO, VIP, or PACAP) activates K^+ channels and suppresses inward current conductance in smooth muscle cells, which thereby reduces the amplitude of slow waves and attenuates contractile force[18].

In rhythmic GI tract parts (e.g., antrum part of the stomach), slow waves -generated by ICC-MY- depolarize smooth muscle cells to induce the opening of voltage-dependent L-type Ca^{2+} channels. The electrical activity of slow waves is propagated through networks of ICC and conducted passively to smooth muscle cells through gap junctions. These low-resistance connections between ICC and smooth muscle cells facilitate the propagation of electrical events from one cell to another[4].

The regulation of muscle tone (e.g., fundus part of the stomach which is devoid of ICC-MY), however, is not mediated by changes in smooth muscle membrane potential or slow wave generation but by signaling cascades initiated mainly by enteric neurotransmitters acting directly on smooth muscle receptors or indirectly via ICC-IM[4].

1.8 Peristalsis

Peristalsis is a distinctive pattern of smooth muscle contraction that propels foodstuffs distally through the GI tract. It was first described by Bayliss and Starling as a type of motility

wholly mediated by the enteric nervous system in which there is contraction above and relaxation below the segment being stimulated[19]. It can be evoked by stroking, initiated by the release of serotonin (5-HT) from mucosal enterochromaffin cells which acts upon 5-HT receptors of enteric sensory nerve terminals in mucosa causing the release of the sensory neurotransmitter calcitonin gene-related peptide (CGRP)[20]. Peristalsis can also be elicited by radial stretch, which activates the intramuscular nerve terminals of extrinsic sensory neurons which have axonal projections to myenteric neurons[21].

Peristaltic reflex consists of an ascending and descending phases. During the descending phase, circular muscle relaxes and longitudinal muscle contracts, while during the ascending phase, circular muscle contracts and longitudinal muscle relaxes. This reciprocal contraction and relaxation of the two muscle layers maintain the dimensions of the segment. VIP, PACAP, and NO are released during and responsible for the descending relaxation of circular muscle, while acetylcholine, substance P, and NKA are released during and responsible for the ascending contraction of circular muscle[22].

1.9 Signaling for smooth muscle contraction

An essential step in smooth muscle contraction is phosphorylation of the 20 kDa regulatory myosin light chain (MLC_{20}) by a Ca^{2+}/calmodulin-dependent or -independent myosin light chain kinase (MLCK) which transfers the phosphate group from ATP to either Ser^{19} or Thr^{18} hydroxyl groups of MLC_{20}. This phosphorylation activates the actin-activated myosin ATPase and actin-myosin interaction, which thereby initiates smooth muscle contraction.

An increase in intracellular free Ca^{2+} concentration induces activation of Ca^{2+}/CaM-dependent MLCK and the phophorylation of MLC_{20} and thus muscle contraction. The decrease in intracellular level of Ca^{2+} induces dissociation of the Ca^{2+}-CaM-MLCK complex, resulting in

dephosphorylation of the MLC_{20} by myosin light chain phosphatase (MLCP) and thus smooth muscle relaxation[9,23]. Thus, the phosphorylation level of MLC_{20} is determined by the opposing activities of MLCK and MLCP and both of these enzymes' activities are well-regulated in smooth muscle.

1.9.1 MLCK regulation

As mentioned previously, smooth muscle tone is regulated by signaling cascades initiated by enteric neurotransmitters acting directly on smooth muscle receptors. In circular smooth muscle cells, contractile agonists activate PLC-β1 via Gαq coupled receptors (e.g., muscarinic m3 receptors) by Gαq binding to PLC-β1's COOH-terminal tail[24]. PLC-β1 hydrolyzes PIP2 into DAG and IP3. An increase in IP3 leads to the binding of IP3 to the high affinity IP3 receptor/Ca^{2+} channel on the sarcoplasmic reticulum, resulting in the release of Ca^{2+} into the cytosol. Of the two IP3 receptor isoforms (IP3R-I and IP3R-III) expressed in smooth muscle cells, only IP3R-I mediates Ca^{2+} release[25].

In longitudinal smooth muscle cells, Ca^{2+} mobilization is dependent on a mandatory step involving Ca^{2+} influx via voltage-gated Ca^{2+} channels[25]. Upon contractile agonist stimulation, both Gq- and Gi-coupled receptors activate cytoplasmic PLA2 resulting in phosphatidylcholine hydrolysis into arachidonic acid which induces membrane depolarization and opening of voltage-gated Ca^{2+} channels. The entry of Ca^{2+} stimulates cyclic ADP ribose formation and induces synergistic Ca^{2+}- and cyclic ADP ribose-induced Ca^{2+} release via ryanodine receptors/Ca^{2+} channels[26].

MLCK activity is strictly dependent on $[Ca^{2+}]i$ which, upon agonist stimulation, increases as a result of Ca^{2+} influx into the cytosol through voltage-gated channels and/or the release of Ca^{2+} from intracellular stores. Resting levels of $[Ca^{2+}]i$ (70-100nM) increases up to 8-fold during maximum contraction.

Four Ca^{2+} ions bind to calmodulin (CaM) cofactor which then binds to and activates MLCK[27]. The transient high levels of $[Ca^{2+}]i$ are then extruded from the cell and/or up taken into the sarcoplasmic Ca^{2+} stores. This decrease in the intracellular level of Ca^{2+} induces dissociation of the Ca^{2+}-CaM-MLCK complex, which thereupon decreases MLCK activity. MLC_{20} phosphorylation and contraction, however, are maintained by Ca^{2+}-independent MLCKs and regulated inhibition of MLCP activity in a process called Ca^{2+} sensitization[23].

Moreover, MLCK activity was shown to be regulated by protein kinases that act to provide negative feedback mechanisms. Stull and coworkers have found that MLCK is phosphorylated by CaMKII, and this phosphorylation decreases the activity of MLCK by decreasing the affinity of the enzyme for calmodulin. It was found that $[Ca^{2+}]i$ required for the half-maximum activation of CaMKII equals 500 nM, whereas that for MLCK activation is only 250 nM, suggesting a role for CaMKII in inactivation of MLCK when smooth muscle is hyperactivated and $[Ca^{2+}]i$ rises above some critical level[28]. A similar mechanism has been proposed recently with AMP kinase (AMPK) in which AMPK phosphorylates MLCK at Ser^{815} leading to decreased activity of MLCK. It was found that ablation of AMPK augmented contraction, suggesting rapid MLCK attenuation and suppression of contraction by AMPK[29]. In addition, p21-activated protein kinase 1 (PAK1) was shown to attenuate smooth muscle contraction by phosphorylating and inactivating MLCK[30].

1.9.2 MLCP regulation

While MLCK-mediated contraction is strictly dependent on $[Ca^{2+}]i$, agonist-induced MLC_{20} phosphorylation and contraction can be maintained even after $[Ca^{2+}]i$ returns to basal levels via two ways; MLC_{20} phosphorylation by Ca^{2+}-independent MLCKs and regulated inhibition of MLCP.

An important step in maintaining contraction via MLCP inhibition involves activation of RhoA via a cascade leading to sequential agonist-mediated activation of $Gq/G\alpha_{13}$ and Rho guanine nucleotide exchange factor (Rho-GEF) [30,31]. Activated Rho A (Rho-GTP) is translocated to the plasma membrane where it activates both Rho kinase -mainly Rho kinase II, the predominant smooth muscle isoform- and PLD[32]. Hydrolysis of phosphatidylcholine by PLD yields phosphatidic acid, which is dephophorylated to diacylglycerol, resulting in sustained activation of Ca^{2+}-dependent and -independent PKC isozymes. Rho kinase and PKC act concurrently and cooperatively to inhibit MLCP activity[9].

The same receptors that initiate Ca^{2+} mobilization and MLCK-mediated MLC_{20} phosphorylation and contraction also engage a distinct G protein-dependent pathway that mediates Ca^{2+}-independent MLC_{20} phosphorylation and contraction via negative regulation of MLCP. Some receptors (e.g., m3 receptors) are coupled to RhoA via G_{13} only, whereas others (e.g., SIP2 and motilin receptors) are coupled to RhoA via both Gq and G_{13}[30,33,34].

Structurally, MLCP holoenzyme consists of three subunits; a 37 kDa catalytic subunit of type 1 phosphatase (ppicδ), a 110 to 130 kDa regulatory subunit, known as myosin phosphatase target subunit I or MYPT1, and a 20 kDa subunit of unknown function. MYPT1 binding to the catalytic subunit enhances MLCP catalytic activity[35].

Phosphorylation of MYPT1 at Thr^{696} by Rho kinase promotes dissociation of the catalytic and regulatory subunits of MLCP and inhibits its catalytic activity [36]. Rho kinase also phophorylates Thr^{853} within the myosin-binding domain on MYPT1 upon which the enzyme dissociates from myosin and decreases the efficiency of the enzyme by decreasing availabilty of the substrate[31]. On the other hand, phosphorylation of an adjacent Ser^{695} by cAMP- or cGMP-dependent protein kinase (PKA and PKG, respectively) blocks the ability of Rho kinase to phosphorylate Thr^{696} and so restores MLCP activity [37].

PKC, mainly PKC-ε and PKC-δ, phosphorylates CPI-17, a 17 kDa endogenous inhibitor of MLCP, at Thr^{38} and greatly enhancing its ability to inhibit MLCP [38]. Thus, a dual Rho-dependent mechanism (i.e., via Rho kinase and PKC activation) causes sustained inhibition of MLCP. The relative involvement of Rho-mediated pathways-Rho kinase/MYPT1 and PKC/CPI-17- in MLCP inhibition appears to be receptor-specific. Most $Gq/_{13}$-coupled receptors (e.g., m3, S1P2, motilin) engage both pathways. ETA receptors engage only Rho kinase/MYPT1 while LPA3 receptors engage only PKC/CPI-17[33,34,39,40].

Zipper interacting protein kinase (ZIPK) was also found to inhibit MLCP. It is a serine/threonin kinase expressed in various tissues including smooth muscle and is a member of the death–associated protein kinase (DAP) family[41]. ZIPK co-localizes with MLCP and is phosphorylated following activation of Rho kinase-dependent pathway during carbachol stimulation of rabbit bladder. The phosphorylated ZIPK, in turn, phosphorylates the myosin-binding subunit at Thr^{696}, considerably faster and even more effective than Rho kinase[42,43]. Niiro and Ikebe, however[44], have demonstrated that MYPT1 is a poor substrate for ZIPK, and instead, ZIPK acts as a Ca^{2+}-independent MLCK that directly phosphorylates MLC_{20} at both Ser^{19} and Thr^{18} in absence of Ca^{2+}. It has been suggested that the myofilament-bound ZIPK may mediate Rho kinase–dependent phosphorylation of MYPT1 and inhibition of MLCP and thus could be the link between the activated plasma membrane-bound Rho kinase and MYPT1.

Integrin-linked kinase (ILK) is another myofilament-bound Ca^{2+}-independent MLCK. It mediates MLC_{20} phosphorylation, at both Ser^{19} and Thr^{18}, and smooth muscle contraction through Gi-coupled receptors. These receptors sequentially activate ILK through certain pathway involving PI3-kinase activation via $G\beta\gamma i$[45].

1.10 Regulation of smooth muscle contractility by thin filament-associated proteins

The thin filaments are defined as those filaments 6–8 nm in diameter and composed of filamentous actin. They are different from the intermediate filaments (10 nm), the myosin filaments (15-18 nm), and the microtubules (~24 nm)[46]. Some proteins have been suggested to bind actin and possibly regulate smooth muscle contraction. Thin filament-associated proteins include: Tropomyosin (Tm), caldesmon (CaD), calponin (CaP), and smoothelin.

1.10.1 Tropomyosin (Tm)

Tm is a coiled-coil α-helix that spans seven actin monomers. Individual molecules interact head to tail, thereby creating a continuous strand along the actin filament[47]. Functionally, X-ray and fluorescent resonance energy transfer studies have shown that activation of smooth muscle leads to movement and displacement of Tm away from actin monomers, i.e., exposing myosin-binding sites on actin for myosin binding and thus forming cross-bridges[48,49]. Moreover, Tm is necessary for full inhibition of actomyosin ATPase activity by CaD[50]. Two Tm isoforms appear to be specific to smooth muscle; α-Tm and β-Tm. PKC-mediated phosphorylation and displacement of TM is associated with smooth muscle contraction by enhancing the cooperative activation of actomyosin[51].

1.10.2 Calponin (CaP)

Calponin was first found in smooth muscle cells as a striated muscle troponin-like protein with a proposed function in the regulation of smooth muscle contraction[52]. Calponin is now well-known as a family of actin filament-associated proteins of 34-37 kDa expressed in both smooth muscle and non-muscle cells. Three isoforms of calponin have been found in the vertebrates as the products of three homologous genes[53]; a basic calponin (h1-calponin), which is the chicken gizzard calponin ortholog, a neutral calponin (h2-calponin), and an acidic calponin (h3-calponin). h1-calponin is specific to differentiated smooth muscle cells and up-regulated during post-natal development, while both h2 and h3-calponins are expressed in both muscle and non-muscle

tissues[54]. There is an in vitro experimental evidence that calponin inhibits actin-activated myosin ATPase[55].

In vitro phosphorylation of CaP (most probably at Ser^{175} and Thr^{184}) by several kinases (such as PKC-ε) resulted in the loss of its ability to bind F-actin to inhibit both actomyosin Mg^{2+}-ATPase activity[56] and unloaded shortening velocity[57].

1.10.3 Caldesmon (CaD)

Caldesmon is another actin-binding protein that is present in both smooth muscle and non-muscle cells. The heavier smooth muscle isoform (h-caldesmon, 87 kDa) is found in differentiated 'contractile' smooth muscle cells, whereas the lighter isoform (i-caldesmon, 57 kDa) is expressed in both non-muscle cells and 'synthetic' smooth muscle cells[58]. Caldesmon binds myosin, actin, tropomyosin, and calmodulin and inhibits the actin-activated myosin ATPase by blocking the interaction of actin and myosin[59] and/or inhibiting a kinetic step of the actomyosin ATPase cycle[60]. Inhibition of contraction by caldesmon can be released by its binding to Ca^{2+}/calmodulin[61] or via posttranslational phosphorylation at Ser^{789} [62]. Immunocytochemical studies of chicken gizzard smooth muscle have revealed that CaD is colocalized with contractile proteins, while CaP is associated with both contractile and cytoskeletal proteins[63].

1.10.4 Smoothelin

Smoothelins are smooth muscle α actin stress fibers-binding proteins that are specifically and abundantly expressed in contractile smooth muscle cells, absent or limited in non-contractile and proliferative smooth muscle cells or cells with smooth muscle-like features, and are the only marker that differentiates between smooth muscle cells and myofibroblasts[64]. They are encoded by a single-copy gene via dual promoter system that generates two major isoforms containing a troponin T-like domain; A (59 kDa) and B (110 kDa) isoforms[65]. Lack of smoothelin-A, the main

isoform in visceral smooth muscle, decreases intestinal contractions in response to both receptor-mediated (e.g., ACh) and non receptor-mediated contractile agonists (e.g., KCl), but the mechanism of regulation is yet unknown[66].

1.11 Signaling for relaxation

Smooth muscle relaxation is initiated by targeting MLC_{20} dephosphorylation. This involves either MLCK inactivation and/or removal of MLCP inhibition. Most agents cause relaxation by stimulating the production of cAMP (e.g., VIP and its homologue PACAP) or cGMP (e.g., nitric oxide [NO]) leading to activation of PKA, PKG or both. Cyclic AMP-activated PKA and cGMP-activated PKG are the main enzymes that induce relaxation in smooth muscle. They target different components of the contractile signaling pathways that attenuate MLCK activity and/or augment MLCP activity which eventually induce dephosphorylation of MLC_{20} and thus smooth muscle relaxation[9].

1.11.1 Cyclic nucleotide regulation:

The levels of cAMP and cGMP in gastrointestinal smooth muscle depend on the rates of their synthesis by cyclases and degradation by phosphodiesterases (PDEs). Cyclic AMP, which is produced in ~10-fold greater amounts than cGMP, is generated from ATP via the membrane-bound adenylate cyclase (AC) -type V and VI- and is rapidly degraded by the cAMP-preferring PDE3 and cAMP-specific PDE4. On the other hand, cGMP is generated from GTP via the soluble guanylate cyclase (sGC) and is rapidly degraded by cGMP-specific PDE5. PKA inhibits AC while PKG inhibits sGC. Both PDE3 and PDE4 are activated by PKA, but only PDE3 is inhibited by cGMP. On the other hand, PDE5 is activated by PKG. When both cAMP and cGMP are present, PDE5 is also activated by PKA[67-69]. So, regulatory feedback from the protein kinases inhibits synthesis and accelerates degradation, and thereby maintains the levels of cyclic nucleotides within a narrow range.

Although cAMP preferentially activates PKA, it can, at higher concentrations, also cross-reactivate PKG[70]. An increase in both cAMP and cGMP, such as that brought about by corelease of NO, VIP, and PACAP from the same or adjacent nerve terminals, is the physiological norm during nerve-induced relaxation of the gut. Inhibition of PDE3 by cGMP enhances cAMP levels, whereas activation of PDE5 by PKA and PKG greatly increases its affinity for the more abundant cAMP. Under these conditions, PKG is activated by both cGMP and cAMP [69,71].

In addition to degradation by phosphodiesterases, cyclic nucleotides elimination pathways comprise active export into the extracellular space via members of the multidrug resistance protein (MRP) family (the other name is ABC transporters). MRPs bind and hydrolyze ATP, providing the energy to transport their substrates across membrane barriers. Among the MRP family membes, MRP4 and MRP5 have been shown to be competent in the transport of cAMP and cGMP respectively[72].

1.11.2 PKA and PKG targets

PKA and PKG indirectly target MLCK inactivation by primarily decreasing $[Ca^{2+}]i$. Both PKA and PKG can inhibit Ca^{2+} mobilization by inhibiting IP3 formation in circular muscle and arachidonic acid formation in longitudinal muscle. Inhibition of IP3 formation in circular muscle involves phosphorylation of RGS4, leading to more rapid degradation of Gαq-GTP and inhibition of PLC-β1 activity. PKG-mediated phosphorylation of SERCA2 and sarcoplasmic reticulum IP3 receptors accelerates Ca^{2+} reuptake into the stores and inhibits IP3-induced Ca^{2+} release, respectively. In addition, both kinases inhibit the activity of membrane Ca^{2+} channels and stimulate the activity of membrane K^{+} channels, leading to hyperpolarization of the plasma membrane and interruption of Ca^{2+} influx into the cell, a mechanism that is important in relaxtion of rhythmic contraction[9].

Moreover, PKG and PKA augment MLCP activity by different ways; first, they phosphorylate the activated form of RhoA (Rho-GTP) at Ser^{188} leading to its inactivation and translocation back to the cytosol [73]. Second, both enzymes can phosphorylate MYPT1 at Ser^{695}, preventing the inhibitory regulation of Rho kinase-mediated phosphorylation of MYPT1 at Thr^{696} [37]. Finally, both kinases are able to phosphorylate (at Ser^{13}) and enhance the activity of telokin, a smooth muscle-specific endogenous activator of MLCP [74].

1.12 Phasic and tonic smooth muscles

Based on the membrane properties, activation speed and contractile behavior, smooth muscles have been classified as either phasic or tonic[23]. Phasic muscles, like those in the distal stomach (or antrum), ileum, and taenia coli, generate action potentials, shorten rapidly, and typically produce spontaneous and rapid contractions and do not maintain force for extended periods of time. These muscles exhibit variable tones on which are superimposed rhythmic or phasic contractions driven by cycles of membrane depolarization and repolarization known as slow waves, which are believed to be generated by ICC. Tonic smooth muscles, on the other hand, do not generate action potentials or spontaneous contractions, but are specialized to contract slowly and maintain contractile force for long durations. Examples of tonic smooth muscles include proximal stomach (or fundus), sphincters, and gall bladder[9].

The phasic and tonic behavior of smooth muscles may also be related to differences in content and isoform composition of contractile proteins and intracellular signaling molecules that regulate the activities of myosin light chain kinase (MLCK) and myosin light chain phosphatase (MLCP). For example, previous studies have shown that phasic muscle differs from the tonic muscle in the relative abundance of the ratio of acidic to basic isoforms of the 17 kDa essential light chain and the seven amino acid-inserted to non-inserted myosin heavy chain isoforms (SMA/SMB isoforms)[75,76].

MLCK activity is stimulated by an increase in Ca^{2+} via Ca^{2+}/calmodulin complex, and inhibited by Ca^{2+}/calmodulin-dependent protein kinase II in a feedback mechanism. Moreover, recent studies have shown that smooth muscle contraction is attenuated by phosphorylation and inactivation of MLCK via AMP-dependent kinase (AMPK). MLCP activity is inhibited via PKC-mediated phosphorylation of the endogenous inhibitor CPI-17, and activated via PKA- and PKG-dependent phosphorylation of the endogenous activator telokin. PKA and PKG are the two main kinases responsible for smooth muscle relaxation by targeting different components in the signaling pathways of MLCK and MLCP. They are activated by an elevation in cAMP and cGMP respectively, the level of which is dependent on the balance between their generation by cyclases and degradation by phosphodiesterases.

It is not known, however, whether the expression and regulation of the signaling molecules that regulate MLCK and MLCP are different in phasic and tonic smooth muscle. The purpose of our study is to comprehensively compare the content and regulation of the different signaling molecules that regulate MLCK and MLCP as well as highlighting the differences in the contractile and thin-filament associated proteins in phasic versus tonic smooth muscle of the gastrointestinal tract.

1.13 Stomah"proximal vs. distal"

The purpose of this study is to comprehensively compare the content and regulation of different contractile proteins and signaling pathways that regulate MLCK and MLCP activity in phasic versus tonic smooth muscle of the gastrointestinal tract as well as highlighting other aspects of general significance in smooth muscle physiology. This thesis explores these differences in the antrum (represents phasic smooth muscles) versus the fundus (represents tonic smooth muscles) parts of the stomach, and so, I found it valuable to have some physiological

anatomy and membrane potential characteristics of the stomach and brief description of some gastric disorders that are related to the improper smooth muscle function in this organ.

The main motor function of the stomach is to serve as an active reservoir that stores and mixes ingested food as well as modulates its rate of emptying into the duodenum. Stomach is divided into two major functional areas; the proximal stomach and the distal stomach. The proximal stomach consists of the fundus and the upper body (or corpus). The primary function of the proximal stomach is to accommodate ingested food. The distal stomach consists of the lower body and the antrum. The primary function of distal stomach is to regularly push digested food into the duodenum in a well-coordinated fashion[77].

The membrane potential of gastric smooth muscle exhibits a characteristic gradient decreasing from −48 mV in the fundus to −71 mV in the antrum[78]. Unlike the distal stomach, the proximal stomach membrane potential does not demonstrate phasic changes in potential, in other words it is electrically quiescent (without slow waves). Consequently, under basal conditions, the fundus exhibits tone rather than pulsation which, in turn, can be modulated by small changes in neural and hormonal inputs[79]. Fundus is suitable for receiving (i.e., vagal-mediated receptive relaxation) and discharging (i.e., tonic contraction) a meal upon inhibitory (hyperpolarizing) or stimulatory (depolarizing) inputs respectively.

It is believed that corpus is the site of spontaneous pacemaker activity or slow wave generation in the stomach[80]. Slow waves originating in the corpus paropagate to and pace antral muscle. Unlike the fundus, the distal body of the stomach and the antrum exhibit phasic rather than tonic motor activity. This is often seen on endoscopy as a powerful ring-shaped peristaltic wave, which initiates in the mid to distal body of the stomach, picking up strength as it drives towards the pylorus where it abruptly terminates[81]. As contractions or electrical activity corresponding to contractions reach pylorus, the pylorus begins to open or relax.

The frequency and direction of the phasic motor activity are tightly coupled with the gastric slow wave generated by phasic depolarization of the interstitial cells of Cajal[82]. A slow wave frequency of three cycles per minute is present during both the resting and active phases of gastric motor activity. Neurohumoral activators increase the slow wave amplitude and this initiates a coupled peristaltic response that grinds and triturates food into a fine particulate suspension, ready for passage into the duodenum[83].

In a number of disease states or conditions, these peristaltic contractions of the stomach and/or the opening and closing of the pylorus is irregular. Gastroparesis or delayed gastric emptying may result in insufficient contractions to churn food, move food through the pylorus, and/or open the pylorus, resulting in gastro retention of food[84]. In another motility disorder known as dumping syndrome, the stomach empties at an abnormally high rate into the small intestine causing various gastrointestinal disorders[84].

SIGNIFICANCE

Although, the initial classification was based on membrane properties and contractile behavior, recent studies suggests that these muscle types exhibit differences in several cellular properties, from membrane activation, cell signaling to the actin-myosin interaction. Previous studies suggest that the phasic and tonic behavior of smooth muscles may be related to differences in content and isoform composition of contractile proteins. Understanding the differences in the signaling pathways that regulate MLCK and MLCP activities and cGMP levels using biochemical, molecular and functional approaches, and antrum (distal stomach) and fundus (proximal stomach) of rabbit stomach as models of phasic and tonic smooth muscle, respectively, is the major question of inquiry of the present study. An understanding of the mechanisms that regulate tone and relaxation at the intracellular levels is important in the pathophysiology and may provide new insights for the development of therapeutic agents that should act on smooth muscle in the gut to treat motility disorders as well as in other regions such as airways and vascular smooth muscle where similar intracellular mechanisms may prevail.

To understand the biochemical basis of phasic and tonic contractile phenotype, I have undertaken a systematic analysis of signaling proteins whose expression and activity are important in the regulation of MLCK and MLCP activity and cGMP levels. The signaling

proteins are AMPK (MLCK activity), Rho kinase, ZIP, CPI-17 and telokin (MLCP activity) and PDE5 and MRP5 (cGMP levels).

HYPOTHESIS AND SPECIFIC AIMS

The following are the Specific Aims and underlying hypotheses.

Specific Aim 1: Identification of differences in the signaling pathways mediating termination of MLCK activity and muscle contraction.

Hypothesis. Expression and function of AMPK-dependent pathway involved in the termination of Ca^{2+}/CaM-dependent MLCK activity are higher in phasic muscle than tonic muscle.

Specific Aim 2: Identification of differences in the signaling pathways mediating MLCP inhibition and sustained muscle contraction.

Hypothesis. Expression and function of Rho kinase/ZIPK/MYPT1 and PKC/CPI-17 pathways involved in the suppression of MLCP activity are higher in tonic muscle than phasic muscle.

Specific Aim 3: Identification of differences in the signaling pathways mediating termination of cGMP signaling and muscle relaxation.

Hypothesis. Expression and function of cGMP degradation (PDE5) and efflux (MRP5) are higher in tonic muscle than phasic muscle.

CHAPTER 2

MATERIALS AND METHODS

2.1 Materials

[^{125}I]cGMP, [γ-^{32}P]ATP, and [^{32}P]Pi were obtained from PerkinElmer Life Sciences, Boston, MA; Collagenase CLS type II and soybean trypsin inhibitor were obtained from Worthington, Freehold, NJ; Western blotting, Dowex AG-1 X 8 resin (100-200 mesh in formate form), chromatography material and protein assay kit, Tris-HCl Ready Gels were obtained from Bio-Rad Laboratories, Hercules, CA; antibodies to MLCK, AMPK, Rho kinase II, PKC-ε, ZIPK, telokin, CPI-17, PDE5, MYPT1, phospho-MLC_{20}, α-actin, smoothelin, tropomyosin, caldesmon, calponin-1, and MRP5 were obtained from Santa Cruz biotechnology, Santa Cruz, CA; myelin basic protein (MBP) was obtained from Upstate Biotechnology; Y27632, STO609, Phorbol 12-myristate 13-acetate (PMA), cGMP, PKI(6-22) amide were obtained from Calbiochem, La Jolla, CA; RKRSRAE was obtained from Peninsula Laboratories, Belmont, CA; RNAqueous^{TM} kit was obtained from Ambion, Austin, TX; Effectene Transfection Reagent, QIAEX®II Gel extraction Kit and QIAprep®Spin Miniprep Kit were obtained from QIAGEN Sciences, Maryland; PCR reagents were obtained from Applied Biosystems, Roche; SuperScript^{TM} II Reverse Transcriptese and TOPO TA Cloning® Kit Dual Promoter were obtained from Invitrogen, CA; Dulbecco's

modified Eagle's medium (DMEM) was obtained from Fisher Scientific. All other chemicals were obtained from Sigma, St. Louis, MO.

New Zealand white rabbits (weight: 4-5 lbs) were purchased from RSI Biotechnology, Clemmons, NC and killed by injection of euthasol (100 mg/kg), as approved by the Institutional Animal Care and Use Committee of the Virginia Commonwealth University. The animals were housed in the animal facility administered by the Division of Animal Resources, Virginia Commonwealth University. All procedures were conducted in accordance with the Institutional Animal Care and Use Committee of the Virginia Commonwealth University.

2.2 Methods

2.2.1 Collection of tissue

Rabbits were sacrificed by injection of Euthasol (100 mg/kg body weight) into the ear vein. The stomach was rapidly removed, emptied of its contents and placed in a cold smooth muscle buffer with the following composition: NaCl 120 mM, KCl 4 mM, KH_2PO_4 2.6 mM, $CaCl_2$ 2.0 mM, $MgCl_2$ 0.6 mM, HEPES (N-2-hydroxyethylpiperazine-N' 2-ethanesulfonic acid) 25 mM, glucose 14 mM, and essential amino mixture 2.1% (pH 7.4)[85-87].

2.2.2 Preparation of dispersed gastric smooth muscle cells

Smooth muscle cells from the circular muscle layer of the antrum and fundus were isolated by sequential enzymatic digestion of muscle strips, filtration, and centrifugation as described previously [32,85-87]. The tissue was cut into thin slices using a Stadie-Riggs tissue slicer and then the slices were incubated for 30 min in a smooth muscle buffer at 31°C containing 0.1% collagenase (300 U/ml) and 0.01% soybean trypsin inhibitor (w/v). The tissue was continuously gassed with 100% oxygen during the entire isolation procedure. The partly digested tissues were

washed twice with 50-ml of collagenase-free smooth muscle buffer and the muscle cells were allowed to disperse spontaneously for 30 min in collagenase-free medium. Cells were harvested by filtration through 500 μm Nitex and centrifuged twice at 350 g for 10 min to eliminate broken cells and organelles. The cells were counted in a hemocytometer and it is estimated that 95% of the cells excluded trypan blue. The experiments were done within 2-3 h of cell dispersion.

2.2.3 Permeabilization of smooth muscle cells

Dispersed muscle cells were permeabilized by incubation for 10 min with 35 μg/ml of saponin in a medium containing 20 mM NaCl, 100 mM KCl, 5 mM $MgSO_4$, 1 mM NH_2PO_4, 25 mM $NaHCO_3$, 0.34 mM $CaCl_2$ and 1 mM EGTA with 1% bovine serum albumin[25]. The cells were centrifuged at 350 *g* for 5 min, washed free of saponin, and resuspended in the same medium with 1.5 mM ATP and ATP-regenerating system (5 mM creatine phosphate and 10 U/ml creatine phosphokinase).

2.2.4 Preparation of cultured gastric smooth muscle cells

Dispersed muscle cells isolated from the antrum and fundus were resuspended in DMEM containing penicillin (200 U/ml), streptomycin (200 μg/ml), gentamycin (100 μg/ml), amphotericin B (2.5 μg/ml) and 10% fetal bovine serum (DMEM-10). The muscle cells were plated at a concentration of 5 X 10^5 cells/ml and incubated at 37°C in a CO_2 incubator. DMEM-10 medium was replaced every three days for 2-3 weeks until confluence was attained. The muscle cells in confluent primary cultures were trypsinized (0.5 mg trypsin/ml), re-plated at a concentration of 2.5 X 10^5 cells/ml and cultured under the same conditions. All experiments were done on cells in the first passage. Previous studies have determined the purity of cultured muscle

cells with smooth muscle-specific γ-actin[88]. Cultured muscle cells were starved in serum-free medium for 24 hours before each use.

2.2.5 Expression of MRP5, α-actin, β-actin, γ-actin, and myosin isoforms (SM1, SM2, SMA, SMB) by RT-PCR

Total RNA was isolated from freshly dispersed smooth muscle cells with TRIzol® reagent (Invitrogen) and cultured gastric muscle cells using ULTRASPECT™ reagent from both antrum and fundus regions of the stomach and then treated with TURBO DNase (Ambion) . RNA from each preparation was reversely transcribed using the SuperScript™ II system containing 50 mM Tris–HCl (pH 8.3), 75 mM KCl, 3 mM $MgCl_2$, 10 mM dithiothreitol (DTT), 0.5 mM deoxynucleoside triphosphates (dNTP), 2.5 μM random hexamers and 200 units of reverse transcriptase in a 20 μl reaction volume. The reactions were carried out at room temperature for 10 min and at 42°C for 50 min, and terminated by heating at 70°C for 15 min. Three μl of the reversely transcribed cDNA was amplified in a final volume of 50 μl by PCR in standard conditions (2 mM $MgCl_2$, 200 μM dNTP, 2.5 units Taq polymerase) with specific primers designed based on conserved sequences in human, rat and mouse cDNAs (Table 1). PCR was performed for 30 cycles. For each experiment, a parallel control without reverse transcriptase was processed. The amplified PCR products were analyzed on 1.5% agarose gel containing 0.1 μg/ml ethidium bromide.

2.2.6 Expression of telokin, CPI-17, α-tropomyosin, β-tropomyosin h-caldesmon, h1-calponin, and smoothelin-A and smoothelin-B by Real Time PCR

Real-time PCR was performed on cDNA samples synthesized from total RNA isolated from freshly dispersed smooth muscle cells and whole gastric tissue from antrum and fundus with TRIzol® reagent (Invitrogen) and from antrum and fundus cultured gastric muscle cells with the

StepOne™ Real-Time PCR System (Applied Biosystem, Foster city, CA) and the intercalating dye, SYBRgreen. Methods for total RNA isolation and cDNA synthesis were followed for the real-time PCR experiments. PCR conditions were optimized on the gradient thermal cycler on the StepOne™ Real-Time PCR System. For each cDNA sample, real-time PCR was conducted in a 20 µl reaction volume containing Quantitect™ SYBRgreen PCR Mastermix (Qiagen, Mississauga, ON). The following time and temperature profile was used for the real-time PCR reactions: 95 ˚C for 5 min; 50 cycles of a series consisting of 15 s at 94 ˚C, 30 s at 52 ˚C, 30 s at 72 ˚C; and a final extension of 5 min at 72 ˚C. The optimal annealing temperatures were determined empirically for each primer set. The sequences of specific primers are listed in Table 1.

Real-time PCR reactions were performed in triplicate. Each primer set generated only one PCR product, and the identity and integrity of these products were confirmed by electrophoresis on 1.5% agarose gel containing 0.1 µg/ml ethidium bromide and sequencing of the individual bands. The fluorescent threshold value was calculated using the StepOne™ Real-Time PCR System software. The absence of peaks in water controls suggested a lack of primer-dimer formation.

Quantification of gene expression. Two general types of quantification strategies can be performed in quantitative RT-PCR (qRT-PCR). The levels of expressed genes may be measured by an absolute quantification or by a relative qRT-PCR. The absolute quantification approach relates the PCR signal to input copy number using a calibration curve[89].

Relative quantification relates the PCR signal of the target transcript in a treatment group to that of another sample such as an untreated control. Relative quantification of a target gene in relation to another gene (reference gene or housekeeping gene) can be calculated on the basis of

delta delta CT values (CT, called as well CP, is the cycle number at which the fluorescence generated within a reaction crosses the threshold. CT reflects the point during the reaction at which a sufficient number of amplicons has accumulated). There are several mathematical models to calculate the relative expression ratio (R), based on the comparison of the diverse cycle differences. Among them are the delta delta CT method [90] and the efficiency corrected calculation model[91]. In these models, the target-gene expression is normalized to the expression of one or more non-regulated housekeeping genes. The choice of an internal control to normalize the expression of the gene of interest is critical to the interpretation of experimental real-time PCR results. The housekeeping gene expression must not be influenced by the applied treatment[92].

Delta delta CT method

$$\Delta\Delta CT = (C_{T,\,Tag} - C_{T,\,HKG})_{\,Treatment} - (C_{T,\,Tag} - C_{T,\,HKG})_{\,Control}$$

$$R = 2^{-\Delta\Delta C_T}$$

Where, HKG is the housekeeping gene and Tag, the evaluated gene.

Following the criteria for choosing the reference genes and delta delta method, in this study GAPDH was selected as reference gene. After normalization, the data for antrum were expressed as the fold-change in mRNA expression relative to that obtained for fundus.

2.2.7 Transfection of dominant negative mutants and minigene constructs into cultured smooth muscle cells.

Wild type telokin and phosphorylation-deficient telokin (S13A) were subcloned into the multiple cloning site (*EcoR I*) of the eukaryotic expression vector pcDNA3. Recombinant plasmid

Table 1. Real-time and RT-PCR primer sequences. Primers for amplification of different genes from smooth muscle tissue. AMPK; AMP kinase, MLCK; myosin light chain kinase, ZIPK; zipper interacting protein kinase, CPI-17; PKC potentiated inhibitor 17 kDa protein, PDE5; phosphodiesterase 5, MRP5; multi-drug resistance protein 5, Tm; tropomyosin, CaD; caldesmon, CaP; calponin, GAPDH; Glyceraldehyde 3-phosphate dehydrogenase, SMA/B; smooth muscle myosin (isoforms A and B), SM1/2; smooth muscle myosin (isoforms 1 and 2).

Primer set	Forward 5'→3'	Reverse 3'→5'	Size (bp)
AMPK	TATGGTGGTCCACAGAGATTTGA	TTTGCATTCATGTGTGCATCA	63
MLCK	GCCGAGCAGATGGATTTCC	CTCTCCTCCTCAGACACAGTCTTG	71
Rho Kinase	CCAAACCTCTCTGGCATGTCTT	TTAACATGGCATCTTCGACATTCT	64
ZIPK	ATCCGCCACCCCAACAT	TCAGCACCACATCTGTCTTGTTC	64
Telokin	AACGGGCAATGCTGTGAGA	GCCCTGAGATCATTGCCATAG	69
CPI-17	GAGCAAGCTGCAGTCCCCGT	GATCCACTTCTCCACGTCCA	116
PDE5	CTATTCCCTGTTCCTTGTCTGTGA	CAAAGAGGCGGCTGATAAGAA	65
MRP5	GCAAGAGCCCTGCTGCGTCA	CTGTGTGCAGGCGATGGGCA	151
α-actin	GTCACTTCCCTGCTCTGT	GCTTTGGATAGGCATGACT	97
β-actin	CCCTCCATCGTGCACCGCAA	CTCGTCTCGTTTCTGCGCCGT	100
γ –actin	ATCAGGCCCGCGACACTCGT	GCCGCCAGTGTGCTCTAAAGGT	70
α-Tm	CTGAAGCCGATGTAGCGTCTCTG	ACGCTCCTGGGCACGATCCA	75
β-Tm	CCTCCCTGAACCGCCGCATT	TGACAAGACGCTCCTGCGCC	67
h-CaD	CAGAAGGGAAGTCGGTAAATGAAA	GGGCAGCTGTCTGAAGTTTATCTTCTT	61
h1-CaP	GGTGAAGCCCCACGACAT	CAAAGCCAGGAGGGTGGACTG	86
Smoothelin-A	GCTGGTAAAAACCAAAAAGTCCTAA	GCTTTTTGCCCATGATCATCA	107
Smoothelin-B	ATGAGGAGCGCAAGCTGATC	GGCAGCCTCAATCTCCTGAGC	65
GAPDH	GCCTGGAGAAAGCTGCTAAGTATG	CCTCGGATGCCTGCTTCA	60
SMA/B	CAGTCCATTCTCTGCACAGG	TCATTCTTGACCGTCTTGGC	197/218
SM1/2	TGAAGCAGAGGGACAAGAAG	TTCTGGTAGGAACGAACGAG	230/291

DNAs were transiently transfected into the muscle in primary culture using Effectene Transfection Reagent (QIAGEN) for 48 h. Cells were co-transfected with 2 μg of pcDNA3 vector and 1 μg of pGreen Lantern-1 DNA. Transfection efficiency was monitored by the expression of the green fluorescent protein using FITC filters. Control cells were transfected with vector alone. Analysis by fluorescence microscopy showed that approximately 80% of the cells were transfected[30,93].

2.2.8 Immunokinase assay

Activities of MLCK, AMPK, PKC, ZIPK, and Rho kinase were measured by an immunokinase assay as previously described[30,34,39,93-96]. Muscle cells were washed one time with PBS, and then were lysed with buffer containing 50 mM Tris-HCl (pH 7.5),150 mM NaCl, 0.1 % SDS, 0.5% sodium deoxycholate, 1% NP-40, 10 mM sodium pyrophosphate, and protease inhibitor cocktail (2 μl/ml, BD Biosciences). The homogenates were centrifuged at 10,000 rpm for 10 min at 4 °C. The supernatant containing cytosolic protein was transferred to a fresh tube and 5 μl of the specific antibody was added to each tube and incubated for 2 h at 4 °C.

At the end of two hours, Protein A/G agarose was added to each tube and the mixture was reincubated at 4 °C for overnight and washed 3 times with lysis buffer. The pellets were re-suspended in 50 μl of kinase buffer containing 100 mM Tris-HCl (pH 7.4), 1 M KCl, 50 mM $MgCl_2$, 10 mM EDTA, and 1 mM DTT. Twenty microliters of the immunoprecipitates were added to the reaction mixture containing 100 mM Tris-HCl (pH 7.4), 1 M KCl, 50 mM $MgCl_2$, 1 mM DTT, 1 mM ATP, and 10 μCi of [γ-^{32}P] ATP (3,000 Ci/mol) along with 5 μg of myelin basic protein (for Rho kinase II, ZIPK an dPKC), or 1 μg purified recombinant MLCK (for AMPK), followed by incubation for 15 min at 37 °C. Phosphorylation of myelin basic protein or MLCK

was absorbed onto phosphocellulose disks, and free radioactivity was removed by washing 3 times with 75 mM H_3PO_4. The amount of radioactivity on the disks was measured by liquid scintillation. The results are expressed as counts per milligram protein per minute.

2.2.9 Cyclic GMP-dependent protein kinase (PKG) assay

PKG activity was measured by the method of Jiang et al [97]. One milliliter of cell suspension was incubated in HEPES medium with 8-Br-cGMP for 90 s at 31^0C. The reaction was stopped by rapid centrifugation, and the pellet was rinsed with a medium containing 50 mM Tris-HCl (pH 7.4), 10 mM EDTA, 0.5 mM IBMX, 10 mM β-mercaptoethanol, and 100 mM NaCl and homogenized in 0.5 ml ice-cold medium. The mixture was centrifuged at 48, 000 *g* for 15 min and the supernatant was used as a source of protein kinaase. PKG activity was measured in a volume of 60 µl containing 50 mM Tris, 10 mM $MgCl_2$, 100 µM [^{32}P]ATP, 50 µM synthetic heptapeptide histone H2B [Arg-Lys-Arg-Ser-Arg-Ala-Glu (RKRSRAE)], and 0.25 mg/ml of bovine serum albumin. The assay was done in the presence or absence of 10 µM of cGMP and 1 µM PKI (6-22 amide) and was initiated by the addition of 20 µl of cell supernatants (50 µg protein) to the reaction mixture. PKG activity was calculated as pmoles/mg protein and expressed as the ratio of activity in the presence or absence of 10 µM cGMP (-cGMP/+cGMP).

2.2.10 Western blot analysis

Muscle cells were solubilized in Triton X-100-based lysis buffer plus protease and phosphatase inhibitors (100 µg/ml PMSF, 10 µg/ml aprotinin, 10 µg/ml leupeptin, 30 mM sodium fluoride and 3 mM sodium vanadate). After centrifugation of the lysates at 20000 *g* for 10 min at 4 °C, the protein concentrations of the supernatant were determined with a Dc protein assay kit from Bio-Rad. Equal amounts of proteins were fractionated by SDS/PAGE, and transferred on to

nitrocellulose membrane. Blots were blocked in 5% (w/v) non-fat dried milk/TBS-T [tris-buffered saline (pH 7.6) plus 0.1% Tween-20] for 1 h and then incubated overnight at 4 °C with various primary antibodies in TBS-T plus 1% (w/v) non-fat dried milk (Table 2). After incubation for 1 h with horseradish-peroxidase-conjugated corresponding secondary antibody (1:2000; 10 μg/ml, Pierce) in TBS-T plus 1% (w/v) non-fat dried milk, immunoreactive proteins were visualized using SuperSignal Femto maximum sensitivity substrate kit (Pierce). All washing steps were performed with TBS-T. The protein bands were identified by enhanced chemiluminescence reagent.

Quantification of protein bands obtained on western blot was done by densitometric analysis of the Details view of the Odyssey software using the median method for calculation of background. The average intensity obtained for each band was normalized to that of β-actin for the same lane. The band intensity of each treatment was then calculated as a percent value of normalized value of the control lane. The percent value of the control was used for statistical analysis.

2.2.11 Radioimmunoassay for cGMP.

Cyclic GMP levels were measured by radioimmunoassay, as previously described [70]. Suspensions of smooth muscle cells (10^6 cells/ml) were stimulated for 1 min with GSNO in the presence of 100 μM IBMX, and the reaction was terminated with 10% trichloroacetic acid. Samples were centrifuged, and the supernatant was extracted with diethyl ether and lyophilized. Samples were resuspended in Na-acetate buffer (pH 6.2) followed by acetylation with triethylamine-acetic anhydride for 10 min. cGMP was measured in duplicate using 100-μl aliquots, and the results are expressed as picomoles per milligram of protein.

Table 2. Primary antibodies. Primary antibodies and their catalogue number, company of production, product size and dilution ratio.

Antibody	Catalog #	Product size (kDa)	Company name	Dilution
AMPKα1 (C-20)	sc-19128	63	SANTA CRUZ	1/1000
MYLK (L-18)	sc-9452	210/135	SANTA CRUZ	1/1000
Rock-2 (H-85)	sc-5561	160	SANTA CRUZ	1/1000
ZIP-kinase (C-19)	sc-8161	52	SANTA CRUZ	1/1000
MYPT1 (N-15)	sc-17433	130	SANTA CRUZ	1/1000
MRCL3/MRLC2/MYL9 (FL-172)	sc-15370	20	SANTA CRUZ	1/1000
Telokin	sc-22226	17	SANTA CRUZ	1/1000
CPI-17 (N-20)	sc-17561	17	SANTA CRUZ	1/1000
PKC ε (17)	sc-56944	82	SANTA CRUZ	1/1000
PDE5	2395	100	CELL SIGNALING	1/1000
MRP5 (C-17)	sc-5780	185	SANTA CRUZ	1/1000
PKG	7721301		PROMEGA	1/1000
β-actin	AC1978	42	SIGMA	1/5000
Tropomyosin (FL-284)	sc-28543	35-45	SANTA CRUZ	1/1000
Caldesmon (H-300):	sc-15374	90-150	SANTA CRUZ	1/1000
Calponin 1 (CALP)	sc-58707	33-36	SANTA CRUZ	1/1000

2.2.12 Phosphorylation of MLCK and AMPK

Phosphorylation of MLCK and AMPK was determined from the amount of ^{32}P incorporated into the enzyme after immunoprecipitation with MLCK or AMPK antibody respectively. A 10 ml suspension of smooth-muscle cells (4×10^6 cells/ml) was prelabelled with 0.5 mCi/ml of [^{32}P]Pi for 3 h. Samples (1 ml) were treated with ACh in the presence or absence of various agents. The reaction was terminated with an equal volume of lysis buffer, containing 1% (v/v) Triton X-100, 0.5% SDS, 10 mM EDTA, 1 mM PMSF, 10 μg/ml leupeptin, 100 μg/ml aprotinin, 10 mM sodium pyrophosphate, 50 mM NaF and 0.2 mM sodium vanadate. The cell lysates were separated from the insoluble material by centrifugation at 13000 g for 15 min at 4 °C, precleared with 40 μl of Protein A–Sepharose and incubated with antibody to MLCK or AMPK for 2 h at 4 °C. After addition of Protein A–Sepharose (40 μl), the lysates were incubated for 1 h. The immunoprecipitates were washed five times with 1 ml of wash buffer containing 10 mM Tris/HCl (pH 7.4), 150 mM NaCl and 0.5% Triton X-100, and extracted with SDS sample buffer. The samples were resolved by SDS/PAGE and ^{32}P-labelled MLCK and AMPK were visualized by autoradiography, and the amount of radioactivity in the bands was counted.

2.2.13 Assay for phosphodiesterase 5 (PDE5) activity

PDE5 activity was measured in immunoprecipitates of PDE5 by the method of Wyatt et al. [98]. PDE5 was immunoprecipitated from lysates of dispersed gastric smooth-muscle cells (3×10^6 cells/ml) using an anti-PDE5 antibody, and the immunoprecipitates were washed in a solution of 50 mM Tris/HCl (pH 7.5), 200 mM NaCl and 5 mM EDTA. The immunoprecipitates were then incubated for 15 min at 30 °C in a reaction mixture containing 100 mM Mes (pH 7.5), 10 mM EDTA, 0.1 M magnesium acetate, 0.9 mg/ml BSA, 20 μM cGMP and [^3H] cGMP. The

samples were boiled for 3 min, chilled for 3 min and then incubated at 30 °C for 10 min in 20 mM Tris/HCl (pH 7.5) containing 10 µl of *C. atrox* snake venom (10 µg/µl). The samples were added to DEAE-Sephacel A-25 columns and the radioactivity in the effluent was counted. The results were expressed as cpm/mg of protein.

2.2.14 Immunoblot analysis of MLC_{20} and CPI-17 phosphoproteins.

Phosphorylation of MLC_{20} and CPI-17 was determined by immunoblot analysis with phosphospecific antibodies as described preciously [30]. Muscle cells were treated with ACh or Ca^{2+} for 30 s or 10 min and solubilized on ice in a medium containing 20 mM Tris·HCl (pH 8.0), 1 mM DTT, 100 mM NaCl, 0.5% SDS, 0.75% deoxycholate, 1 mM PMSF, 10 µg/ml leupeptin, and 100 µg/ml aprotinin. The lysate proteins were resolved by SDS-PAGE and transferred onto polyvinylidene difluoride membranes. The membranes were incubated for 12 h with phosphospecific antibodies to MLC_{20} (Ser^{19}) or CPI-17 (Thr^{38}) and then incubated for 1 h with horseradish peroxidase-conjugated secondary antibodies. The bands were identified by enhanced chemiluminescence. Quantification of protein bands obtained on western blot was done by densitometric analysis as described above.

2.2.15 Measurement of contraction and relaxation in dispersed smooth muscle cells

Contraction in freshly dispersed gastric circular smooth muscle cells was determined by scanning micrometry[93]. An aliquot (0.4 ml) of cells containing approximately 10^4 cells/ml was treated with 100 µl of medium containing acetylcholine (ACh, 0.1 µM) for 30 s or 10 min and the reaction was terminated with 1% acrolein at a final concentration of 0.1%. Acrolein kills and fixes cells without affecting the cell length. The resting cell length was determined in control experiments in which muscle cells were incubated with 100 µl of 0.1% bovine serum albumin

without the ACh. The mean lengths of 50 muscle cells treated with various agonists was measured by scanning micrometry and compared with the mean lengths of untreated cells. The contractile response was expressed as the percent decrease in mean cell length from control cell length.

Relaxation was measured in intact muscle cells contracted with ACh (0.1 µM). Muscle cells were treated for 1 minute with GSNO followed by ACh for 30 s or 10 min. The reaction was terminated with 1% acrolein. The length of 50 cells treated with acetylcholine was measured in sequential microscopic fields by scanning micrometry. Relaxation was expressed as percent increase in the length of cells contracted with ACh.

2.2.16 Transfection of cultured smooth muscle cells with MRP5 siRNA

Confluent smooth muscle cells in the first passage on six-well plates were transiently transfected with the control vector or vector encoding MRP5 siRNA using Lipofectamine 2000 according to the manufacturer's instructions (Invitrogen). Briefly, 2 µg of the vector in 125 µl Opti-MEM medium were mixed with 5 µl Lipofectamine 2000 in 125 µl Opti-MEM. The mixture was incubated at room temperature for 20 min and added to wells containing 1.5 ml DMEM with 10% FBS for 1 day. The medium was then replaced with DMEM with 10% FBS plus antibiotics for 2 days. Cells were maintained for a final 24 h in DMEM without FBS before experiments were started.

2.3. Experimental approach

1. We have used two approaches to determine the differences in smooth muscle contraction and relaxation signaling pathways in antrum versus fundus parts of the stomach. In the first approach, freshly dispersed muscle cells were used to examine expression of various

proteins by western blot, enzyme activities by immuno kinase assay, protein phosphorylation, and smooth muscle contraction and relaxation in response to various reagents. In the second approach, cultured muscle cells in the first passage were used for various molecular and biochemical studies. The purity of cultured muscle cells was determined using markers for smooth muscle, interstial cells of Cajal, enteric neurons and endothelial cells. Use of cultured muscle cells is essential for mRNA expression by RT-PCR and real time PCR and for the expression of phosphorylation-deficient mutants of telokin cDNAs.

2. Permeabilized muscle cells were used to preclude the effects of 8-Br-cGMP on mechanisms upstream of Ca^{2+} generation.

3. The concentrations of inhibitors used in the present study was based on the previous studies in smooth muscle cells and shown to be maximally effective in eliciting an inhibitory response[30,32-34,93].

2.4 Statistical analysis

The results were expressed as means ± S.E. of *n* experiments and analyzed for statistical significance using Student's *t*-test for paired and unpaired values. Each experiment was performed on cells obtained from different animals. Differences among multiple groups were tested using ANOVA and checked for significance using Fisher's protected least significant difference test. A statistical software program was used (GraphPad software, San Diego, CA). A probability of $p<0.05$ was considered significant.

CHAPTER 3

DIFFERENTIAL EXPRESSION OF PROTEINS ASSOCIATED WITH THE CONTRACTILE FILAMENTS IN SMOOTH MUSCLE OF ANTRUM AND FUNDUS

Previous studies using esophagus and lower esophageal sphincter as models of phasic and tonic smooth muscle, respectively, have demonstrated that the expression of various contractile proteins is tissue specific and related to the function of the muscle [99,100]. Initially, studies were carried out to examine whether the expression of contractile proteins is different in muscle cells from antrum and fundus and correlates with the phasic and tonic phenotypes of the muscle, respectively.

The mRNA expression levels of various contractile proteins were analyzed using specific primers by both RT-PCR and qRT-PCR in cultured muscle cells in the first passage. As shown previously [101], the use of confluent cultures of smooth muscle in the first passage ensured the absence of neural, endothelial, or interstitial cell contaminants.

Specific primers were designed based on known sequences in rabbit, if available, or based on the conserved sequences in human, rat, and mouse cDNAs (Table 1). In an initial evaluation, the accuracy of the designed primers was evaluated with agarose gels followed by sequencing of amplicons generated with the primers. Moreover, the formation of primer-dimers and the PCR efficiency of the primer sets were examined. Both the size and the sequence of all

real time RT-PCR amplicons were confirmed. Melt curve analyses showed single peaks for all samples. The PCR efficiencies were calculated from standard curves. The values of the PCR efficiencies were higher than 90%, and the difference among them was not greater than 5%. These findings validated the design of primers and satisfied the requirements for use of the $2^{-\Delta\Delta CT}$ quantification method, described previously in the Materials and Methods section.

GAPDH expression was chosen to normalize the expression of the contractile proteins. The GAPDH amplicon was utilized to normalize and calculate the quantitative expression of various genes. Thus, a quantitative comparison between antrum and fundus tissue was calculated with the $2^{-\Delta\Delta CT}$ method by normalizing the ΔCT counts to GAPDH expression.

3.1 Actins

Expression of six different isoforms of actin with similar levels of acto-myosin ATPase activating property has been demonstrated in smooth muscle tissues. α- and γ-actin isoforms were found to be located primarily within the contractile apparatus, while β-actin is a highly conserved protein and shown to be the cytoskeletal actin isoform. The expression of α-actin is predominant in vascular smooth muscles, while expression of γ-actin is predominant in visceral smooth muscles. The expression of α, β and γ-actin isoforms were examined in antrum and fundus smooth muscle using isoform-specific primers (Table 1). A PCR product with predicted size was detected for α-actin (97bp), γ- actin (70bp) or β-actin (100bp) in muscle cells from both antrum and fundus of rabbit stomach. The differences in the expression levels were analyzed by qRT-PCR. The results showed that expression of α-actin was 11-fold ($p<0.001$, $n=3$) greater in muscle cells from fundus compared to muscle cells from antrum, whereas the expression of γ-actin was ~3-fold ($p<0.05$, $n=3$) greater in muscle cells from antrum than fundus (Figure 1). There was no

significant difference in the expression of β-actin between muscle cells from antrum and fundus (Figure 1).

3.2 Tropomyosins

Expression two different isoforms of tropomyosin has been demonstrated in smooth muscle tissues [102]. Expression of both α-tropomyosin and β-tropomyosin was measured in muscle cells of antrum and fundus. The differences in the expression levels were analyzed by qRT-PCR. The results showed that expression of α-tropomyosin was 5-fold greater, and β-tropomyosin was 2-fold greater in muscle cells from antrum compared to fundus (Figure 2).

Expression of tropomyosin was also examined in the two regions of the stomach by western blot analysis using an antibody that recognizes all the isoforms of tropomyosin. Results showed expression of 2 protein bands with ~45 kDa in the muscle cells from antrum, but only one band in muscle cells from fundus. The molecular weight of the protein bands corresponds to the expected molecular weight of tropomyosin isoforms (35-45 kDa). Comparing the densities of protein bands in the two regions revealed higher expression in muscle cells from antrum compared to fundus and this is consistent with higher expression of mRNA (Figure 2).

3.3 Calponin and Caldesmon

Calponin and caldesmon are thin filament associated proteins that were shown to regulate smooth muscle contraction. They are differentially expressed in phasic (e.g., esophagus) versus tonic (e.g., lower esophageal sphincter) smooth muscles[99,100]. Expression of h-caldesmon and h1-calponin was analyzed by qRT-PCR in muscle cells from antrum and fundus. The results showed that the expression of h1-calponin was 2-fold higher and h-caldesmon was 3-fold higher ($p<0.05$, $n=3$) in muscle cells from antrum compared to fundus. Western blot analysis using antibody to h1-calponin or h-caldesmon demonstrated expression of h1-calponin (~35 kDa) and h-caldemon

(~100 kDa) in both antrum and fundus, and confirmed higher expression in muscle cells from antrum compared to fundus (Figure 3).

3.4 Smoothelin

Expression two different isoforms of smoothelin has been demonstrated in smooth muscle tissues [103]. Expression of smoothelin-A isoform was found to be predominant in visceral smooth muscle cells, whereas expression of smoothelin-B isoform was found to be predominant in vascular smooth muscle. Expression of smoothelin-A and -B isoforms was analyzed by qRT-PCR in muscle cells from antrum and fundus. The results showed that expression of smoothelin-A was 4-fold ($p<0.05$, $n=3$) higher in muscle cells from antrum compared to fundus, whereas expression of smoothelin-B was 3-fold higher ($p<0.05$, $n=3$) in fundus compared to antrum (Figure 4).

3.5 Myosin heavy chain

The smooth muscle myosin is a hexamer with a pair of heavy chains (220 kDa), a pair of 20 kDa regulatory light chains or myosin light chains (MLC_{20}) and a pair of 17 kDa essential light chains. Myosin heavy chain is encoded by a single gene, but alternative splicing at two sites can create four different variants of this ~ 200 kDa polypeptide (SM1, SM2, SM-A and SM-B isoforms). Expression of myosin heavy chain isoforms (SM1, SM2, SM-A and SM-B) was determined by RT-PCR. PCR product of expected size was obtained using specific primers for SM1 (330 bp) and SM2 (291 bp) only in antrum, and the expression of SM1 appears to be greater than SM2 (Figure 5). However, no detectable PCR product was obtained in fundus using same primers for SM1 and SM2. Expression of SM-A and SM-B was also analyzed using specific primers for SM-A and SM-B. Expression of both SM-A (197 bp) and SM-B (218 bp) isoforms was detected in fundus, but only SM-B was detected in antrum (Figures 5). Expression of SM-B

appears to be higher in muscle cells from antrum compared to fundus. The results are consistent with the higher expression of SM-B isoform in phasic muscle [75].

Figure 1. Expression of α-, β-, and γ- actin. Total RNA isolated from cultured (first passage) gastric circular muscle cells from antrum and fundus using RNAqueous prep kits (Ambion, Austin, Tx) was reverse transcribed using 2 μg of total RNA using qScript cDNA prep kits (Quanta, Gaithersburg, MD). The cDNA was amplified with specific primers for α-, β-, and γ-actin. PCR products of expected size (97 bp, 100 bp, and 70 bp) were obtained with α-, β-, and γ-actin primers, respectively. The sequences of specific primers are listed in Table 1. Quantitative real-time polymerase chain reaction (qRT-PCR) was used to measure RNA levels of α-actin, γ-actin and β-actin. For each cDNA sample, real-time PCR was conducted in a 20 μl reaction volume containing Quantitect™ SYBRgreen PCR Mastermix (Qiagen, Mississauga, ON). Real-time PCR reactions were performed in triplicate. Each primer set generated only one PCR product, and the identity and integrity of these products were confirmed by electrophoresis in agarose gel in the presence of ethidium bromide and sequencing of the individual bands (inset: representative PCR products of α-actin, γ-actin and β-actin). Standard curves for each amplicon were generated from a dilution series of cDNA and results were quantified and reported using the $2^{-\Delta\Delta C_T}$ method based on GAPDH amplification. GAPDH amplicon thresholds remained constant. Relative quantification of a target gene in relation to reference gene was calculated on the basis of delta delta CT values. Results demonstrated that α-actin mRNA levels are higher, while γ-actin mRNA levels are lower in fundus compared to antrum. β-actin mRNA levels were similar in antrum and fundus. Values represent the means ±SEM of 3 separate experiments. *$p<0.05$ versus fundus; **$p<0.001$ versus antrum

Figure 1

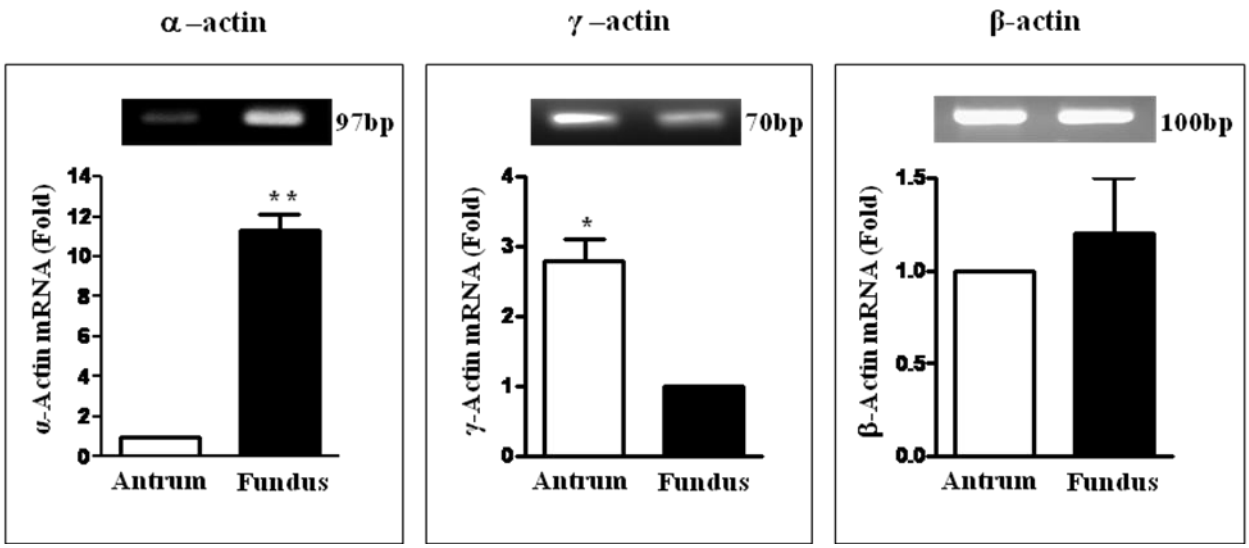
α –actin
97bp
α-Actin mRNA (Fold)
14
12
10
8
6
4
2
0
**
Antrum
Fundus
γ –actin
70bp
γ-Actin mRNA (Fold)
4
3
2
1
0
*
Antrum
Fundus
β-actin
100bp
β-Actin mRNA (Fold)
1.5
1.0
0.5
0.0
Antrum
Fundus

Figure 2. Expression of α- and β-tropomyosin. Total RNA was isolated from cultured (first passage) muscle cells from antrum and fundus using RNAqueous prep kits (Ambion, Austin, Tx) was reverse transcribed using 2 μg of total RNA using qScript cDNA prep kits (Quanta, Gaithersburg, MD). The cDNA was amplified with specific primers for α- or β-tropomyosin. PCR products of expected size (75bp, and 67bp,) were obtained with α-or β-tropomyosin primers respectively. The sequences of specific primers are listed in Table 1. Quantitative real-time polymerase chain reaction (qRT-PCR) was used to measure RNA levels of α- or β-tropomyosin. For each cDNA sample, real-time PCR was conducted in a 20 μl reaction volume containing Quantitect™ SYBRgreen PCR Mastermix (Qiagen, Mississauga, ON). Real-time PCR reactions were performed in triplicate. Each primer set generated only one PCR product, and the identity and integrity of these products were confirmed by electrophoresis in agarose gel in the presence of ethidium bromide and sequencing of the individual bands. Standard curves for each amplicon were generated from a dilution series of cDNA and results were quantified and reported using the $2^{-\Delta\Delta C_T}$ method based on GAPDH amplification. GAPDH amplicon thresholds remained constant. Relative quantification of a target gene in relation to reference gene was calculated on the basis of delta delta CT values. Results demonstrated that both α- and β-tropomyosin mRNA levels are higher in antrum compared to fundus. Inset: Representative western blot results of tropomyosin expression. Cell lysates containing equal amounts of total proteins were separated with SDS-PAGE and expression of tropomyosin was analyzed using an antibody that recognizes all the isoforms of tropomyosin. Values represent the means ±SEM of 3 separate experiments. *$p<0.05$ versus fundus; **$p<0.001$ versus fundus.

Figure 2

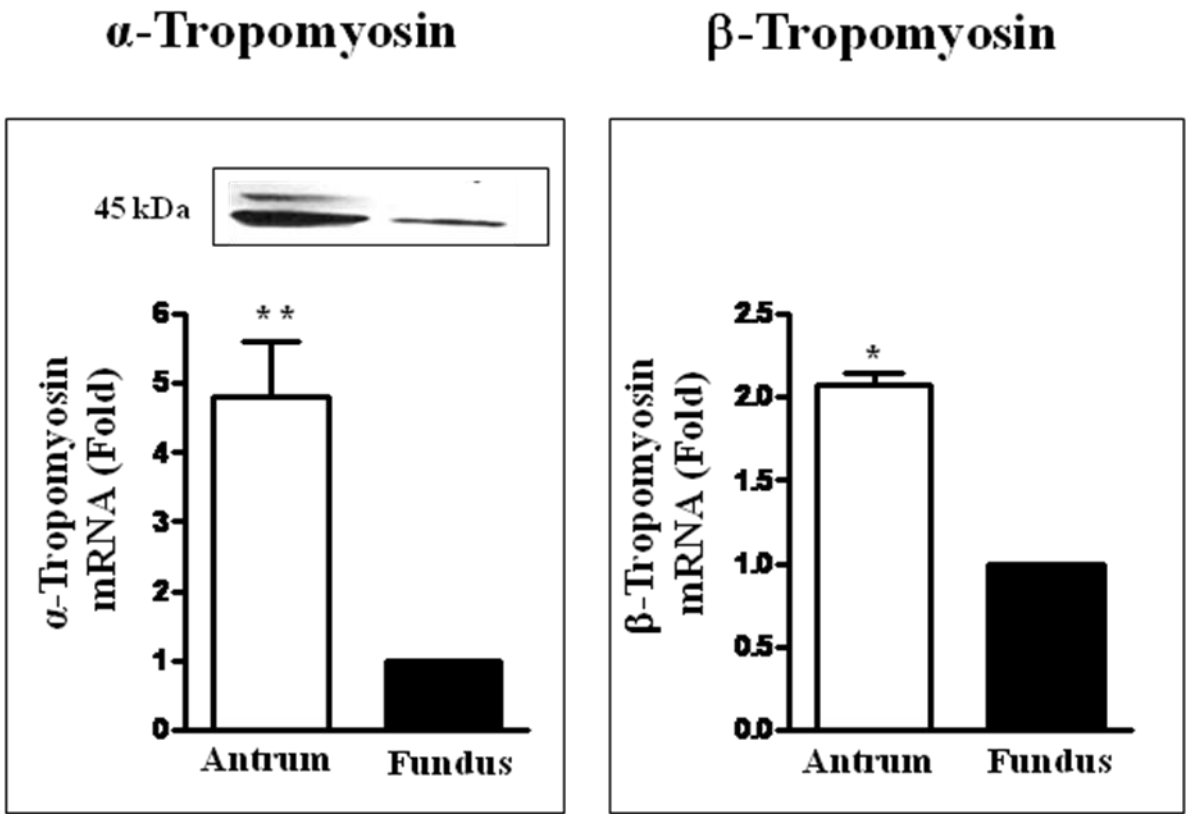
α-Tropomyosin
β-Tropomyosin
45 kDa
α-Tropomyosin mRNA (Fold)
β-Tropomyosin mRNA (Fold)
**
*
Antrum
Fundus
Antrum
Fundus

Figure 3. Expression of h1-calponin and h-caldesmon. Total RNA isolated from cultured (first passage) muscle cells from antrum and fundus was reverse transcribed using 2 μg of total RNA. The cDNA was amplified with specific primers for h1-clponin and h-caldesmon. PCR products of expected size (86 bp and 61 bp) were obtained with h1-clponin and h-caldesmon primers respectively. The sequences of specific primers are listed in Table 1. Quantitative real-time polymerase chain reaction (qRT-PCR) was used to measure RNA levels of h1-clponin and h-caldesmon. For each cDNA sample, real-time PCR was conducted in a 20 μl reaction volume containing Quantitect^{TM} SYBRgreen PCR Mastermix. Real-time PCR reactions were performed in triplicate. Each primer set generated only one PCR product, and the identity and integrity of these products were confirmed by electrophoresis in agarose gel in the presence of ethidium bromide and sequencing of the individual bands. Standard curves for each amplicon were generated from a dilution series of cDNA and results were quantified and reported using the $2^{-\Delta\Delta C_T}$ method based on GAPDH amplification. Relative quantification of a target gene in relation to reference gene was calculated on the basis of delta delta CT values. Results demonstrated that both h1-calponin and h-caldesmon levels are higher in antrum compared to fundus. Inset: Representative western blot results of calponin and caldesmon expression. Cell lysates containing equal amounts of total proteins were separated with SDS-PAGE and expression of calponin or caldesmon was analyzed using selective antibody. Values represent the means ±SEM of 3 separate experiments. *$p<0.05$ versus fundus.

Figure 3

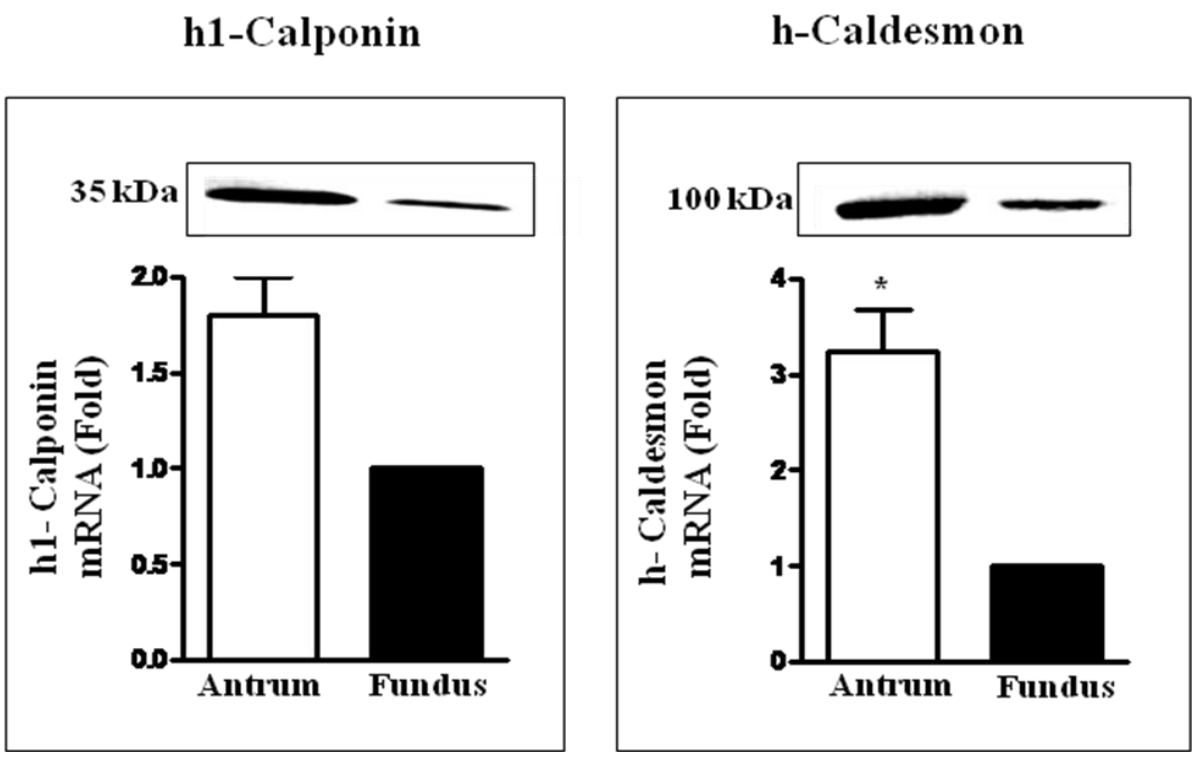
h1-Calponin
35 kDa
h1- Calponin mRNA (Fold)
2.0
1.5
1.0
0.5
0.0
Antrum
Fundus
h-Caldesmon
100 kDa
h- Caldesmon mRNA (Fold)
*
4
3
2
1
0
Antrum
Fundus

Figure 4. Expression of smoothelin-A and smoothelin-B. Total RNA isolated from cultured (first passage) muscle cells from antrum and fundus was reverse transcribed using 2 μg of total RNA. The cDNA was amplified with specific primers for smoothelin-A and smoothelin-B. PCR products of expected size (107 bp and 65 bp) were obtained with smoothelin-A and smoothelin-B primers, respectively. The sequences of specific primers are listed in Table 1. Quantitative real-time polymerase chain reaction (qRT-PCR) was used to measure RNA levels of smoothelin-A and smoothelin-B. For each cDNA sample, real-time PCR was conducted in a 20 μl reaction volume containing Quantitect™ SYBRgreen PCR Mastermix. Real-time PCR reactions were performed in triplicate. Each primer set generated only one PCR product, and the identity and integrity of these products were confirmed by electrophoresis by electrophoresis in agarose gel in the presence of ethidium bromide and sequencing of the individual bands. Standard curves for each amplicon were generated from a dilution series of cDNA and results were quantified and reported using the $2^{-\Delta\Delta C_T}$ method based on GAPDH amplification. Relative quantification of a target gene in relation to reference gene was calculated on the basis of delta delta CT values. Results demonstrated that expression of smoothelin-A is higher in antrum compared to fundus, whereas expression of smoothelin-B is higher in fundus compared to antrum. Values represent the means ±SEM of 3 separate experiments. **$p<0.001$ versus fundus for smoothelin-A, and versus antrum for smoothelin-B.

Figure 4

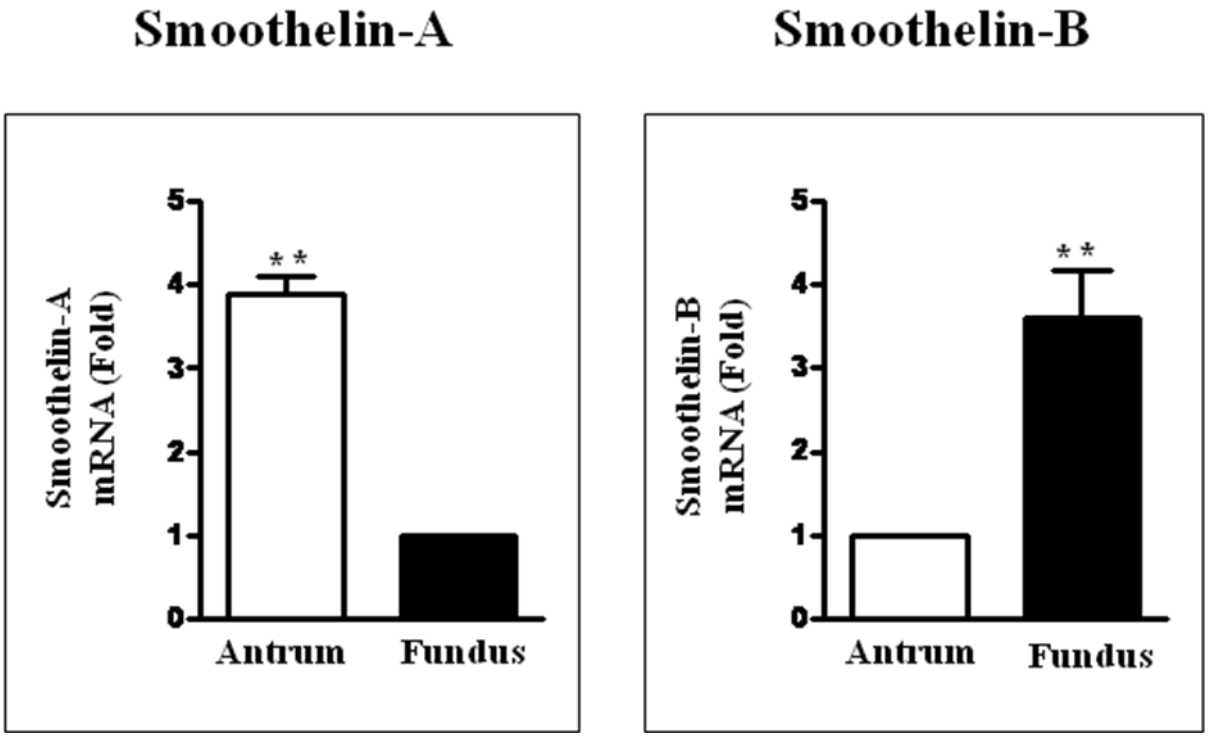
Smoothelin-A
Smoothelin-A mRNA (Fold)
0
1
2
3
4
5
* *
Antrum
Fundus
Smoothelin-B
Smoothelin-B mRNA (Fold)
0
1
2
3
4
5
* *
Antrum
Fundus

Figure 5. Expression of myosin heavy chain isoforms (SM1/2 and SMA/B). Total RNA isolated from cultured (first passage) gastric circular muscle cells from antrum and fundus was reverse transcribed using 2 µg of total RNA. The cDNA was amplified with specific primers for SM1/2 or SM-A/SM-B. PCR products of expected size (330/291 bp and 197/218 bp) were obtained with SM1/2 or SM-A/SM-B primers respectively. The sequences of specific primers are listed in Table 1. Primers for SM1/2 generated two PCR products only in antrum, whereas primers for SM-A/SM-B generated one PCR product, corresponding to SM-B, in antrum and 2 products corresponding to both SM-A and SM-B isoforms in fundus. Results show representative PCR products of myosin heavy chain isoforms separated by electrophoresis in agarose gel in the presence of ethidium bromide and visualized by a ChemiImager Fluorescence system.

Figure 5

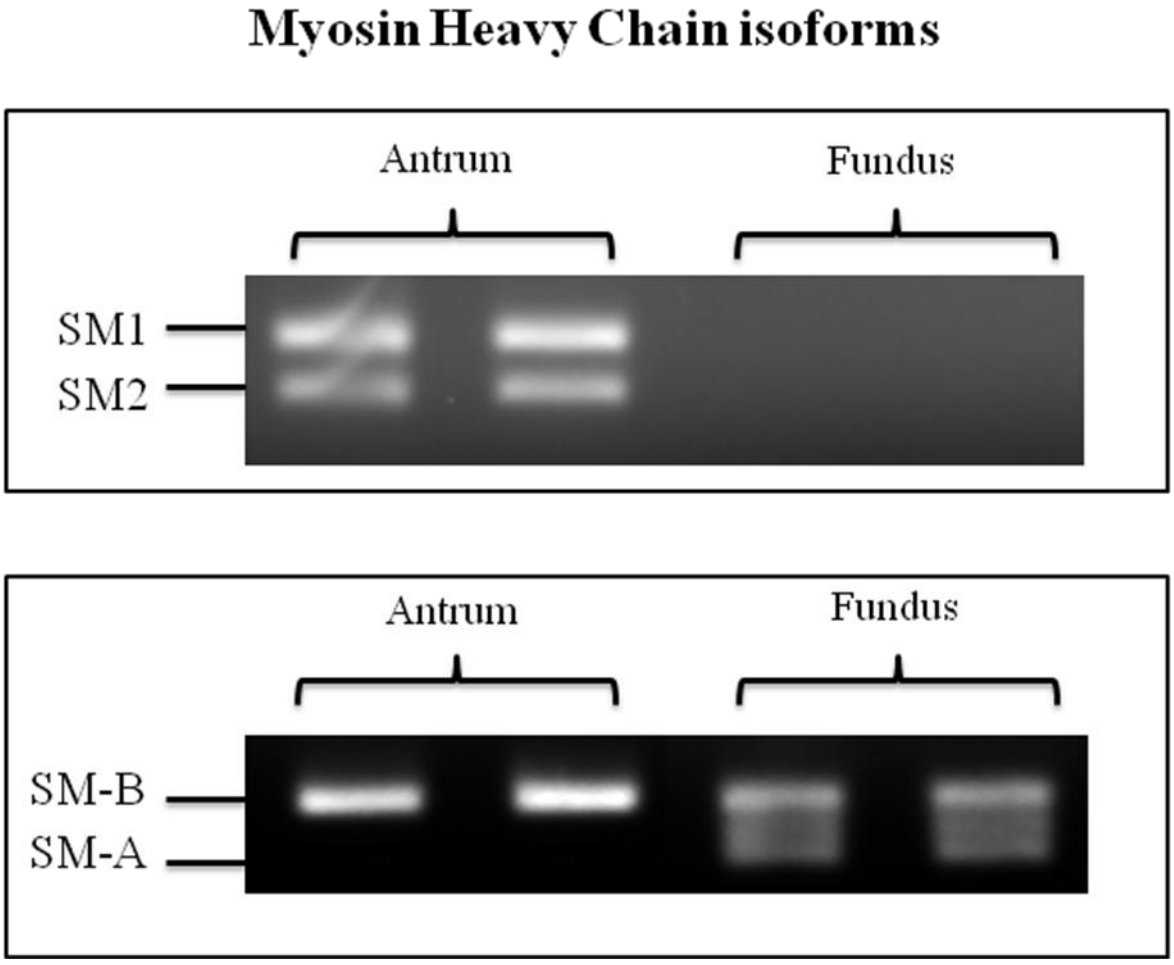
Myosin Heavy Chain isoforms
Antrum
Fundus
SM1
SM2
Antrum
Fundus
SM-B
SM-A

CHAPTER 4

DIFFERENTIAL REGULATION OF MLCK ACTIVITY AND INITIAL MUSCLE CONTRACTION IN ANTRUM AND FUNDUS

In gastrointestinal smooth muscle, contraction-induced by Gq-coupled receptor agonists (e.g., acetylcholine) consists of a transient Ca^{2+}-dependent phase and reflects sequential activation of PLC-β1, IP_3-depedent Ca^{2+} release, Ca^{2+}/CaM-dependent activation of MLCK and phosphorylation of Ser^{19} on MLC_{20}, leading to interaction of actin and myosin and muscle contraction. The levels of MLC_{20} phosphorylation and contraction are dependent on relative activities of MLCK and MLCP. Ca^{2+}/CaM complex stimulates MLCK activity and the affinity of MLCK for Ca^{2+}/CaM is regulated by several mechanisms. Recent studies have demonstrated that agonist-induced MLCK activity is regulated by AMPK in vascular smooth muscle. Stimulation of AMPK activity was mediated by an upstream Ca^{2+}/CaM-dependent protein kinase kinase-β (CaMKK-β), which phosphorylates AMPK at Thr^{172} and thus stimulates AMPK activity[104]. *We postulated that the rapid termination of contraction and MLCK activity by AMPK could contribute to the phasic phenotype of antrum.*

4.1 Expression and activation of AMPK

Expression of AMPK, by both qRT-PCR and western blot, and stimulation of AMPK activity in response to ACh (0.1μM) and depolarizing concentrations of KCl (20 mM) were determined in muscle cells from antrum and fundus. AMPKα1 mRNA was expressed in muscle cells from both antrum and fundus and the expression was 3-fold ($p<0.001$, $n=3$) greater in antrum compared to fundus (figure 6). AMPK protein expression was examined in the two regions of the stomach by western blot using selective antibody to AMPKα1, the smooth muscle predominant isoform[105]. The results confirmed the expression of AMPKα1 of predicted size (63 kDa) in the homogenates of smooth muscle cells of both antrum and fundus. Comparing the densities of protein bands in the two regions revealed a ~ 6-fold higher expression of AMPK in antrum compared to fundus ($p<0.001$, $n=4$) and this is consistent with the higher expression of AMPK mRNA in antrum compared to fundus (figure 6).

Basal and agonist-stimulated AMPK activity was measured by immunokinase assay using recombinant MLCK as substrate. Although, the expression levels are different, basal AMPK activity was not significantly different in antrum (7561±860 cpm/mg protein) and fundus (5741±602 cpm/mg protein). Treatment of freshly dispersed muscle cells with ACh (0.1 μM) significantly increased AMPK activity in antrum (567±34% increase; 44357±3672 cpm/mg protein above basal level), but not in fundus (Figure 7). The results are consistent with higher expression of AMPK in antrum.

Previous studies have shown that AMPK activity is stimulated by several upstream kinases including CaMKK-β, LKB1, and TAK1. CaMKK-β links AMPK activity with increase in intracellular Ca^{2+}. Freshly dispersed smooth muscle cells from both antrum and fundus were treated with ACh (0.1 μM) in the presence or absence of STO609 (10 μM), a selective

inhibitor of CaMKKβ, BAPTA (10 μM), a selective Ca^{2+} chelator, or calmidazolium (10μM), a selective CaM antagonist.

The increase in ACh-induced AMPK activity was blocked by pre-treatment of cells with STO609 (83±6% inhibition, $p<0.001$, n=4), BAPTA (77±12% inhibition), or calmidazolum (89±8% inhibition) (Figures 7, 8, 9). These results suggest that stimulation of AMPK activity in muscle cells from antrum is mediated by CaMKKβ in a Ca^{2+}/calmodulin-dependent manner.

To examine whether stimulation of AMPK activity can be mediated by an increase intracellular Ca^{2+} without receptor activation, muscle cells were treated with depolarizing concentrations of KCl (20 mM) for 30 s and AMPK activity was measured. KCl significantly increased AMPK activity in antrum (513±26% increase; 38801± 3120 cpm/mg protein above basal level, but not in fundus (Figure 10). The extent of stimulation in antrum was similar to that induced by ACh. KCl-induced AMPK activity was blocked by pre-treatment of cells with BAPTA (89±8% inhibition, $p<0.001$) or calmidazolium (82±6% inhibition) (Figures 10 and 11).

Further evidence for the involvement of phosphorylation in the stimulation of AMPK activity was obtained by measurement of AMPK phosphorylation in cells labeled with [^{32}P]Pi followed by immunoblot with AMPKα1 antibody in both antrum and fundus. ACh induced significant phosphorylation of AMPK in muscle cell from antrum (2156±402 cpm/mg protein), but had no effect in muscle cells from fundus (Figure 12).

Figure 6. Expression of AMPKα1. Total RNA isolated from cultured (first passage) muscle cells from antrum and fundus was reverse transcribed using 2 μg of total RNA. The cDNA was amplified with specific primers for AMPKα1. The sequences of specific primers are listed in Table 1. Quantitative real-time polymerase chain reaction (qRT-PCR) was used to measure RNA levels of AMPKα1. For each cDNA sample, real-time PCR was conducted in a 20 μl reaction volume containing TaqMan Gene Expression master Mix. Real-time PCR reactions were performed in triplicate. Each primer set generated only one PCR product (63 bp), and the identity and integrity of these products were confirmed by electrophoresis in agarose gel in the presence of ethidium bromide and sequencing of the individual bands. Relative quantification of a target gene in relation to reference gene was calculated on the basis of delta delta CT values. Results demonstrated that mRNA levels of AMPKα1 are higher in antrum compared to fundus. Inset: Representative western blot results of AMPKα1 expression. Cell lysates containing equal amounts of total proteins were separated with SDS-PAGE and expression of AMPKα1 was analyzed using selective antibody for AMPKα1. Membranes were reblotted to measure β-actin. Protein bands visualized with enhanced chemiluminescence, images were quantified and densitometric values were calculated after normalization to β-actin density. Results are expressed as fold increase over the expression of AMPKα1 in fundus. Values represent the means ±SEM of 3 separate experiments. **$p<0.001$ versus fundus.

Figure 6

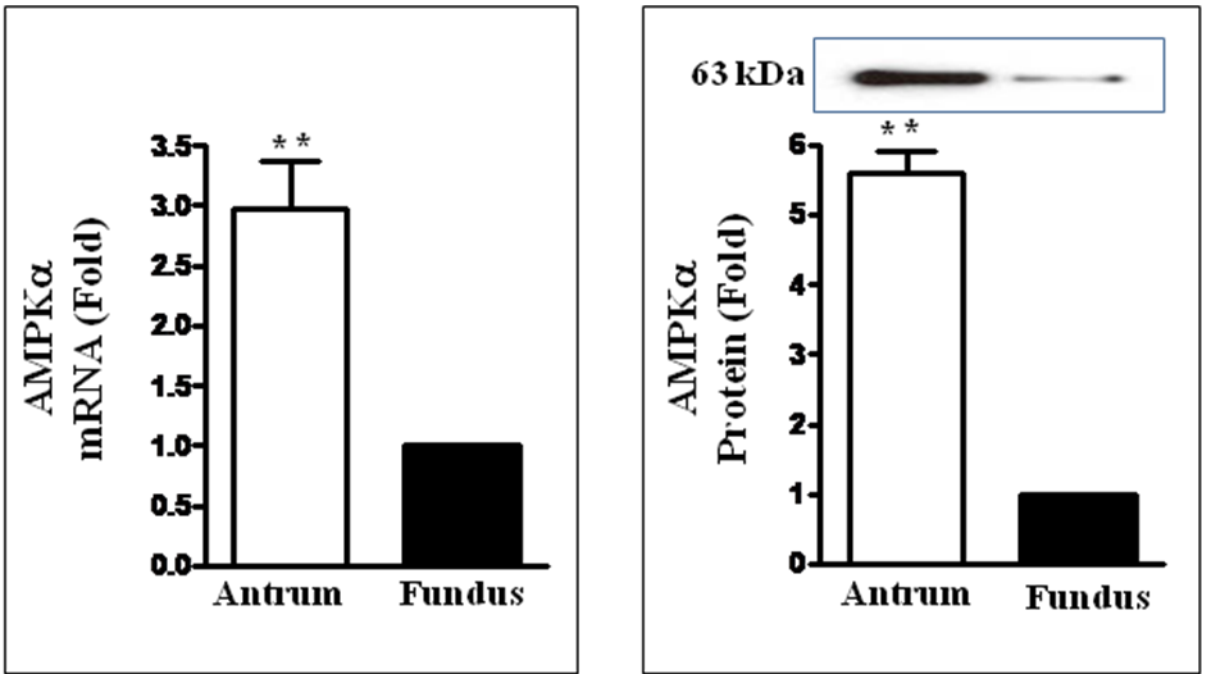
AMPKα
mRNA (Fold)
3.5
3.0
2.5
2.0
1.5
1.0
0.5
0.0
* *
Antrum
Fundus
63 kDa
AMPKα
Protein (Fold)
6
5
4
3
2
1
0
* *
Antrum
Fundus

Figure 7. Stimulation of AMPK activity by ACh and sensitivity to CAMKKβ antagonist. One milliliter of cell suspension (2 x 10^6 cells/ml) freshly dispersed muscle cells from antrum and fundus were treated with ACh (0.1 μM) for 30 s in the presence or absence of STO609 (1 μM), a selective inhibitor of CaMKKβ. The cells were homogenized in the lysis buffer and the protein content in the supernatants was measured. AMPK was immunoprecipitated from lysates containing equal amounts of protein and the activity was measured in immunoprecipitates using purified recombinant MLCK as substrate and [^{32}P]ATP. The amount of radioactivity absorbed onto phosphocellulose disks reflecting kinase activity was measured by liquid scintillation and the results are expressed as counts per milligram protein per minute. ACh stimulated AMPK activity selectively in antrum and the stimulation was blocked by pretreatment of cells with STO609. Values represent the means ±SEM of 4-5 separate experiments. **$p<0.001$ versus basal activity in the absence of ACh.

Figure 7

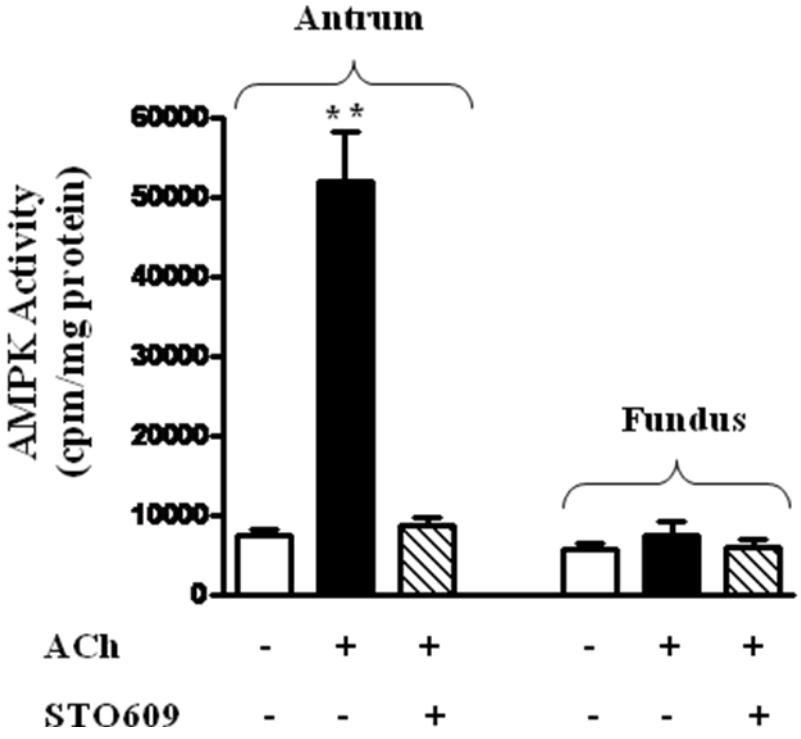
Antrum
Fundus
AMPK Activity
(cpm/mg protein)
60000
50000
40000
30000
20000
10000
0
* *
ACh - + + - + +
STO609 - - + - - +

Figure 8. Ca^{2+}-dependent stimulation of AMPK activity by ACh. One milliliter of cell suspension (2 x 10^6 cells/ml) freshly dispersed muscle cells from antrum and fundus were treated with ACh (0.1 μM) for 30 s in the presence or absence of BAPTA (10 μM), an intracellular Ca^{2+} chelator. The cells were homogenized in the lysis buffer and the protein content in the supernatants was measured. AMPK was immunoprecipitated from lysates containing equal amounts of protein and the activity was measured in immunoprecipitates using purified recombinant MLCK as substrate and [^{32}P]ATP. The amount of radioactivity absorbed onto phosphocellulose disks reflecting kinase activity was measured by liquid scintillation and the results are expressed as counts per milligram protein per minute. ACh stimulated AMPK activity selectively in antrum and the stimulation was blocked by pretreatment of cells with BAPTA. Values represent the means ±SEM of 4-5 separate experiments. **$p<0.001$ significant increase above basal activity induced by ACh; ##$p<0.05$ significant inhibition of ACh-stimulated activity by BAPTA.

Figure 8

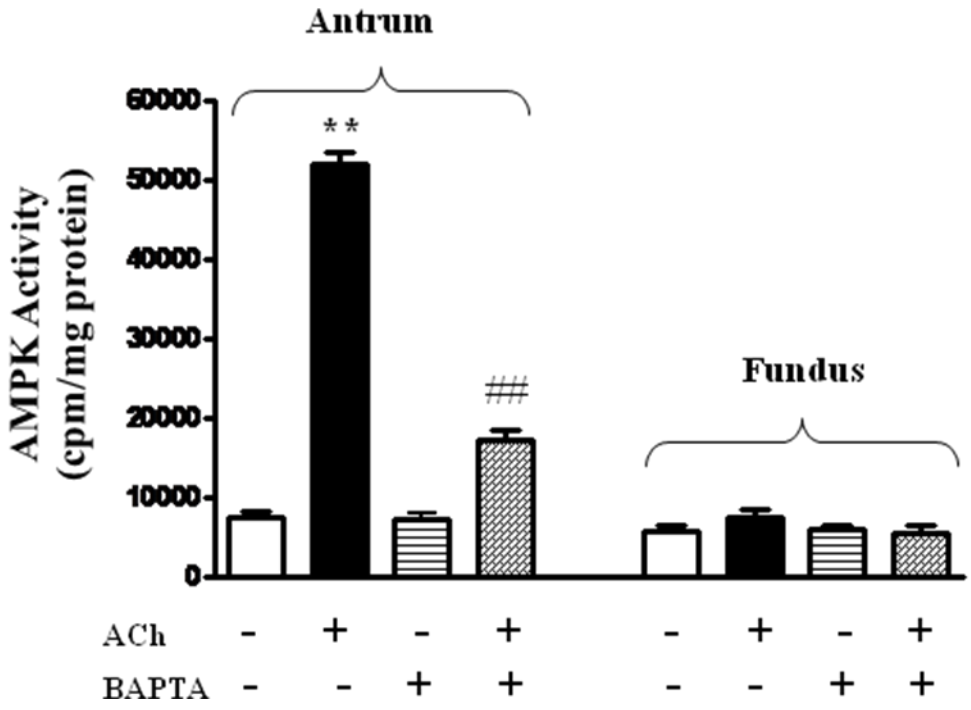
Antrum
Fundus
AMPK Activity
(cpm/mg protein)
60000
50000
40000
30000
20000
10000
0
**
##
ACh - + - + - + - +
BAPTA - - + + - - + +

Figure 9. Calmodulin-dependent stimulation of AMPK activity by ACh. One milliliter of cell suspension (2 x 10^6 cells/ml) freshly dispersed muscle cells from antrum and fundus were treated with ACh (0.1 µM) for 30 s in the presence or absence of calmidazolium (10 µM), a calmodulin antagonist. The cells were homogenized in the lysis buffer and the protein content in the supernatants was measured. AMPK was immunoprecipitated from lysates containing equal amounts of protein and the activity was measured in immunoprecipitates using purified recombinant MLCK as substrate and [^{32}P]ATP. The amount of radioactivity absorbed onto phosphocellulose disks reflecting kinase activity was measured by liquid scintillation and the results are expressed as counts per milligram protein per minute. ACh stimulated AMPK activity selectively in antrum and the stimulation was blocked by pretreatment of cells with calmidazolium. Values represent the means ±SEM of 4-5 separate experiments. **$p<0.001$ significant increase above basal activity induced by ACh; ##$p<0.05$ significant inhibition of ACh-stimulated activity by calmidazolium.

Figure 9

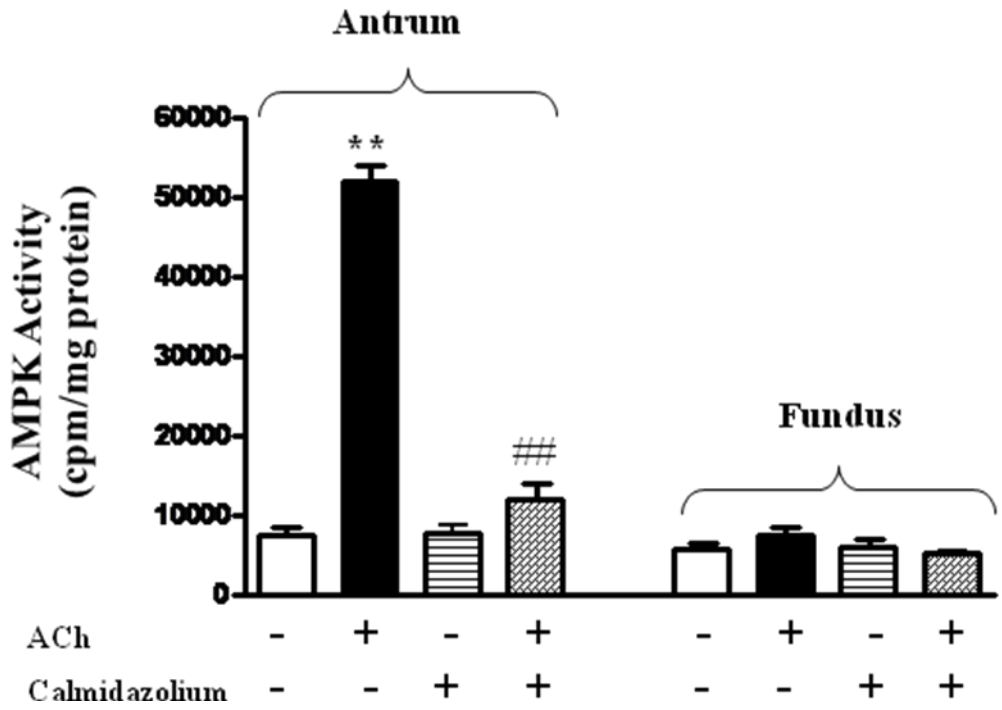
Antrum
Fundus
AMPK Activity
(cpm/mg protein)
60000
50000
40000
30000
20000
10000
0
**
##
ACh
Calmidazolium
- + - + - + - +
- - + + - - + +

Figure 10. Ca^{2+}-dependent stimulation of AMPK activity by KCl. One milliliter of cell suspension (2 x 10^6 cells/ml) freshly dispersed muscle cells from antrum and fundus were treated with KCl (20 mM) for 30 s in the presence or absence of BAPTA (10 µM), an intracellular Ca^{2+} chelator. The cells were homogenized in the lysis buffer and the protein content in the supernatants was measured. AMPK was immunoprecipitated from lysates containing equal amounts of protein and the activity was measured in immunoprecipitates using purified recombinant MLCK as substrate and [^{32}P]ATP. The amount of radioactivity absorbed onto phosphocellulose disks reflecting kinase activity was measured by liquid scintillation and the results are expressed as counts per milligram protein per minute. KCl stimulated AMPK activity selectively in antrum and the stimulation was blocked by pretreatment of cells with BAPTA. Values represent the means ±SEM of 4-5 separate experiments. **$p<0.001$ significant increase above basal activity induced by KCl; ##$p<0.05$ significant inhibition of KCl-stimulated activity by BAPTA.

Figure 10

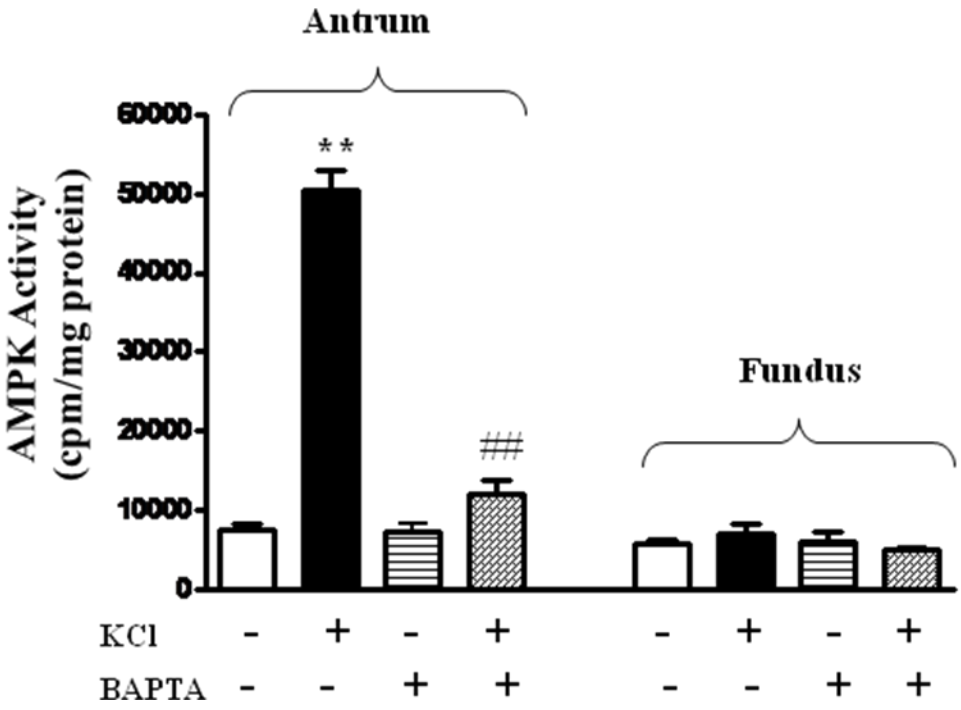
Antrum
Fundus
AMPK Activity
(cpm/mg protein)
60000
50000
40000
30000
20000
10000
0
**
##
KCl - + - + - + - +
BAPTA - - + + - - + +

Figure 11. Calmodulin-dependent stimulation of AMPK activity by KCl. One milliliter of cell suspension (2 x 10^6 cells/ml) freshly dispersed muscle cells from antrum and fundus were treated with KCl (20 mM) for 30 s in the presence or absence of calmidazolium (10 μM), a calmodulin antagonist. The cells were homogenized in the lysis buffer and the protein content in the supernatants was measured. AMPK was immunoprecipitated from lysates containing equal amounts of protein and the activity was measured in immunoprecipitates using purified recombinant MLCK as substrate and [^{32}P]ATP. The amount of radioactivity absorbed onto phosphocellulose disks reflecting kinase activity was measured by liquid scintillation and the results are expressed as counts per milligram protein per minute. KCl stimulated AMPK activity selectively in antrum and the stimulation was blocked by pretreatment of cells with calmidazolium. Values represent the means ±SEM of 4-5 separate experiments. **$p<0.001$ significant increase above basal activity induced by KCl; ##$p<0.05$ significant inhibition of KCl-stimulated activity by calmidazolium.

Figure 11

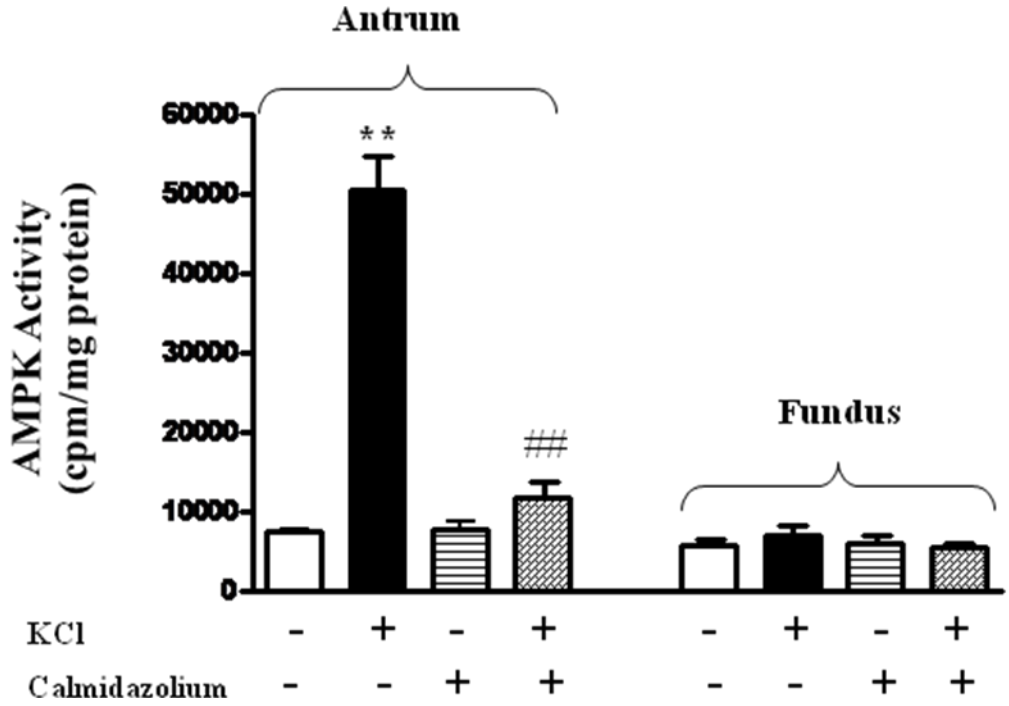
Antrum
Fundus
AMPK Activity
(cpm/mg protein)
60000
50000
40000
30000
20000
10000
0
**
##
KCl
Calmidazolium
- + - + - + - +
- - + + - - + +

Figure 12. Phosphorylation of AMPK by ACh. Ten milliliter of cell suspension (2 x 10^6 cells/ml) freshly dispersed muscle cells from antrum and fundus were labeled with ^{32}P and the cells were incubated with ACh for 30s. AMPK was immunoprecipitated from the cell lysates containing equal amount of protein, extracted with Laemmeli buffer and separated by electrophoresis on SDS-PAGE. Phosphorylated AMPK was visualized by autoradiography, and the amount of radioactivity in the protein band was measured. The results are expressed as counts per milligram protein per minute. Values represent the means ±SEM of 3 separate experiments. **$p<0.001$ significant increase in phosphorylation above basal level induced by ACh.

Figure 12

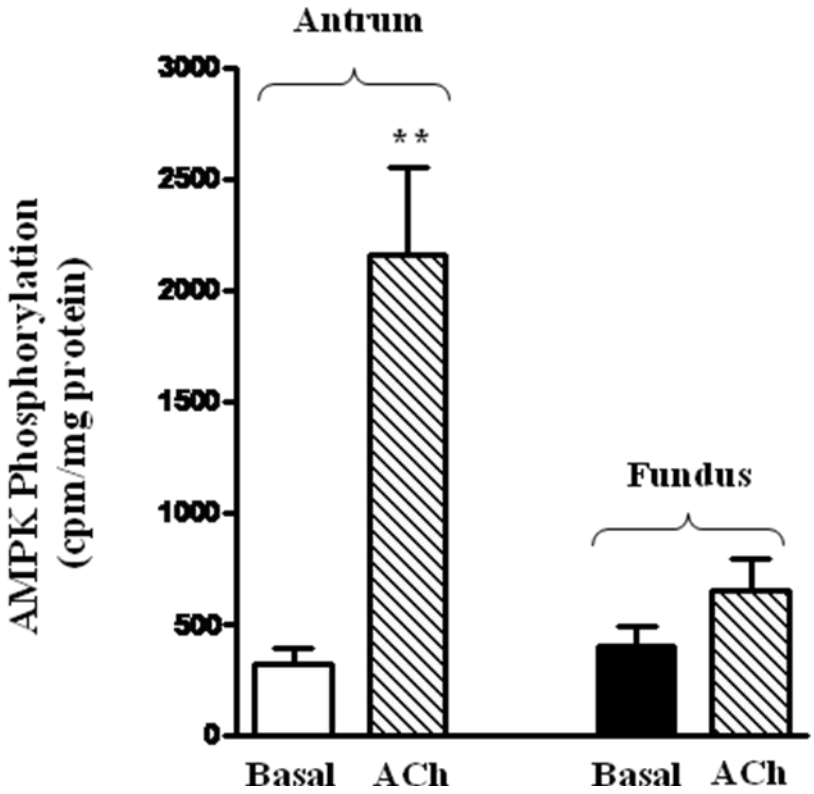
Antrum
Fundus
AMPK Phosphorylation
(cpm/mg protein)
3000
2500
2000
1500
1000
500
0
**
Basal
ACh
Basal
ACh

4.2 Feedback inhibition of MLCK activity

MLCK is the main enzyme responsible for MLC_{20} phosphorylation, and thus smooth muscle contraction. Expression of MLCK, by both qRT-PCR and western blot, and stimulation of MLCK activity in response to ACh (0.1μM) were determined in muscle cells from antrum and fundus. MLCK mRNA was expressed in muscle cells from both antrum and fundus, and the expression was 3-fold higher ($p<0.05$ n=3) in antrum compared to fundus (Figure 13). MLCK protein expression was examined in the two regions of the stomach by western blot using selective antibody to MLCK. Results confirmed the expression of MLCK of predicted size (135 kDa) in the homogenates of smooth muscle cells from both antrum and fundus (Figure 13). Comparing the densities of protein bands in the two regions revealed that there was nearly 2-fold higher expression MLCK in muscle cells from antrum compared to fundus.

Basal and agonist-stimulated MLCK activity was measured by immunokinase assay using MLC_{20} as substrate. Basal MLCK activity was not significantly different in antrum (1249±116 cpm/mg protein) and fundus (1464±236 cpm/mg protein). Treatment of freshly dispersed muscle cells with ACh (0.1 μM) significantly increased MLCK activity in antrum (943±56% increase, 12721±1038 cpm/mg protein above basal level, $p<0.001$, n=4) and fundus (821±56% increase; 12045±1306 cpm/mg protein above basal level, $p<0.001$, n=4) (Figure 14).

Despite higher expression of MLCK in antrum, agonist-stimulated MLCK activity in antrum and fundus was similar. This raised the possibility that MLCK activity might be negatively regulated in antrum via a feedback mechanism involving AMPK. To examine this notion, ACh-stimulated MLCK activity was measured in the presence of STO609, an inhibitor of CaMKK/AMPK pathway. ACh-stimulated MLCK activity was significantly augmented (194±35% increase above

ACh treatment alone, $p<0.001$, $n=4$) in the presence of STO609 in muscle cells from antrum. STO609 had no effect on ACh-stimulated MLCK activity in muscle cells from fundus (Figure 14). These results suggest that MLCK activity is negatively regulated in a feedback mechanism via CaMKKβ/AMPK pathway in antrum, but not in fundus. The results are consistent with the higher expression and activation of AMPK in antrum.

Further evidence for the involvement of AMPK in the regulation of MLCK activity was obtained by measurement of MLCK phosphorylation in cells labeled with [^{32}P]Pi followed by immunoblot with MLCK antibody in both antrum and fundus. ACh induced significant phosphorylation of MLCK in muscle cell from antrum (3562±564 cpm/mg protein), but had no effect in muscle cells from fundus (Fig 15).

4.3 Regulation of initial muscle contraction by CaMKKβ/AMPK pathway

The inhibition of MLCK activity by AMPK in antrum muscle could contribute to its phasic phenotype. To examine the involvement of CaMKK/AMPK pathway in the regulation of muscle contraction, muscle cells from antrum and fundus were treated with different concentrations of ACh for 30 s in the presence or absence of STO609 (10μM) and the decrease in cell length was measured by scanning micrometry. Previous studies in gastrointestinal smooth muscle have demonstrated that the contractile response at 30 s reflects Ca^{2+}/CaM-depedent activation of MLCK. Control cell length in muscle cells from antrum and fundus are similar (95±3 μm in antrum and 102±5 μm in fundus). ACh caused contraction that was concentration-dependent with an EC_{50} of 2±1 nM in antrum and 3±2 nM in fundus and the maximal response to 0.1 μM of ACh was similar in antrum and fundus (27±2% decrease in cell length in antrum and 28±3% decrease in cell length in fundus) (Figure 16). However, pretreatment of cells with STO609 significantly augmented ACh-induced contraction in muscle cells from antrum and

shifted the concentration-response curve to the left (EC_{50} 0.09±0.06 nM). In contrast, STO609 had no effect on contraction in fundus. The results are consistent with the selective augmentation of MLCK activity by STO609 in muscle cells from antrum, and further confirm the inhibitory regulation of MLCK activity by AMPK.

Figure 13. Expression of MLCK. Total RNA isolated from cultured (first passage) muscle cells from antrum and fundus was reverse transcribed using 2 μg of total RNA. The cDNA was amplified with specific primers for MLCK. The sequences of specific primers are listed in Table 1. Quantitative real-time polymerase chain reaction (qRT-PCR) was used to measure RNA levels of MLCK. For each cDNA sample, real-time PCR was conducted in a 20 μl reaction volume containing TaqMan GeneExpression Master Mix. Real-time PCR reactions were performed in triplicate. Each primer set generated only one PCR product (71 bp), and the identity and integrity of these products were confirmed by electrophoresis in agarose gel in the presence of ethidium bromide and sequencing of the individual bands. Relative quantification of a target gene in relation to reference gene was calculated on the basis of delta delta CT values. Results demonstrated that mRNA levels of MLCK are higher in antrum compared to fundus. Inset: Representative western blot results of MLCK expression. Cell lysates containing equal amounts of total proteins were separated with SDS-PAGE and expression of MLCK was analyzed using selective antibody for MLCK. Membranes were reblotted to measure β-actin. Protein bands were visualized with enhanced chemiluminescence, images were quantified and densitometric values were calculated after normalization to β-actin density. Results are expressed as fold increase over the expression of MLCK in fundus. Values represent the means ±SEM of 3 separate experiments. *$p<0.05$ versus fundus.

Figure 13

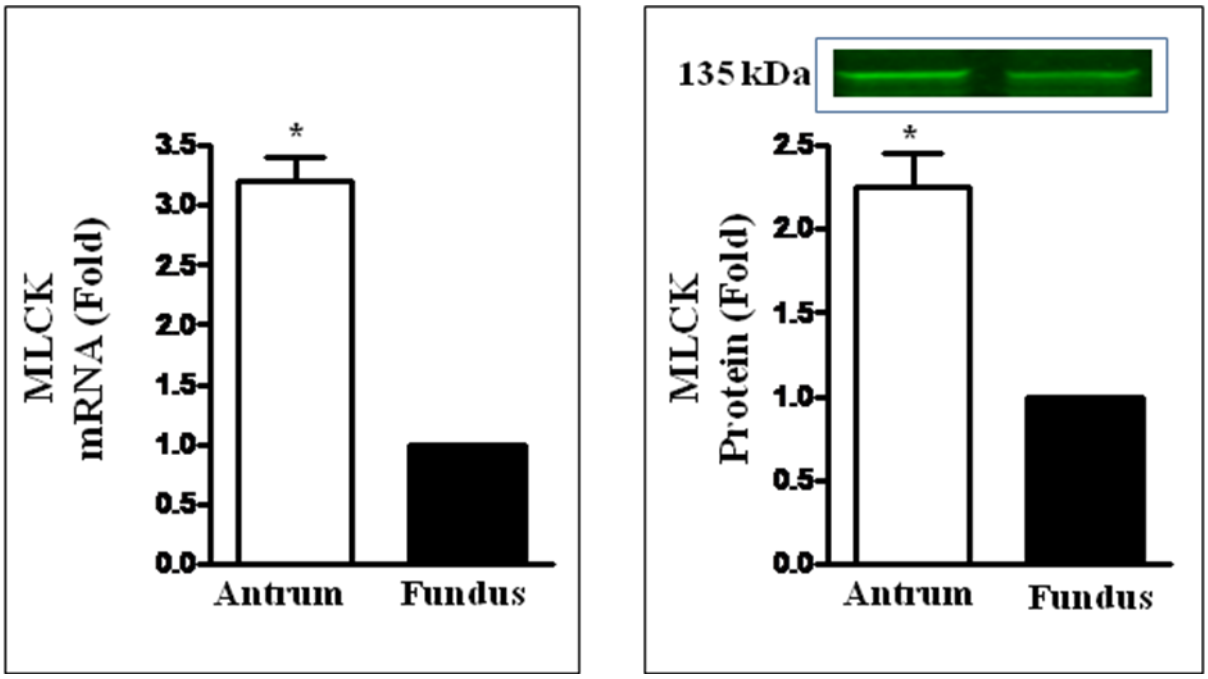
MLCK mRNA (Fold)
3.5
3.0
2.5
2.0
1.5
1.0
0.5
0.0
*
Antrum
Fundus
135 kDa
MLCK Protein (Fold)
2.5
2.0
1.5
1.0
0.5
0.0
*
Antrum
Fundus

Figure 14. Stimulation of MLCK activity by ACh and sensitivity to CAMKKβ antagonist. One milliliter of cell suspension (2 x 10^6 cells/ml) freshly dispersed muscle cells from antrum and fundus were treated with ACh (0.1 μM) for 30 s in the presence or absence of STO609 (1 μM), a selective inhibitor of CaMKKβ/AMPK pathway. The cells were homogenized in the lysis buffer and the protein content in the supernatants was measured. MLCK was immunoprecipitated from lysates containing equal amount of protein and the activity was measured in immunoprecipitates using MLC_{20} as substrate and [^{32}P] ATP. The amount of radioactivity absorbed onto phosphocellulose disks reflecting kinase activity was measured by liquid scintillation and the results are expressed as counts per milligram protein per minute. ACh stimulated MLCK activity in antrum and fundus. Stimulation of MLCK activity was augmented in antrum by pretreatment of cells with STO609, suggesting feedback inhibition of MLCK activity selectively in antrum. Values represent the means ±SEM of 4-5 separate experiments. **$p<0.001$ significant increase in activity above basal level induced by ACh; ##$p<0.05$ significant augmentation of ACh-stimulated MLCK activity by STO609.

Figure 14

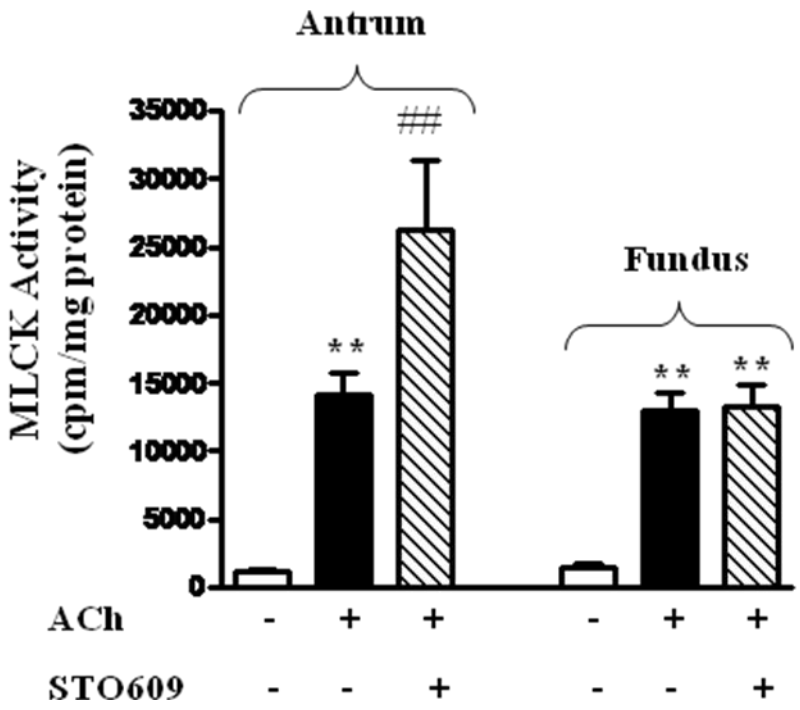
Antrum
Fundus
MLCK Activity
(cpm/mg protein)
35000
30000
25000
20000
15000
10000
5000
0
##
**
**
**
ACh
STO609
- + + - + +
- - + - - +

Figure 15. Phosphorylation of MLCK by ACh. Ten milliliter of cell suspension (2 x 10^6 cells/ml) of freshly dispersed muscle cells from antrum and fundus were labeled with ^{32}P and the cells were incubated with ACh for 30s. MLCK was immunoprecipitated from the cell lysates containing equal amount of protein, extracted with Laemmeli buffer and separated by electrophoresis on SDS-PAGE. Phosphorylated MLCK was visualized by autoradiography, and the amount of radioactivity in the protein band was measured. The results are expressed as counts per milligram protein per minute. Values represent the means ±SEM of 3 separate experiments. **$p<0.001$ significant increase in phosphorylation above basal level induced by ACh.

Figure 15

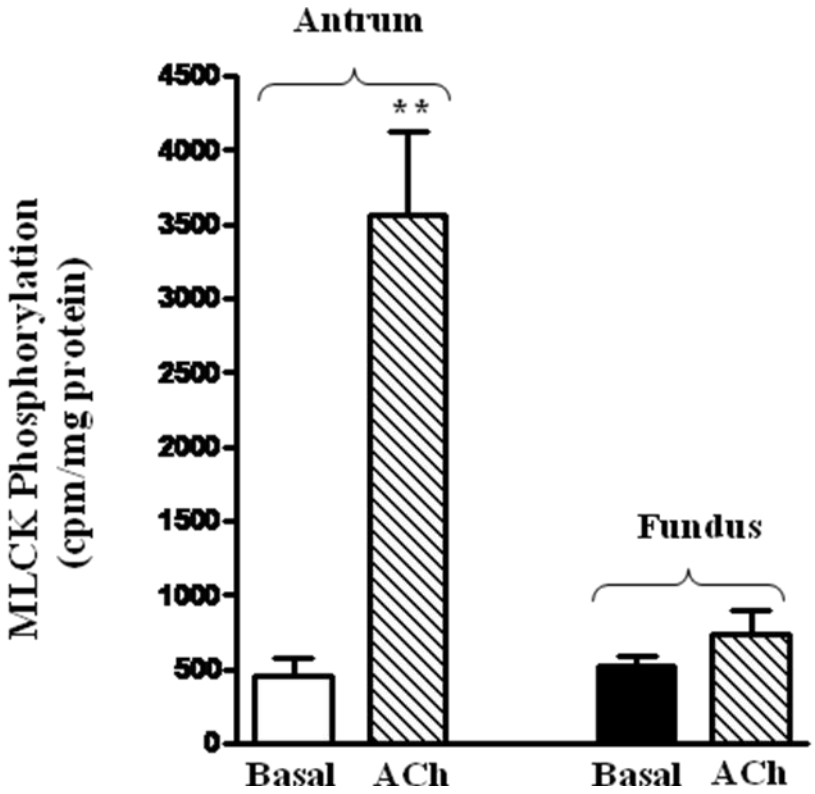
Antrum
MLCK Phosphorylation
(cpm/mg protein)
4500
4000
3500
3000
2500
2000
1500
1000
500
0
**
Fundus
Basal
ACh
Basal
ACh

Figure 16. Effect of STO609 on ACh-induced muscle contraction. Contraction of dispersed muscle cells from antrum and fundus was measured by scanning micrometry in response to different concentrations of ACh in the presence or absence of STO609 (10 μM). Cells were treated with ACh for 30s and pretreated with STO609 for 10 min. Contraction was expressed as percent decrease in cell length from control cell length: control length of muscle cells from antrum 95±3 μm; control length of muscle cells from fundus 102±5 μm. ACh caused contraction that was concentration-dependent in both antrum and fundus and the maximal response to 0.1 μM of ACh was similar in antrum and fundus (27±2% decrease in cell length in antrum and 28±3% decrease in cell length in fundus). STO609 significantly augmented ACh-induced contraction in muscle cells from antrum, but had no effect on contraction in fundus. Values represent the means ±SEM of 4 separate experiments. *$p<0.05$ significant increase in contraction by STO609.

Figure 16

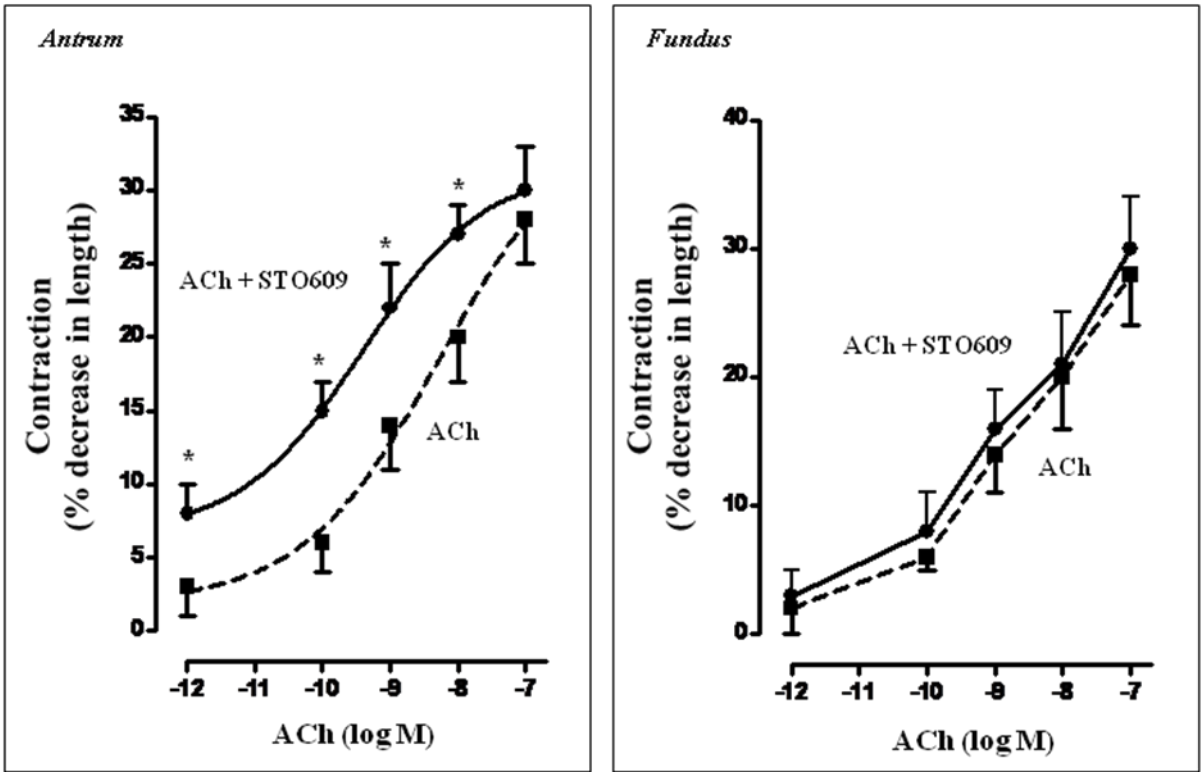
Antrum
Contraction
(% decrease in length)
ACh + STO609
ACh
ACh (log M)
Fundus
Contraction
(% decrease in length)
ACh + STO609
ACh
ACh (log M)

CHPATER 5

DIFFERENTIAL REGULATION OF MLCP ACTIVITY AND SUSTAINED MUSCLE CONTRACTION IN ANTRUM AND FUNDUS

In smooth muscle, inhibition of MLCP activity and sustained MLC_{20} phosphorylation by contractile agonists reflect activation of RhoA via $G\alpha_{13}$ and/or $G\alpha_q$. The pathways that lead to inhibition of MLCP involve phosphorylation of the regulatory subunit of MLCP (MYPT1) via Rho kinase and phosphorylation of CPI-17, an endogenous inhibitor of MLCP, via PKC. A role for ZIPK has also been suggested in the phosphorylation of MYPT1. *We postulated that the higher expression and/or activation of Rho kinase/MYPT1 and PKC/CPI-17 pathways leading to sustained MLC_{20} phosphorylaiton could contribute to the tonic phenotype of fundus.*

5.1 Rho kinase expression and activity

Expression of Rho kinase, by both qRT-PCR and western blot, and stimulation of Rho kinase activity in response to ACh (0.1μM) were determined in muscle cells from antrum and fundus. Rho kinase mRNA was expressed in both antrum and fundus and the expression was 3-fold ($p<0.05$, $n=3$) greater in fundus compared to antrum (Figure 17). Rho kinase protein

expression was examined in the two regions of the stomach by western blot using selective antibody to Rho kinase II, the smooth muscle predominant isoform [32]. Results confirmed the expression of Rho kinase of predicted size (150 kDa) in the homogenates of smooth muscle cells from both antrum and fundus. Comparing the densities of protein bands in the two regions revealed higher expression of Rho kinase in fundus compared to antrum ($p<0.001$, $n=4$) and this is consistent with higher expression of Rho kinase mRNA in fundus compared to antrum (Figure 17).

To determine whether Rho kinase activity level correlates well with its expression profile and thus with the contractile phenotypes in the fundus vs. antrum, freshly dispersed smooth muscle cells from both parts of the stomach were treated with 0.1μM ACh, a $G\alpha q/_{13}$-coupled receptor agonist, for 10 min, and basal and agonist-stimulated Rho kinase activity was measured by immunokinase assay using recombinant myelin basic protein as substrate. Although, the expression levels are different, basal Rho kinase activity was not significantly different in antrum (3242±367 cpm/mg protein) and fundus (4364±503 cpm/mg protein). Treatment of freshly dispersed muscle cells with ACh significantly increased Rho kinase activity in antrum (238±15% increase; 7730±821 cpm/mg protein above basal level, $p<0.001$, $n=5$) and fundus (362±21% increase; 15820±1423 cpm/mg protein above basal level, $p<0.001$, $n=5$) (Figure 18). Consistent with the greater expression of Rho kinase in fundus, agonist-stimulated Rho kinase activity was significantly higher in fundus compared to antrum. Y27632, a selective blocker of Rho kinase, significantly inhibited stimulation of Rho kinase activity in both antrum (90±4% inhibition, $p<0.001$, $n=5$) fundus (96±5 % inhibition, $p<0.001$, $n=5$) (Figure 18).

Figure 17. Expression of Rho kinase II. Total RNA isolated from cultured (first passage) muscle cells from antrum and fundus was reverse transcribed using 2 μg of total RNA. The cDNA was amplified with specific primers for Rho kinase II. The sequences of specific primers are listed in Table 1. Quantitative real-time polymerase chain reaction (qRT-PCR) was used to measure RNA levels of Rho kinase II. For each cDNA sample, real-time PCR was conducted in a 20 μl reaction volume containing Quantitect™ SYBRgreen PCR Mastermix. Real-time PCR reactions were performed in triplicate. Each primer set generated only one PCR product (64 bp), and the identity and integrity of these products were confirmed by electrophoresis in agarose gel in the presence of ethidium bromide and sequencing of the individual bands. Standard curves for each amplicon were generated from a dilution series of cDNA and results were quantified and reported using the $2^{-\Delta\Delta C_T}$ method based on GAPDH amplification. Relative quantification of a target gene in relation to reference gene was calculated on the basis of delta delta CT values. Results demonstrated that mRNA levels of Rho kinase II are higher in fundus compared to antrum. Inset: Representative western blot results of Rho kinaseII expression. Cell lysates containing equal amounts of total proteins were separated with SDS-PAGE and expression of Rho kinase II was analyzed using selective antibody for Rho kinase II. Membranes were reblotted to measure β-actin. Protein bands visualized with enhanced chemiluminescence, images were quantified and densitometric values were calculated after normalization to β-actin density. Results are expressed as fold increase over the expression of Rho kinase II in antrum. Values represent the means ±SEM of 3 separate experiments. **$p<0.001$ versus antrum.

Figure 17

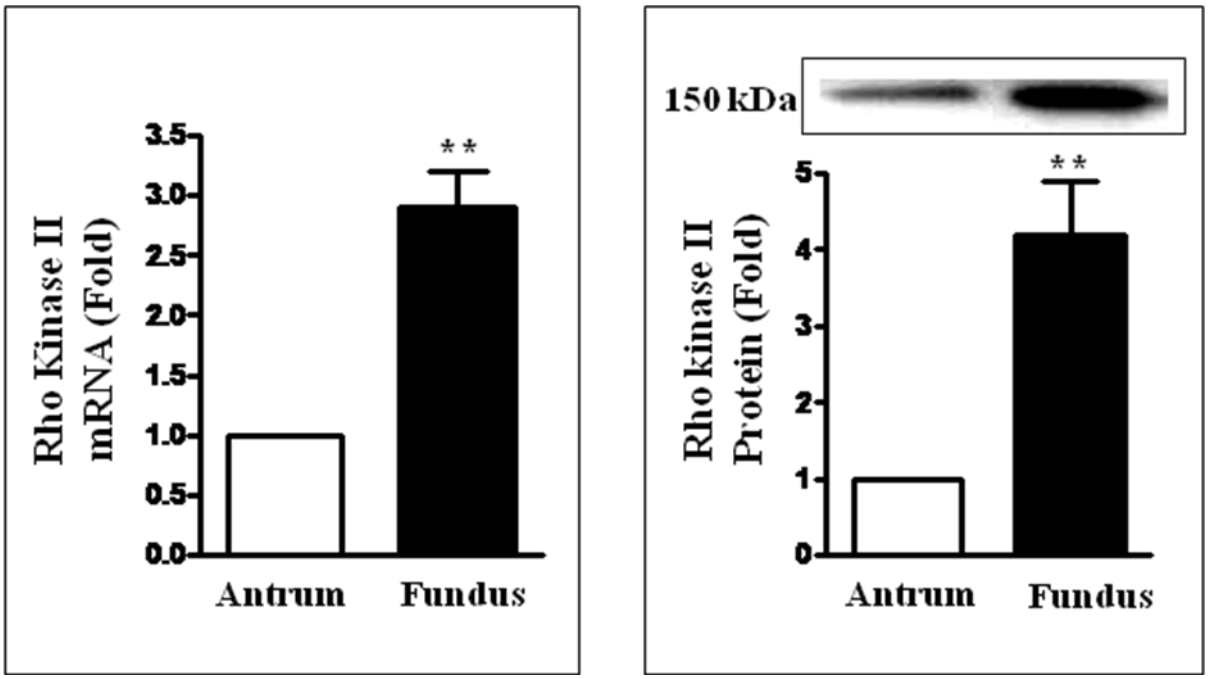
Rho Kinase II
mRNA (Fold)
3.5
3.0
2.5
2.0
1.5
1.0
0.5
0.0
**
Antrum
Fundus
150 kDa
Rho kinase II
Protein (Fold)
5
4
3
2
1
0
**
Antrum
Fundus

Figure 18. Stimulation of Rho kinase activity by ACh. One milliliter of cell suspension (2x 10^6 cells/ml) of freshly dispersed muscle cells from antrum and fundus was treated with ACh (0.1 μM) for 10 min in the presence or absence of Y27632 (1 μM), a selective inhibitor of Rho kinase. The cells were homogenized in the lysis buffer and the protein content in the supernatants was measured. Rho kinase II was immunoprecipitated from lysates containing equal amount of protein and the activity was measured in immunoprecipitates using purified recombinant myelin basic protein as substrate and [^{32}P]ATP. The amount of radioactivity absorbed onto phosphocellulose disks reflecting kinase activity was by measured by liquid scintillation and the results are expressed as counts per milligram protein per minute. ACh stimulated Rho kinase II activity in antrum and fundus and the stimulation was higher in fundus compared to antrum. Y27632 blocked stimulation of Rho kinase activity in both antrum and fundus. Values represent the means ±SEM of 5-6 separate experiments. **$p<0.001$ significant increase in activity above basal level induced by ACh; ##$p<0.05$ significant increase in activity in fundus versus increase in antrum

Figure 18

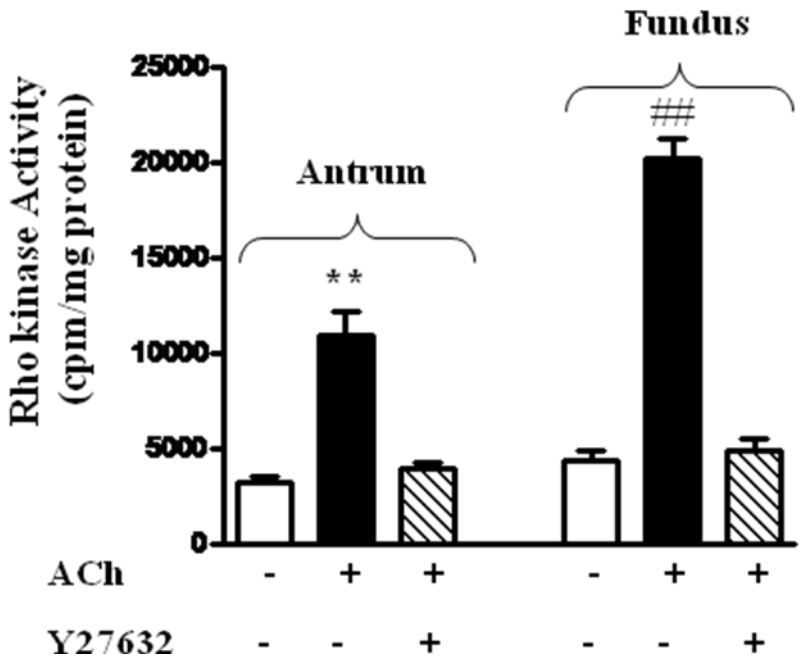
Fundus
Antrum
Rho kinase Activity
(cpm/mg protein)
25000
20000
15000
10000
5000
0
**
##
ACh
Y27632
- + + - + +
- - + - - +

5.2 ZIPK expression and activity

Zipper interacting protein kinase (ZIPK) was also shown to inhibit MLCP activity via phosphorylation of MYPT1 at Thr^{696}. So, it is of interest to reveal any differential expression and activity of this kinase in antrum versus fundus. Expression of ZIPK, by both qRT-PCR and western blot, and stimulation of ZIPK activity in response to ACh (0.1μM) were determined in muscle cells from antrum and fundus. ZIPK mRNA was expressed in both antrum and fundus, and the expression was not significantly different between fundus and antrum (Figure 19). ZIPK kinase protein expression was examined in the two regions of the stomach by western blot analysis using selective antibody to ZIPK. Results confirmed the expression of ZIPK of expected size (52 kDa) in the homogenates of smooth muscle cells from both antrum and fundus. Comparing the densities of protein bands in the two regions revealed no significant difference of ZIPK expression between fundus and antrum (figure 19).

ZIPK activity was measured by immunokinase assay using recombinant myelin basic protein as substrate. Basal ZIPK activity was not significantly different in antrum (3106±308 cpm/mg protein) and fundus (4107±372 cpm/mg protein). Treatment of freshly dispersed muscle cells with ACh (0.1 μM) significantly increased ZIPK activity in antrum (205±11% increase; 6375±438 cpm/mg protein above basal level, $p<0.001$, n=5) and fundus (441±8% increase; 22257±1980 cpm/mg protein above basal level, p0.001, n=5) (Figure 20). Consistent with the greater expression and activation of Rho kinase in fundus, ACh-stimulated ZIPK activity was significantly higher in fundus compared to antrum. ACh stimulated ZIPK activity was blocked by pretreatment of cells with Y27632 (1 μM), a selective Rho kinase inhibitor, in antrum (84±5% inhibition) and fundus (95±5% inhibition) (Figure 20). These results suggest that ZIPK is a downstream target of Rho kinase.

Figure 19. Expression of zipper interacting protein kinase. Total RNA isolated from cultured (first passage) muscle cells from antrum and fundus was reverse transcribed using 2 μg of total RNA. The cDNA was amplified with specific primers for ZIPK. The sequences of specific primers are listed in Table 1. Quantitative real-time polymerase chain reaction (qRT-PCR) was used to measure RNA levels of ZIPK. For each cDNA sample, real-time PCR was conducted in a 20 μl reaction volume containing Quantitect™ SYBRgreen PCR Mastermix. Real-time PCR reactions were performed in triplicate. Each primer set generated only one PCR product (64 bp), and the identity and integrity of these products were confirmed by electrophoresis in agarose gel in the presence of ethidium bromide and sequencing of the individual bands. Standard curves for each amplicon were generated from a dilution series of cDNA and results were quantified and reported using the $2^{-\Delta\Delta C_T}$ method based on GAPDH amplification. Relative quantification of a target gene in relation to reference gene was calculated on the basis of delta delta CT values. Results demonstrated that mRNA levels of ZIPK are not significantly different between fundus and antrum. Inset: Representative western blot results of ZIPK expression. Cell lysates containing equal amounts of total proteins were separated with SDS-PAGE and expression of ZIPK was analyzed using selective antibody for ZIPK. Membranes were reblotted to measure β-actin. Protein bands were visualized with enhanced chemiluminescence, images were quantified and densitometric values were calculated after normalization to β-actin density. Results are expressed as fold increase over the expression of ZIPK in antrum. Values represent the means ±SEM of 3 separate experiments.

Figure 19

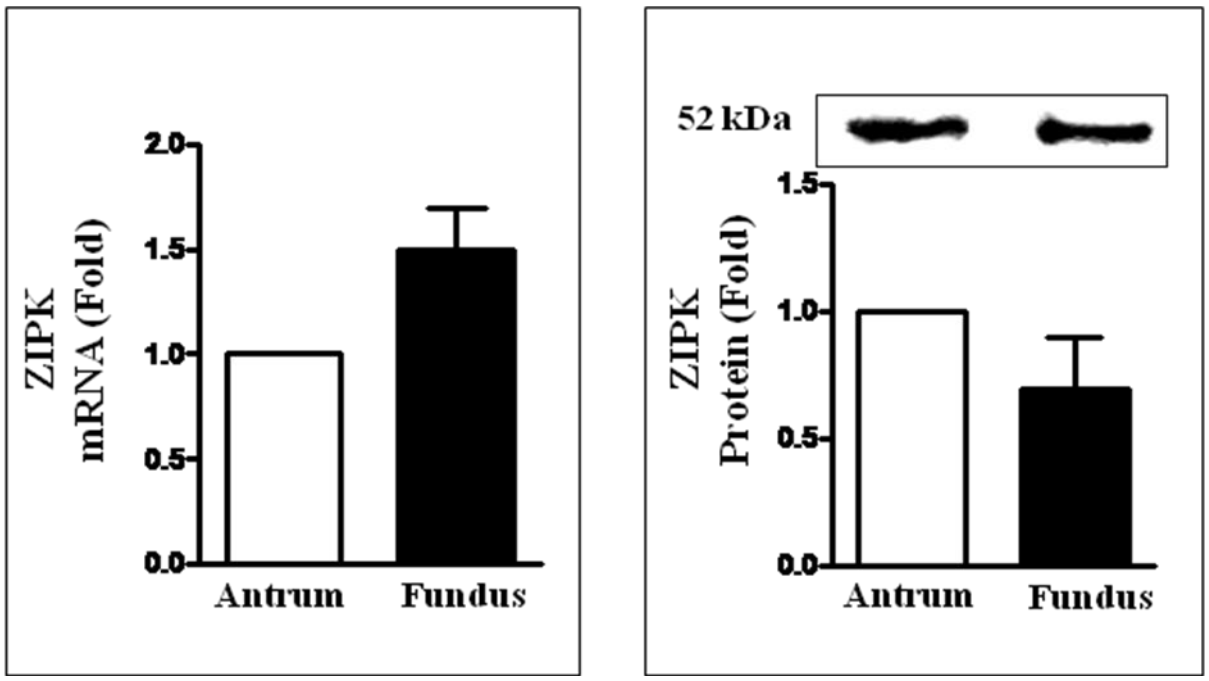
ZIPK
mRNA (Fold)
2.0
1.5
1.0
0.5
0.0
Antrum
Fundus
52 kDa
ZIPK
Protein (Fold)
1.5
1.0
0.5
0.0
Antrum
Fundus

Figure 20. Stimulation of ZIPK by ACh and sensitivity to the Rho kinase inhibitor, Y27632. One milliliter of cell suspension (2x 10^6 cells/ml) of freshly dispersed muscle cells from antrum and fundus was treated with ACh (0.1 μM) for 10 min in the presence or absence of Y27632 (1 μM), a selective inhibitor of Rho kinase. The cells were homogenized in the lysis buffer and the protein content in the supernatants was measured. ZIPK was immunoprecipitated from lysates containing equal amount of protein and the activity was measured in immunoprecipitates using purified recombinant myelin basic protein as substrate and [^{32}P]ATP. The amount of radioactivity absorbed onto phosphocellulose disks reflecting kinase activity was measured by liquid scintillation and the results are expressed as counts per milligram protein per minute. ACh stimulated ZIPK activity in antrum and fundus and the stimulation was higher in fundus compared to antrum. Y27632 blocked stimulation of ZIPK activity in both antrum and fundus. Values represent the means ±SEM of 5-6 separate experiments. **$p<0.001$ significant increase in activity above basal level induced by ACh; ##$p<0.05$ significant increase in activity in fundus versus increase in antrum

Figure 20

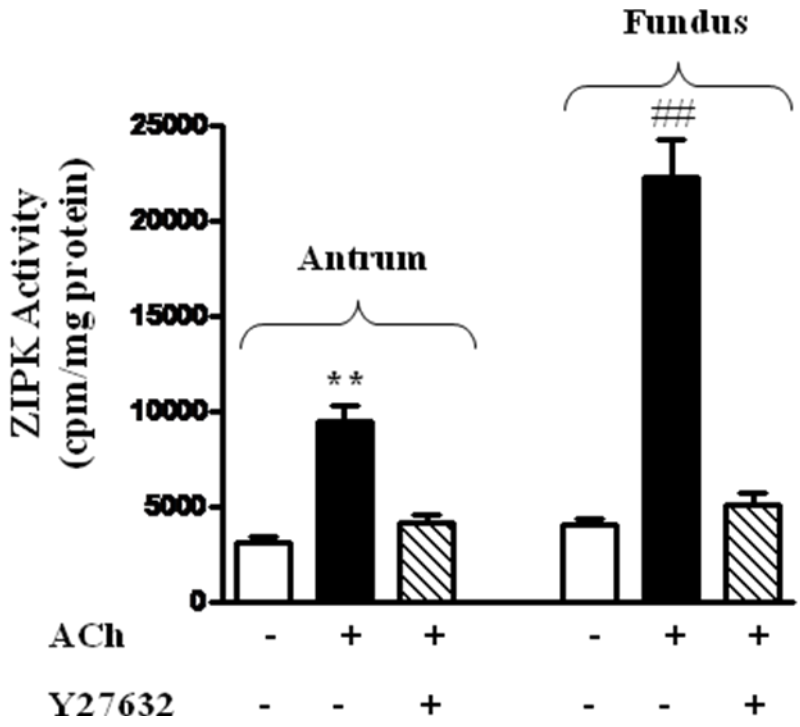
Fundus
##
Antrum
**
ZIPK Activity
(cpm/mg protein)
25000
20000
15000
10000
5000
0
ACh - + + - + +
Y27632 - - + - - +

5.3 Sustained contraction

To examine the involvement of Rho kinase/ZIPK pathway in the regulation of muscle contraction, muscle cells from antrum and fundus were treated with different concentrations of ACh and contractile response at 10 min was measured by scanning micrometry. Previous studies in gastrointestinal smooth muscle have demonstrated that the contractile response at 10 min reflects activation of Rho kinase- and PKC-dependent inhibition of MLCP. Treatment of cells with ACh for 10 min caused contraction that was concentration-dependent with an EC50 of 1.1 ± 0.3 nM in antrum and 0.7±0.03 nM in fundus. The maximal response was significantly greater in muscle cells from fundus (26±2 % decrease in cell length) compared to muscle cells from antrum (18±2% decrease in cell length) (figure 21).

5.4 CPI-17 Expression

As described earlier, sustained MLC_{20} phosphorylation and muscle contraction are mediated by inhibition of MLCP via Rho kinase/MTPT1 and PKC/CPI-17 pathways. Expression of CPI-17, by both qRT-PCR and western blot was determined in muscle cells from antrum and fundus. CPI-17 mRNA was expressed in antrum and fundus and the expression was nearly 4-fold higher in fundus compared to antrum (figure 22). CPI-17 protein expression was examined in the two regions of the stomach by western blot using selective antibody to CPI-17. Results confirmed the expression of CPI-17 of expected size (17 kDa) in the homogenates of smooth muscle cells from both antrum and fundus (Figure 22). Comparing the densities of protein bands in the two regions revealed 4-fold ($p<0.05$) higher expression of CPI-17 in fundus compared to antrum and this is consistent with higher expression of CPI-17 mRNA in fundus compared to antrum.

5.5 PMA-stimulated PKC activity and smooth muscle contraction

Since contractile agonists stimulate both Rho kinase and PKC activities, the singular contribution of PKC/CPI-17 pathway in mediating MLCP inhibition and sustained contraction was examined using phorbol 12-myristate 13-acetate (PMA), a selective activator of PKC. Treatment of cells with PMA caused contraction that was concentration-dependent with an EC50 of 35±5 nM in antrum and 3±2 nM in fundus. The maximal contractile response was significantly greater in muscle cells from fundus (29±2% decrease in cell length) compared to muscle cells from antrum (17±3% decrease in cell length) (figure 23A). However, stimulation of PKC activity in response to PMA was similar in antrum (3245±504 cpm/mg protein above the basal level of 523±102 cpm/mg protein) and fundus (3612±302 cpm/mg protein above the basal level 675±129 cpm/mg protein) (Figure 23B). These results suggest that greater contraction in fundus is not due difference in the PKC activity, but probably due to higher expression of CPI-17 and CPI-17-mediated inhibition of MLCP activity.

Figure 21. ACh-induced sustained muscle contraction. Contraction of dispersed muscle cells from antrum and fundus in response to different concentrations of ACh was measured by scanning micrometry. Cells were treated with ACh (0.1 μM) for 10 min and cntraction was expressed as percent decrease in cell length from control cell length: control length of muscle cells from antrum 95±3 μm; control length of muscle cells from fundus 102±5 μm. ACh caused contraction that was concentration-dependent in both antrum and fundus and the contraction was greater in fundus compared to antrum. The maximal response to 0.1 μM ACh was significantly greater in muscle cells from fundus (26±2 % decrease in cell length) compared to muscle cells from antrum (18±2% decrease in cell length). Values represent the means ±SEM of 4 separate experiments. *$p<0.05$ significant increase in contraction in fundus versus contraction in antrum.

Figure 21

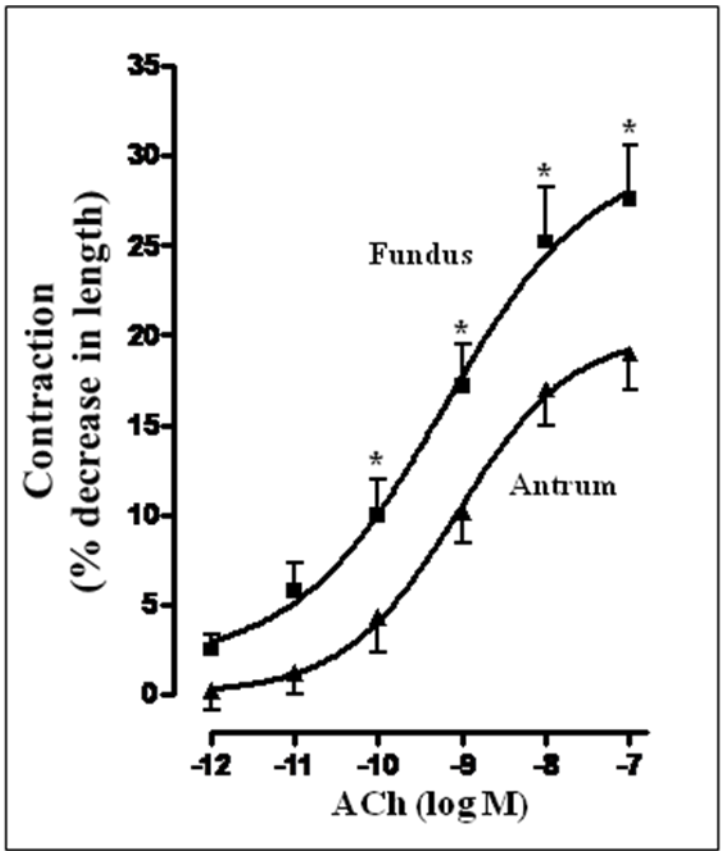
Contraction
(% decrease in length)
35
30
25
20
15
10
5
0
Fundus
Antrum
*
*
*
*
-12
-11
-10
-9
-8
-7
ACh (log M)

Figure 22. Expression of CPI-17. Total RNA isolated from cultured (first passage) muscle cells from antrum and fundus was reverse transcribed using 2 μg of total RNA. The cDNA was amplified with specific primers for CPI-17. The sequences of specific primers are listed in Table 1. Quantitative real-time polymerase chain reaction (qRT-PCR) was used to measure RNA levels of CPI-17. For each cDNA sample, real-time PCR was conducted in a 20 μl reaction volume containing Quantitect™ SYBRgreen PCR Mastermix. Real-time PCR reactions were performed in triplicate. Each primer set generated only one PCR product (116 bp), and the identity and integrity of these products were confirmed by electrophoresis in agarose gel in the presence of ethidium bromide and sequencing of the individual bands. Standard curves for each amplicon were generated from a dilution series of cDNA and results were quantified and reported using the $2^{-\Delta\Delta C_T}$ method based on GAPDH amplification. Relative quantification of a target gene in relation to reference gene was calculated on the basis of delta delta CT values. Results demonstrated that mRNA levels of CPI-17 are significantly higher in fundus compared to antrum. Inset: Representative western blot results of CPI-17 expression. Cell lysates containing equal amounts of total proteins were separated with SDS-PAGE and expression of CPI-17 was analyzed using selective antibody for CPI-17. Membranes were reblotted to measure β-actin. Protein bands visualized with enhanced chemiluminescence, images were quantified and densitometric values were calculated after normalization to β-actin density. Results are expressed as fold increase over the expression of CPI-17 in antrum. Values represent the means ±SEM of 3 separate experiments. **$p<0.05$ versus antrum.

Figure 22

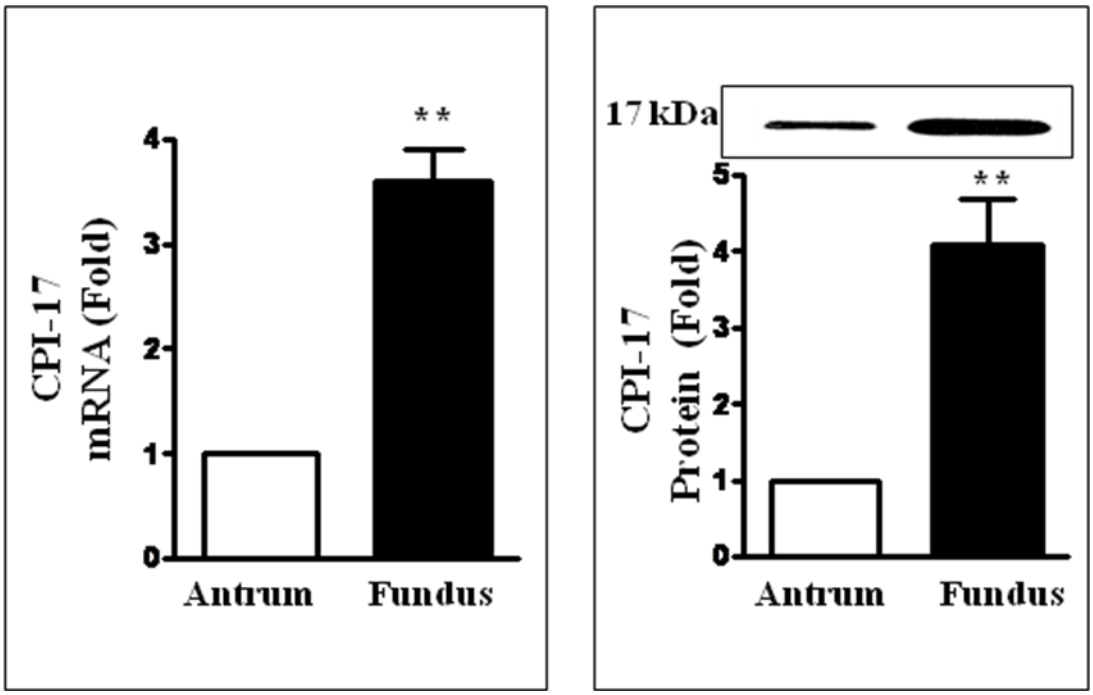
CPI-17
mRNA (Fold)
**
4
3
2
1
0
Antrum
Fundus
17 kDa
CPI-17
Protein (Fold)
**
5
4
3
2
1
0
Antrum
Fundus

Figure 23. PMA-induced sustained muscle contraction and PKC activity. A. Contraction of dispersed muscle cells from antrum and fundus in response to different concentrations of phorbol 12-myristate 13-acetate (PMA) was measured by scanning micrometry. Contraction was expressed as percent decrease in cell length from control cell length: control length of muscle cells from antrum 95±3 μm; control length of muscle cells from fundus 102±5 μm. PMA caused contraction that was concentration-dependent in both antrum and fundus and the contraction was greater in fundus compared to antrum. The maximal response to 1 μM PMA was significantly greater in muscle cells from fundus (29±2 % decrease in cell length) compared to muscle cells from antrum (17±2% decrease in cell length). Values represent the means ±SEM of 4 separate experiments. *$p<0.05$ significant increase in contraction in fundus versus contraction in antrum. **B.** One milliliter of cell suspension (2x 10^6 cells/ml) of freshly dispersed muscle cells from antrum and fundus was treated with PMA (1 μM) for 10 min. The cells were homogenized in the lysis buffer and the protein content in the supernatants was measured. PKC was immunoprecipitated from lysates containing equal amount of protein with a PKC antibody and the activity was measured in immunoprecipitates using purified recombinant myelin basic protein as substrate and [^{32}P]ATP. The amount of radioactivity absorbed onto phosphocellulose disks reflecting kinase activity was by measured by liquid scintillation and the results are expressed as counts per milligram protein per minute above basal levels of 523±102 cpm/mg protein in antrum and 675±129 cpm/mg protein in fundus. PMA stimulated PKC activity was similar in antrum and fundus. Values represent the means ±SEM of 4 separate experiments.

Figure 23

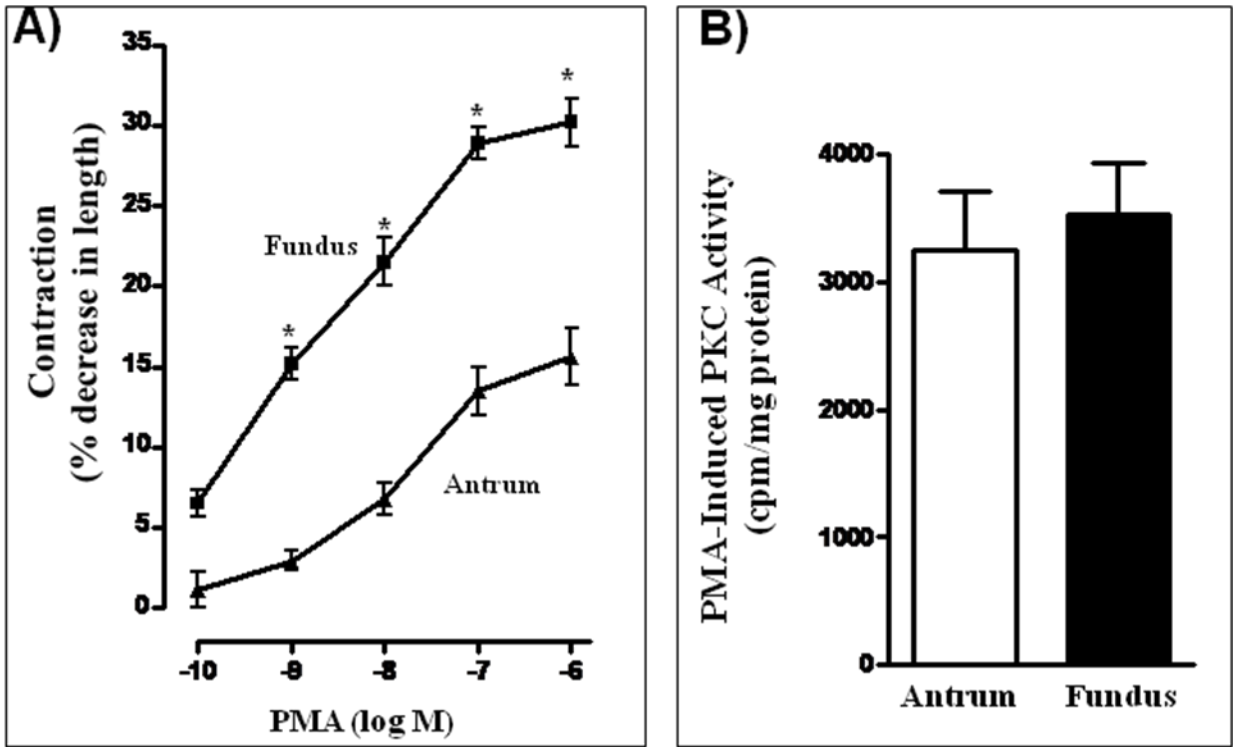
A)
Contraction
(% decrease in length)
35
30
25
20
15
10
5
0
Fundus
Antrum
*
*
*
*
-10
-9
-8
-7
-6
PMA (log M)
B)
PMA-Induced PKC Activity
(cpm/mg protein)
4000
3000
2000
1000
0
Antrum
Fundus

CHAPTER 6

DIFFERENTIAL REGULATION OF MLCP ACTIVITY AND MUSCLE RELAXATION IN ANTRUM AND FUNDUS

In gastrointestinal smooth muscle two endogenous proteins regulate MLCP activity: a 17 kDa inhibitor (CPI-17) and a 17 kDa activator, telokin, also known as kinase-related protein. Telokin is a smooth muscle specific protein and is identical to the C-terminus of MLCK downstream from the kinase and calmodulin binding domains. *We postulated that the higher expression of telokin, and activation MLCP leading to MLC_{20} dephosphorylation could contribute to rapid relaxation and phasic phenotype of antrum.*

6.1 Telokin Expression

Expression of telokin by both qRT-PCR and western blot was determined in muscle cells from antrum and fundus. Telokin mRNA was expressed in both antrum and fundus and the expression was 6-fold higher in antrum compared to fundus (figure 24). Telokin protein expression was examined in the two regions of the stomach by western blot using selective antibody to telokin. Results confirmed the expression of telokin of expected size (17 kDa) in the homogenates of smooth muscle cells from both antrum and fundus (Figure 24). Comparing the

densities of protein bands in the two regions revealed 5-fold higher expression of telokin in antrum compared to fundus and this is consistent with higher expression of telokin mRNA in antrum compared to fundus.

6.2 8-Br-cGMP-stimulated PKG activity and smooth muscle relaxation

Since the relaxant effect of cGMP/PKG pathway on agonist-mediated (e.g., ACh) contraction involves both inhibition of intracellular Ca^{2+} and activation of MLCP, relaxation was measured as inhibition of maximal contraction in response to 0.5 μM Ca^{2+}. Under these experimental conditions, the effect of cGMP/PKG on Ca^{2+} is precluded and reflects stimulation of MLCP activity, probably via telokin. Since termination of cGMP/PKG signaling is different in antrum and fundus and depends on the expression of PDE5 (see next chapter), 8-Br-cGMP, a non-hydrolyzable analog of cGMP, was used to induce muscle relaxation. Treatment of permeabilized muscle cells with 0.5 μM Ca^{2+} caused contraction that was similar in muscle cells from antrum (24±3% decrease in cell length from a basal cell length of 85±3 μm) and fundus (26±2% decrease in cell length from a basal cell length of 92±4 μm). Pretreatment of cells with 8-Br-cGMP (1mM) caused relaxation (i.e., inhibition of contraction) that was concentration-dependent (EC_{50}: antrum, 8±3 μM; fundus, 12±4). Relaxation was significantly higher in antrum compared to fundus at all concentrations of 8-Br-cGMP. The maximal response was significantly greater in muscle cells from antrum (76±4% relaxation) compared to muscle cells from fundus (47±3% relaxation) (figure 25 A). However, stimulation of PKG activity in response to 8-Br-cGMP was similar in antrum (-GMP/+cGMP activity ratio, 2.4±0.4) and fundus (-cGMP/+cGMP activity ratio, 2.2±0.3) suggesting that lower relaxation in fundus was not due to cGMP

degradation via PDE5 or efflux via MRP5, and possibly reflects lower expression of telokin (figure 25 B).

6.3 Telokin-dependent stimulation of MLCP activity

Previous studies have demonstrated that PKG-mediated phosphorylation of telokin at Ser^{13} greatly augments the ability of telokin to stimulate MLCP activity. We tested the role of telokin in cGMP/PKG-mediated relaxation by overexpressing cultured muscle cells with wild type or phosphorylation-deficient telokin (S13A). Relaxation in response to 8-Br-cGMP was measured as decrease in Ca^{2+} (0.5 μM)-induced MLC_{20} phosphorylation. Treatment of cells, containing either wild type or telokin S13A mutant with 0.5 μM Ca^{2+} for 1 minute significantly augmented phosphorylation of MLC_{20} at Ser^{19}. The extent of phosphorylation was similar in both antrum and fundus and consistent with similar levels of contraction as described above. Pretreatment of cells with 8-Br-cGMP inhibited MLC_{20} phosphorylation in both fundus (48±5% inhibition) and antrum (78±6% inhibition) suggesting dephosphorylation of MLC_{20} due to activation of MLCP. The inhibitory effect 8-Br-cGMP was significantly ($p<0.05$, $n=4$) higher in antrum compared to fundus, and reflects higher expression of telokin in antrum compared to fundus (figures 26 and 27).

The inhibitory effect of 8-Br-cGMP on MLC_{20} phosphorylation was significantly attenuated in cells expressing telokin S13A suggesting that the effect of 8-Br-cGMP was due to augmentation of MLCP activity via phosphorylation of telokin at Ser^{13}. Importantly, in the presence of telokin (S13A), the inhibitory effect of 8-Br-cGMP was not significantly different between antrum and fundus (figures 26 and 27). These results provide conclusive evidence for the involvement of telokin in the activation of MLCP and MLC_{20} dephosphorylaiton. Higher

expressions of telokin and MLCP activity in antrum also correlate with the phasic phenotype of this muscle, where rapid contractions and relaxations are needed for optimal organ function.

Figure 24. Expression of telokin. Total RNA isolated from cultured (first passage) muscle cells from antrum and fundus was reverse transcribed using 2 μg of total RNA. The cDNA was amplified with specific primers for telokin. The sequences of specific primers are listed in Table 1. Quantitative real-time polymerase chain reaction (qRT-PCR) was used measure RNA levels of telokin. For each cDNA sample, real-time PCR was conducted in a 20 μl reaction volume containing Quantitect™ SYBRgreen PCR Mastermix. Real-time PCR reactions were performed in triplicate. Each primer set generated only one PCR product (69 bp), and the identity and integrity of these products were confirmed by electrophoresis in agarose gel in the presence of ethidium bromide and sequencing of the individual bands. Standard curves for each amplicon were generated from a dilution series of cDNA and results were quantified and reported using the $2^{-\Delta\Delta CT}$ method based on GAPDH amplification. Relative quantification of a target gene in relation to reference gene was calculated on the basis of delta delta CT values. Results demonstrated that mRNA levels of telokin are significantly higher in antrum compared to fundus Inset: Representative western blot results of telokin expression. Cell lysates containing equal amounts of total proteins were separated with SDS-PAGE and expression of telokin was analyzed using selective antibody for telokin. Membranes were reblotted to measure β-actin. Protein bands were visualized with enhanced chemiluminescence, images were quantified and densitometric values were calculated after normalization to β-actin density. Results are expressed as fold increase over the expression of telokin in fundus. Values represent the means ±SEM of 3 separate experiments. **$p<0.001$ versus fundus.

Figure 24

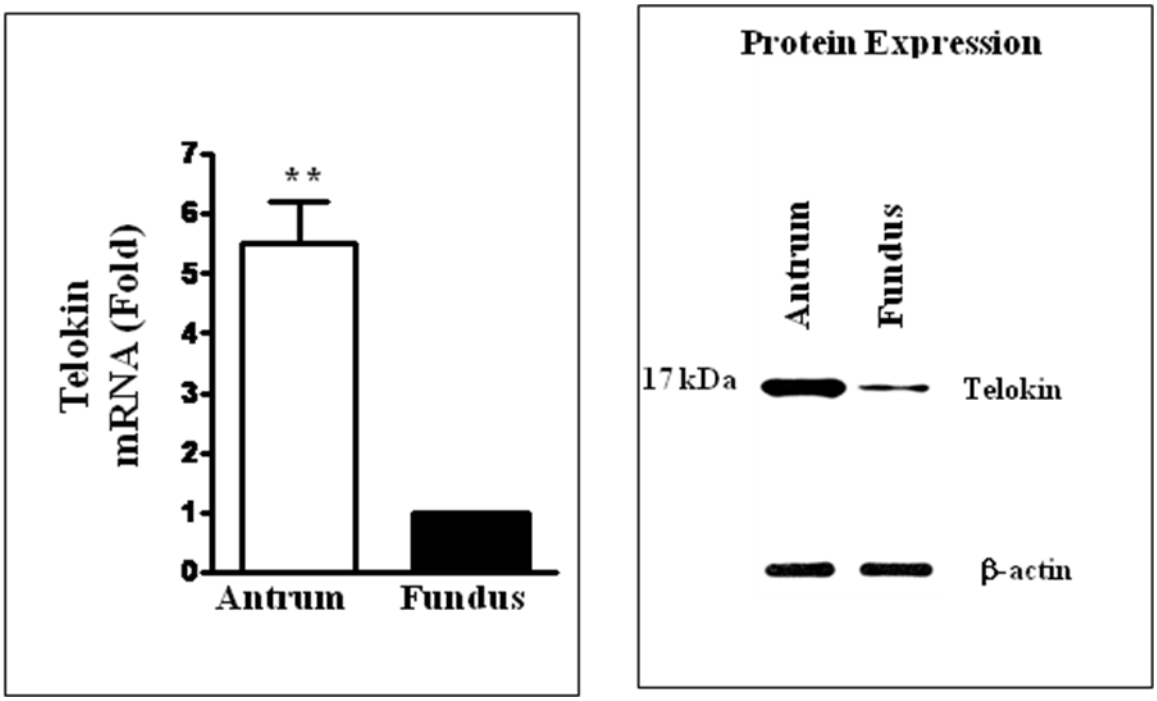
Telokin mRNA (Fold)
7
6
5
4
3
2
1
0
**
Antrum
Fundus
Protein Expression
Antrum
Fundus
17 kDa
Telokin
β-actin

Figure 25. 8-Br-cGMP-induced muscle relaxation and PKG activity. A. Relaxation of dispersed muscle cells from antrum and fundus in response to different concentrations of 8-Br-cGMP was measured by scanning micrometry as decrease in Ca^{2+}-induced contraction. Contraction in response to 0.5 μM Ca^{2+} was measured in permeabilized muscle cells. Contraction was similar in muscle cells from antrum (24±3% decrease in cell length from a basal cell length of 85±3 μm) and fundus (26±2% decrease in cell length from a basal cell length of 92±4 μm). 8-Br-cGMP caused relaxation that was concentration-dependent in both antrum and fundus and the relaxation was greater in antrum compared to fundus. The maximal response to 1 mM 8-Br-cGMP that was significantly greater in antrum (76±4% relaxation) compared to muscle cells from fundus (47±3% relaxation). Values represent the means ±SEM of 4 separate experiments. *$p<0.05$ significant increase in relaxation in antrum versus relaxation in fundus. **B.** One milliliter of cell suspension (2×10^6 cells/ml) of freshly dispersed muscle cells from antrum and fundus was treated with 8-Br-cGMP (1 mM) for 10 min. The cells were homogenized in the lysis buffer and the protein content in the supernatants was measured. PKG activity was measured in the presence or absence of cGMP using a specific substrate RKRSRAE and [^{32}P]ATP, and the results are expressed as the ratio of activity in the absence or presence of cGMP. 8-Br-cGMP-stimulated PKG activity was similar in antrum and fundus. Values represent the means ±SEM of 3 separate experiments.

Figure 25

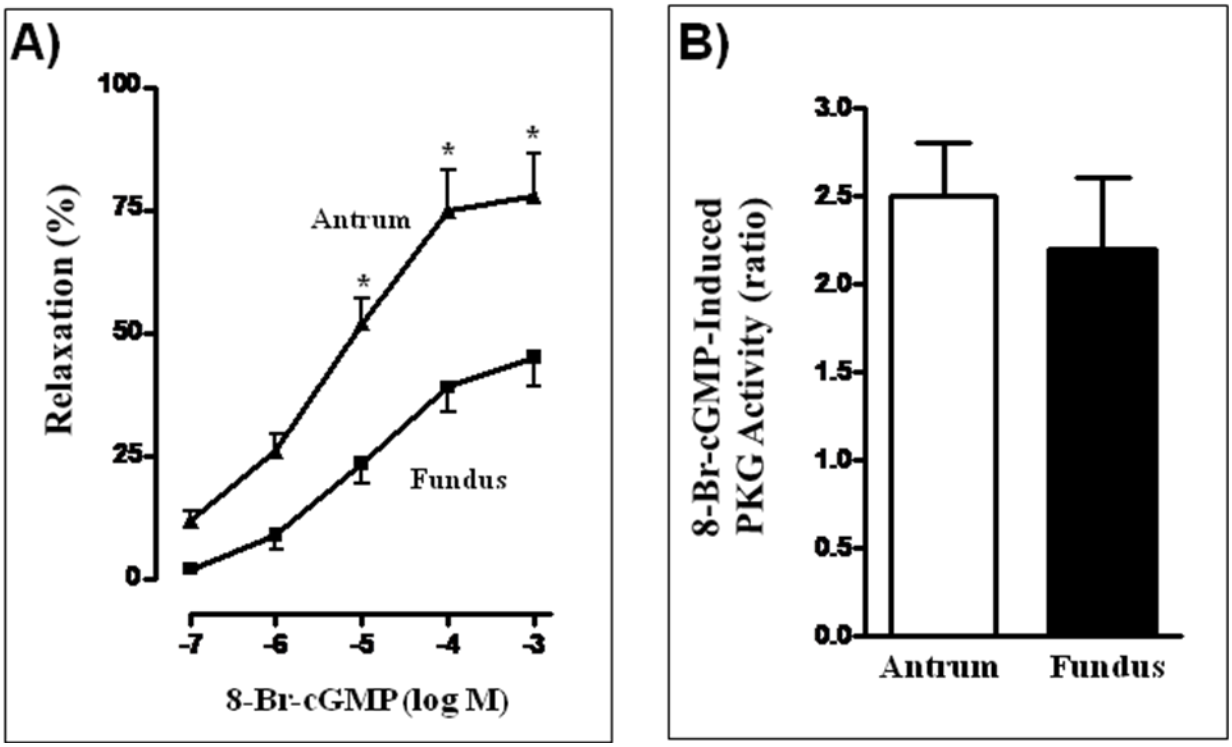
A)
Relaxation (%)
100
75
50
25
0
Antrum
Fundus
*
*
*
-7
-6
-5
-4
-3
8-Br-cGMP (log M)
B)
8-Br-cGMP-Induced
PKG Activity (ratio)
3.0
2.5
2.0
1.5
1.0
0.5
0.0
Antrum
Fundus

Figure 26. Inhibition of Ca^{2+}-induced MLC_{20} phosphorylation by 8-Br-cGMP and the effect of telokin in muscle cells from fundus. Cultured muscle cells from fundus overexpressing wild type telokin or phosphorylation-deficient telokin (telokin S13A) were permeabilized, pretreated with 8-Br-cGMP (1 mM) and then treated with 0.5 µM Ca^{2+}. MLC_{20} phosphorylation was measured in MLC_{20} imunoprecipitates using antibody specific for phospho-Ser^{19} MLC_{20} by immunoblot analysis. Densitometric values were calculated after normalization to MLC_{20} density and the results expressed as percent of control density. Ca^{2+}-induced MLC_{20} phosphorylation was significantly inhibited in cells expressing wild type telokin, but not in cells expressing telokin S13A. Values represent the means ±SEM of 3 separate experiments. **$p<0.001$ significant increase in MLC_{20} phosphorylation by Ca^{2+}, ##$p<0.05$ significant inhibition of Ca^{2+}-induced MLC_{20} phosphorylation by 8-Br-cGMP.

Figure 26

Fundus

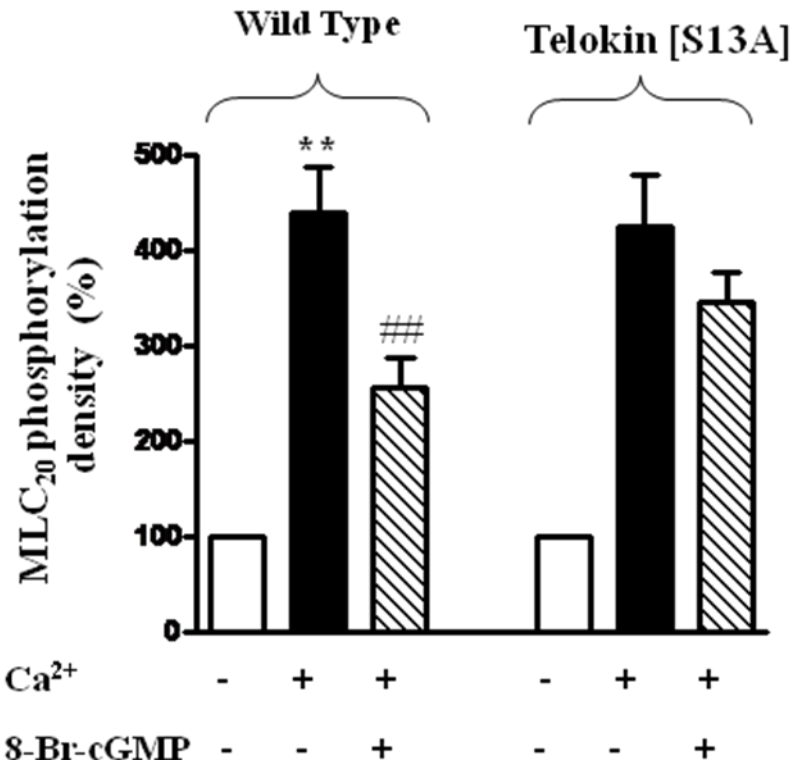

Figure 27. Inhibition of Ca^{2+}-induced MLC_{20} phosphorylation by 8-Br-cGMP and the effect of telokin in muscle cells from antrum. Cultures muscle cells from antrum overexpressing wild type telokin or phosphorylation-deficient telokin (telokin S13A) were permeabilized, pretreated with 8-Br-cGMP (1 mM) and then treated with 0.5 µM Ca^{2+}. MLC_{20} phosphorylation was measured in MLC_{20} imunoprecipitates using antibody specific for phospho-Ser^{19} MLC_{20} by immunoblot analysis. Densitometric values were calculated after normalization to MLC_{20} density and the results expressed as percent of control density. Ca^{2+}-induced MLC_{20} phosphorylation was significantly inhibited in cells expressing wild type telokin, but not in cells expressing telokin S13A. The inhibition of MLC_{20} phosphorylation was significantly greater in antrum (78±6% inhibition) compared to fundus (48±5% inhibition) (compare Figs 26 and 27). Values represent the means ±SEM of 3 separate experiments. **$p<0.001$ significant increase in MLC_{20} phosphorylation by Ca^{2+}, ## $p<0.05$ significant inhibition of Ca^{2+}-induced MLC_{20} phosphorylation by 8-Br-cGMP.

Figure 27

Antrum

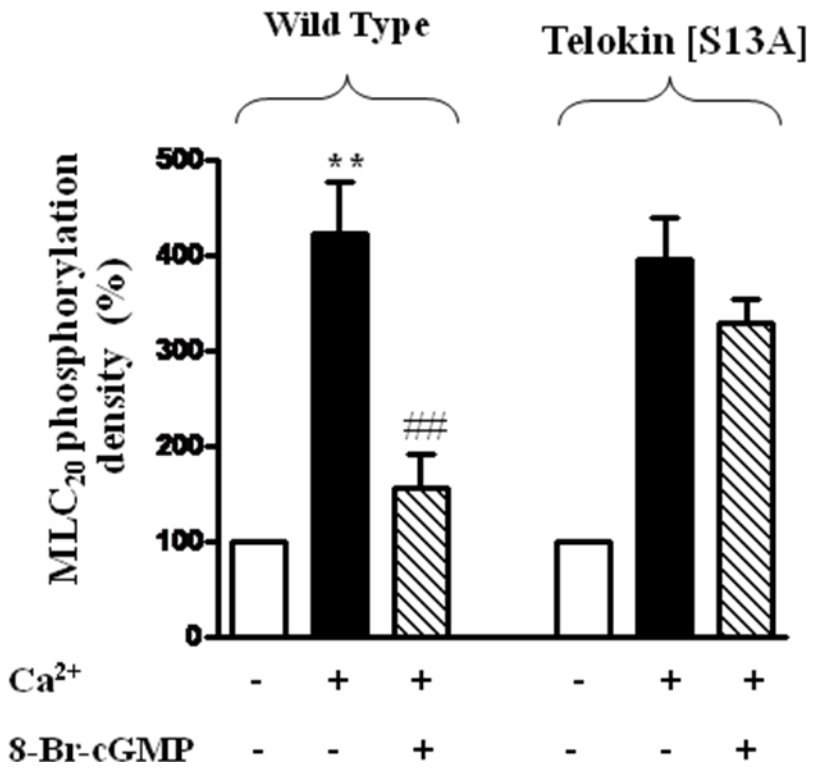

CHAPTER 7

REGULATION OF CYCLIC GMP LEVELS AND MUSCLE RELAXATION IN ANTRUM AND FUNDUS

In the gastrointestinal smooth muscle, the main inhibitory transmitters vasoactive intestinal peptide (VIP) and nitric oxide (NO) induce relaxation through the generation of cAMP and cGMP, and activation of cAMP-dependent protein kinase (PKA) and cGMP-dependent protein kinase (PKG). Although generation of both nucleotides and activation of both kinases are the physiological norm, studies in mice lacking sGC or PKGI suggest an important role for sGC/cGMP/PKG pathway in smooth muscle relaxation [106-108]. The strength and duration of cGMP signaling is regulated by its degradation into inactive 5′GMP via cGMP-specific PDE5, and efflux via ATP-dependent transporter, MRP5. *We postulated that the termination of cGMP effect by both PDE5 and MRP5 in tonic muscle could contribute to rapid return to tonic contractile phenotype following a relaxation.*

7.1 PDE5 Expression and Activity

Expression of PDE5, by both qRT-PCR and western blot, and stimulation of PDE5 activity in response to NO-donor, s-nitrosoglutathione (GSNO), were determined in muscle cells from antrum and fundus. PDE5 mRNA was expressed in both antrum and fundus and the expression was 2-fold higher in fundus compared to antrum (figure 28). PDE5 protein expression

was examined in the two regions of the stomach by western blot using selective antibody to PDE5A, the smooth muscle predominant isoform[109]. Results confirmed the expression of PDE5 of expected size (100 kDa) in the homogenates of smooth muscle cells from both antrum and fundus (figure 28). Comparing the densities of protein bands in the two regions revealed a 3-fold higher expression of PDE5 in fundus compared to antrum and this is consistent with the higher expression of PDE5 mRNA in fundus compared to antrum (Figure 28).

Basal and GSNO-stimulated PDE5 activity was measured by ion-exchange chromatography using [^{3}H]cGMP as substrate. Although, the expression levels are different, basal PDE5 activity was not significantly different in antrum (238±56 cpm/mg protein) and fundus (285±45 cpm/mg protein). Treatment of dispersed muscle cells with GSNO increased PDE5 activity in a concentration-dependent fashion in antrum and fundus. Stimulation of PDE5 activity was significantly higher at concentrations above 10 nM of GSNO in fundus compared to antrum (Figure 29A). The maximal stimulation was also significantly higher ($p<0.05$, $n=6$) in fundus (3212± 245 cpm/mg protein) compared to antrum (2189±310 cpm/mg protein).

Further evidence for higher PDE5 activity in fundus was obtained by measurements of cGMP levels in response to GSNO. GSNO increased cGMP levels in muscle cells from both regions in a concentration-dependent fashion. Basal levels of cGMP are similar in antrum (0.28±0.04 pmol/mg protein) and fundus (0.21±0.03pmol/mg protein). However, GSNO-stimulated cGMP levels were significantly lower in fundus compared to antrum. The maximal stimulation was also significantly lower in fundus (57±3% increase above basal levels) compared to antrum (76±4% increase above basal levels of cGMP) (Figure 29 B). The results are consistent with the higher PDE5 expression and activity in fundus compared to antrum.

Figure 28. Expression of PDE5A. Total RNA isolated from cultured (first passage) muscle cells from antrum and fundus was reverse transcribed using 2 μg of total RNA. The cDNA was amplified with specific primers for PDE5A. The sequences of specific primers are listed in Table 1. Quantitative real-time polymerase chain reaction (qRT-PCR) was used to measure RNA levels of PDE5A. For each cDNA sample, real-time PCR was conducted in a 20 μl reaction volume containing Quantitect™ SYBRgreen PCR Mastermix. Real-time PCR reactions were performed in triplicate. Each primer set generated only one PCR product (65bp), and the identity and integrity of these products were confirmed by electrophoresis in agarose gel in the presence of ethidium bromide and sequencing of the individual bands. Standard curves for each amplicon were generated from a dilution series of cDNA and results were quantified and reported using the $2^{-\Delta\Delta CT}$ method based on GAPDH amplification. Relative quantification of a target gene in relation to reference gene was calculated on the basis of delta delta CT values. Results demonstrated that mRNA levels of PDE5A are significantly higher in fundus compared to antrum. Inset: Representative western blot results of PDE5A expression. Cell lysates containing equal amounts of total proteins were separated with SDS-PAGE and expression of PDE5A was analyzed using selective antibody for PDE5A. Membranes were reblotted to measure β-actin. Protein bands were visualized with enhanced chemiluminescence, images were quantified and densitometric values were calculated after normalization to β-actin density. Results are expressed as fold increase over the expression of PDE5 in antrum. Values represent the means ±SEM of 3 separate experiments. **$p<0.001$ versus antrum.

Figure 28

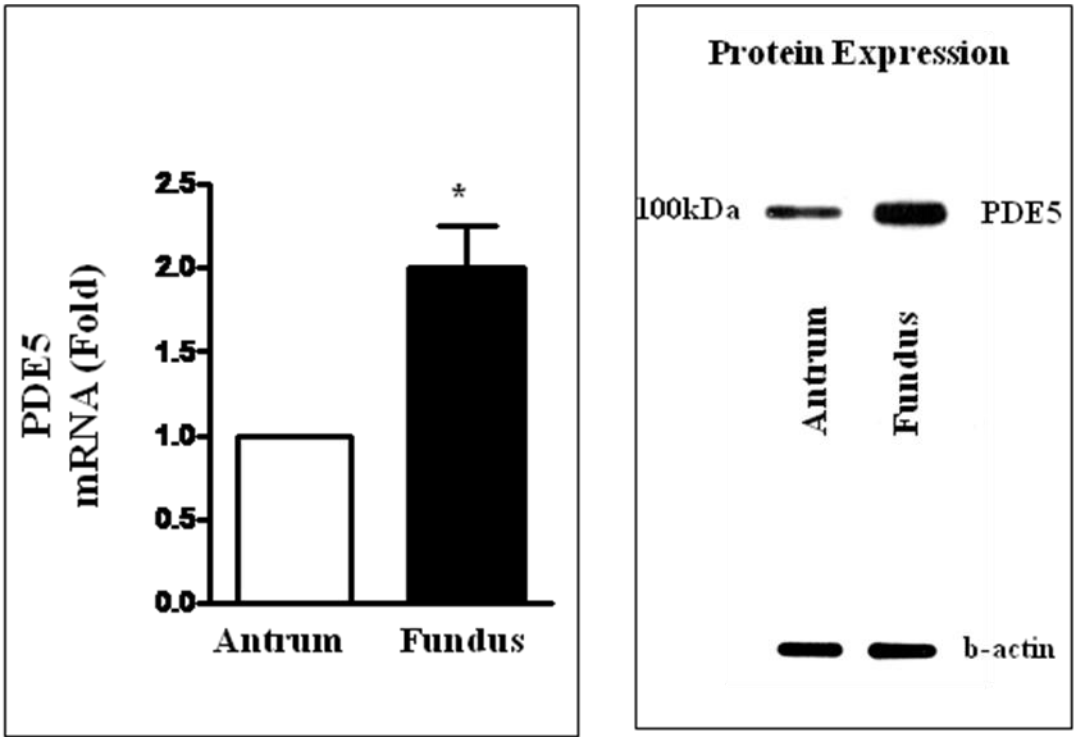
PDE5
mRNA (Fold)
2.5
2.0
1.5
1.0
0.5
0.0
*
Antrum
Fundus
Protein Expression
100kDa
PDE5
Antrum
Fundus
b-actin

Figure 29. Stimulation of PDE5 activity and cGMP formation by GSNO. A. One milliliter of cell suspension (2x 10^6 cells/ml) of freshly dispersed muscle cells from antrum and fundus was treated with different concentrations of s-nitrosoglutathione (GSNO), an NO-donor, for 60 s. The cells were homogenized in the lysis buffer and the protein content in the supernatants was measured. PDE5 was immunoprecipitated from lysates containing equal amount of protein and the activity was measured in immunoprecipitates by liquid chromatography using [3H]cGMP as substrate. The amount of radioactivity in the elutes was measured by liquid scintillation and the results are expressed as counts per milligram protein per minute. GSNO stimulated PDE5 activity in a concentration-dependent manner and the stimulation was significantly higher in fundus compared to antrum. Values represent the means ±SEM of 5-6 separate experiments. *$p<0.05$ significant increase in PDE5 activity in fundus compared to antrum. **B.** One milliliter of cell suspension (2 x 10^6 cells/ml) of freshly dispersed muscle cells from antrum and fundus was treated with different concentrations of s-nitrosoglutathione (GSNO) for 60 s and the reaction was terminated with 10% trichloroacetic acid. Cyclic GMP was measured by radioimmuno assay using [^{125}I]cGMP and the results were expressed as percent increase above basal levels (basal levels in antrum 0.28±0.04 pmol/mg protein; basal level in fundus 0.21±0.03pmol/mg protein). GSNO stimulated cGMP levels in a concentration-dependent manner and the stimulation was significantly lower in fundus compared to antrum. Values represent the means ±SEM of 5 separate experiments. *$p<0.05$ significant lower cGMP levels in fundus compared to antrum.

Figure 29

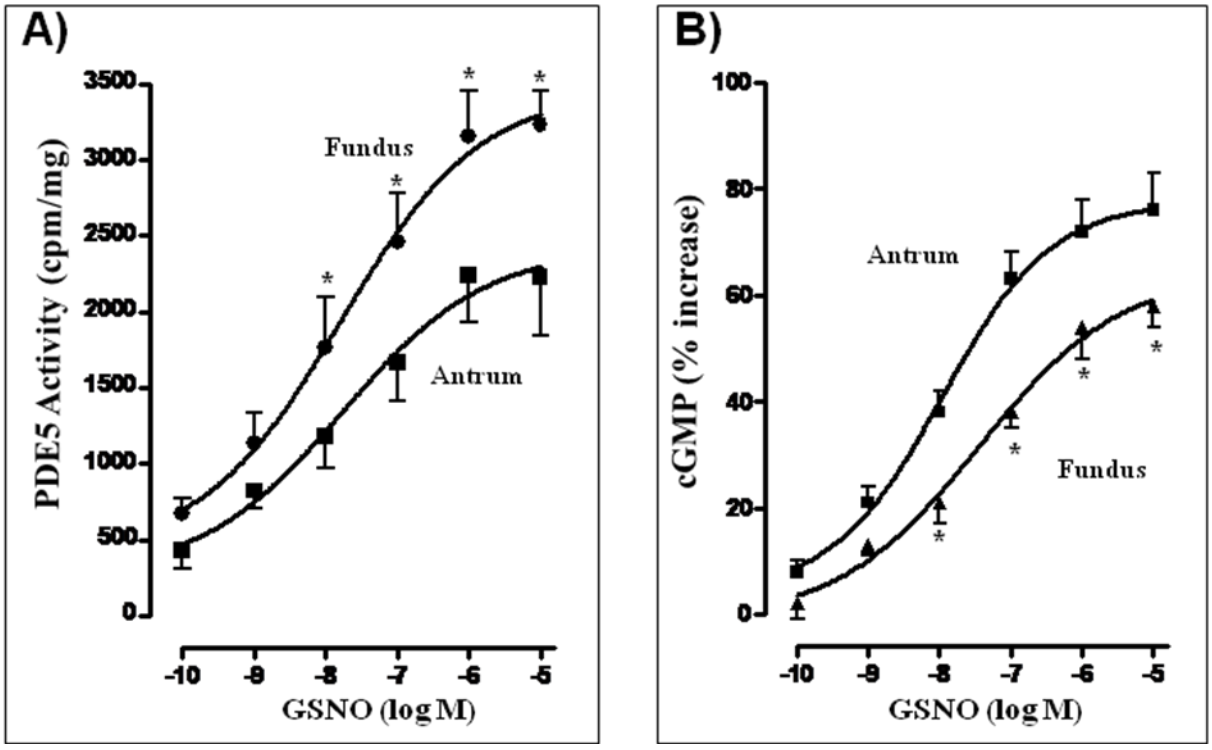
A)
PDE5 Activity (cpm/mg)
3500
3000
2500
2000
1500
1000
500
0
Fundus
Antrum
*
-10
-9
-8
-7
-6
-5
GSNO (log M)
B)
cGMP (% increase)
100
80
60
40
20
0
Antrum
Fundus
*
-10
-9
-8
-7
-6
-5
GSNO (log M)

7.2 MRP5 Expression

Another important mechanism in keeping intracellular cyclic nucleotides within narrow limits is their efflux into the extracellular space via ATP-dependent multidrug resistant proteins (MRPs). MRP5 has been identified as a cGMP export pump in the heart and vasculature, but its expression and function in gastrointestinal smooth muscle are not known. Specific primers for MRP5 were designed based on corresponding conserved sequences in human, rat, and mouse cDNAs (Table 1). MRP5 was detected by RT-PCR using RNA extracted from cultures of whole gastric smooth muscle cells in first passage. Cloning and sequence analysis of the RT-PCR product of MRP5 in the stomach was 98% similar to the corresponding amino acid sequences of human. Expression of MRP5 mRNA was higher in fundus compared to antrum (Figure 30).

MRP5 protein expression was examined in the two regions of the stomach by western blot using selective antibody to MRP5. Results confirmed the expression of MRP5 of expected size (185 kDa) in the homogenates of smooth muscle cells from both antrum and fundus. Comparing the densities of protein bands in the two regions revealed a 5-fold higher expression of MRP5 in fundus compared to antrum (Figure 30).

7.3 cGMP efflux

The function of MRP5 was analyzed by measuring intra- and extracellular cGMP levels in response to GSNO. To exclude the involvement of PDE5 and examine the singular contribution of MRP5 in the regulation of intracellular cGMP levels, experiments were done in the presence of a non-selective PDE inhibitor, IBMX (100 μM). Under these experimental conditions, changes in intracellular cGMP reflect efflux of cGMP, probably via MRP5. GSNO caused an increase in both intra- (146±10% increase above basal level of 0.42±0.05 pmol/mg protein) and extracellular

(65±5% increase above basal level of 0.16±0.03 pmol/mg protein) cGMP levels in antrum, and the increase in intracellular cGMP was greater compared to extracellular cGMP levels. GSNO also caused an increase in both intra- (88±9 above basal level of 0.38±0.04 pmol/mg protein) and extracellular (176±15% increase above basal level of 0.18±0.03 pmol/mg protein) cGMP levels in fundus, and the increase in extracellular cGMP was greater compared to intracellular cGMP levels (Figure 31). Moreover, GSNO-induced cGMP efflux was blocked in cultured muscle cells tranfected with MRP5 siRNA from both antrum and fundus (figure 32) but not in muscle cells tranfected with control siRNA (figure33). The results are consistent with the higher expression of cGMP-specific MRP5 in fundus compared to antrum and also consistent with the tonic phenotype of fundus muscle where rapid restoration of contractile function is required for optimal function.

7.4 NO-induced smooth muscle relaxation

To examine the role of PDE5 and MRP5 pathways in the regulation of muscle function, relaxation of muscle cells from antrum and fundus was measured by scanning micrometry. Muscle relaxation was measured as inhibition of ACh-induced contraction in response to GSNO as described previously. GSNO-induced muscle relaxation was concentration-dependent in both antrum and fundus (Figure 34). Relaxation was significantly lower in fundus compared to antrum and the maximal response was 73±3% in antrum and 58±4% in fundus (Figure 34). The results are consistent with the higher PDE5 and MRP5 functions resulting in lower intracellular cGMP levels in muscle cells from fundus compared to cells from antrum.

Figure 30. Expression of MRP5. A. Total RNA isolated from cultured (first passage) muscle cells from antrum and fundus was reverse transcribed using 2 μg of total RNA. The cDNA was amplified with specific primers for MRP5. The sequences of specific primers are listed in Table 1. The primer set generated only one PCR product (151bp), and the identity and integrity of these products were confirmed by electrophoresis in agarose gel in the presence of ethidium bromide and sequencing of the individual band. Results demonstrated that mRNA levels of MRP5 are higher in fundus compared to antrum. **B.** Representative western blot results of MRP5 expression. Cell lysates containing equal amounts of total proteins were separated with SDS-PAGE and expression of MRP5 was analyzed using selective antibody for MRP5. Membranes were reblotted to measure β-actin. Protein bands were visualized with enhanced chemiluminescence, images were quantified and densitometric values were calculated after normalization to β-actin density. Densitometric values showed that MRP5 expressin was 4-fold higher in fundus compared to antrum. Values represent the means ±SEM of 3 separate experiments. **$p<0.001$ versus antrum.

Figure 30

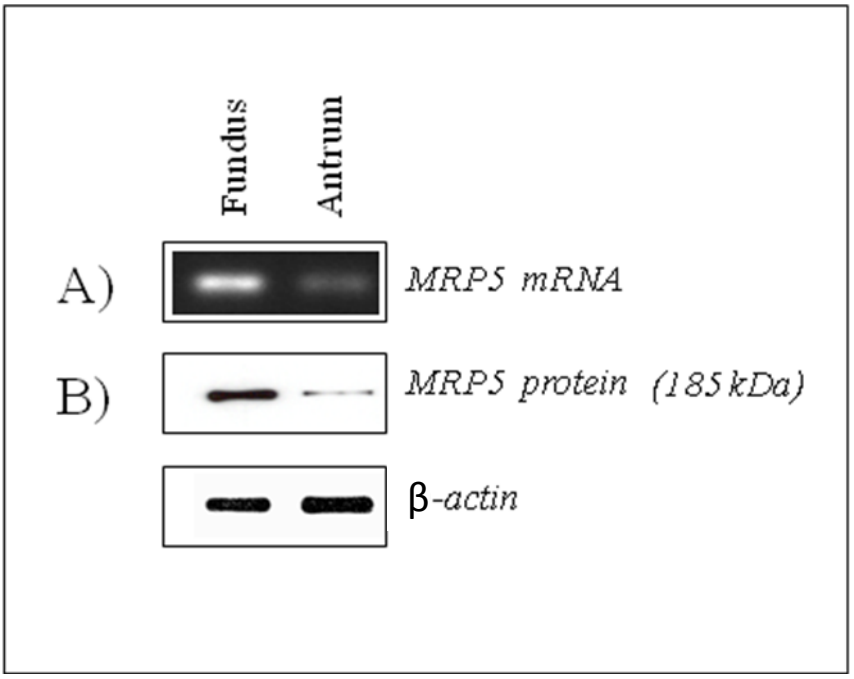

Figure 31. Stimulation of cGMP efflux by GSNO. One milliliter of cell suspension (2 x 10^6 cells/ml) of freshly dispersed muscle cells from antrum and fundus was treated with GSNO for 10 min in the presence of non-specific PDE inhibitor, 100 µM isobutylmethyl xanthine (IBMX). Under these experimental conditions, the effect of PDE5 on cGMP degradation was precluded. Cyclic GMP was measured by radioimmuno assay using [^{125}I]cGMP in the cell pellet and supernatant to reflect intracellular and extracellular cGMP levels, respectively. The results are expressed as percent increase above basal level (antrum: basal intracellular 0.42±0.05 pmol/mg protein; basal extracellular 0.16±0.03 pmol/mg protein; fundus: basal intracellular 0.38±0.04 pmol/mg protein; basal extracellular 0.18±0.03 pmol/mg protein). GSNO stimulated both intra- and extracellular cGMP levels in antrum and fundus. The increase in intracellular levels was higher in antrum compared to extracelluar levels. In contrast, increase in extracellular levels was higher in fundus compared to intracelluar levels. Values represent the means ±SEM of 5 separate experiments. **$p<0.05$ significant increase in cGMP levels by GSNO above basal levels; ##$p<0.05$ significant increase in extracellular cGMP in fundus compared to antrum.

Figure 31

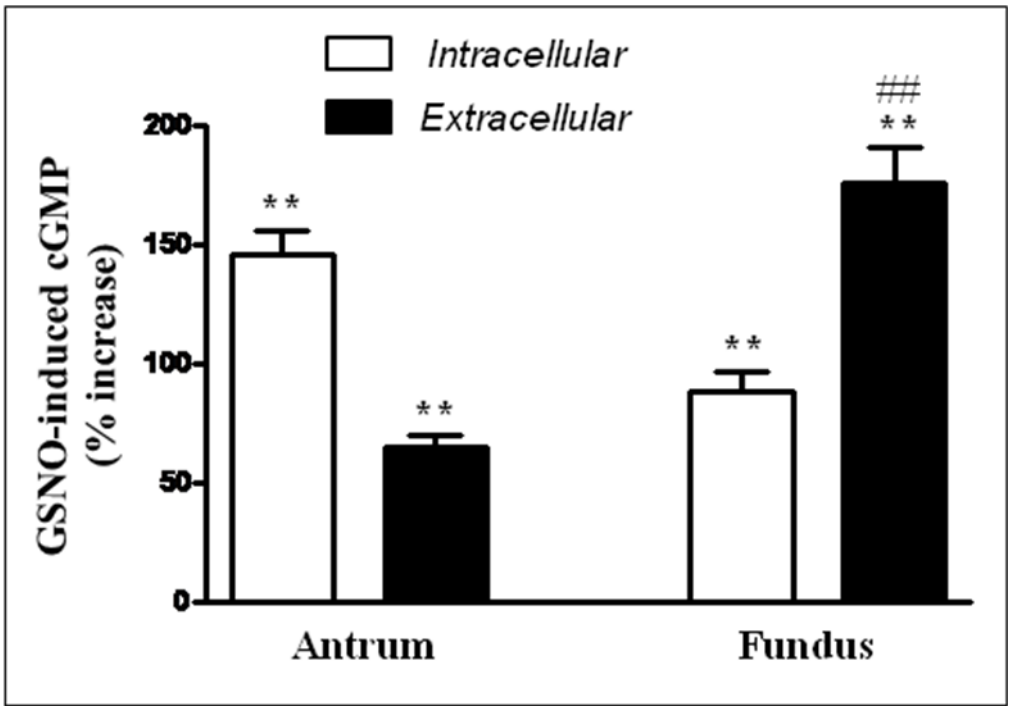
Intracellular
Extracellular
GSNO-induced cGMP
(% increase)
200
150
100
50
0
**
**
**
**
###
Antrum
Fundus

Figure 32. cGMP efflux in cells transfecrted with MRP5 siRNA. Cultures muscle cells transfected with MRP5 siRNA were treated with GSNO for 10 min in the presence of non-specific PDE inhibitor, 100 µM isobutylmethyl xanthine (IBMX). Cyclic cGMP was measured by radioimmuno assay using [^{125}I]cGMP in the cell pellet and supernatant to reflect intracellular and extracellular cGMP levels, respectively. The results are expressed as percent increase above basal level (antrum: basal intracellular 0.38±0.04 pmol/mg protein; basal extracellular 0.13± 0.02 pmol/mg protein; fundus: basal intracellular 0.35± 0.04 pmol/mg protein; basal extracellular 0.16±0.02 pmol/mg protein). GSNO-stimulated extracellular cGMP levels were abolished in cells transfected with MRP5 siRNA in antrum and fundus. Values represent the means ±SEM of 5 separate experiments. **p<0.001 significant increase in cGMP levels by GSNO above basal levels. Left panel: MRP5 expression in cells transfected with control siRNA or MRP5siRNA

Figure 32

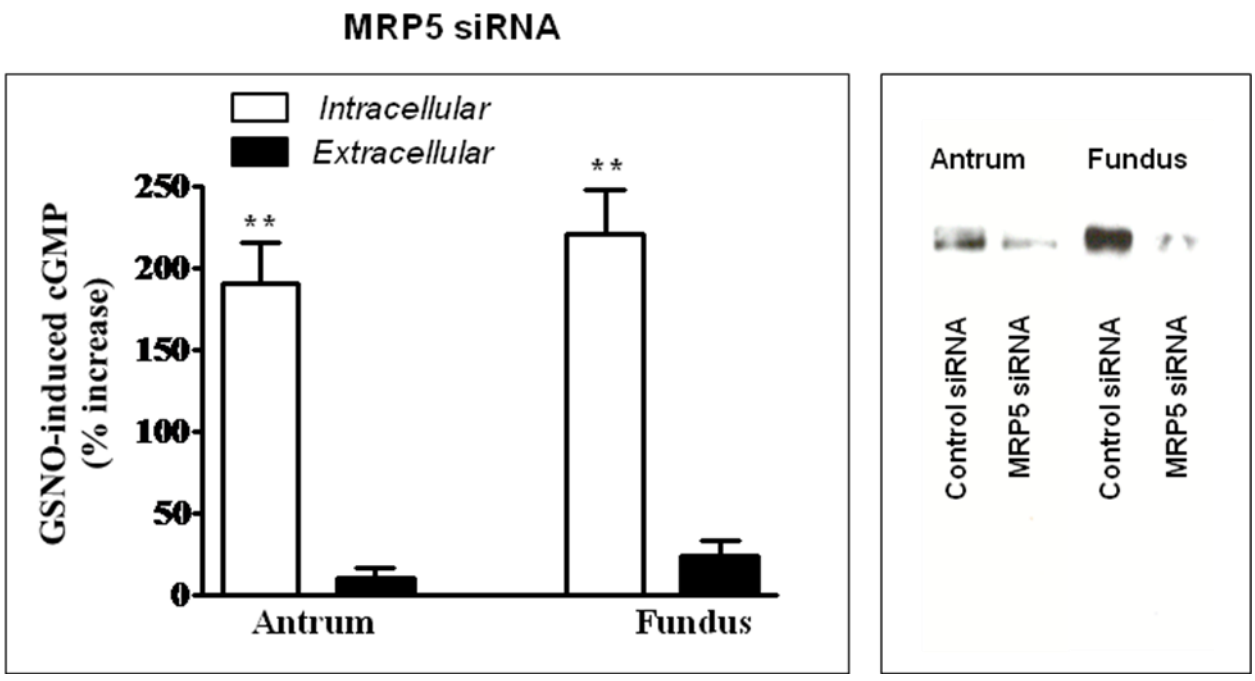
MRP5 siRNA
Intracellular
Extracellular
GSNO-induced cGMP (% increase)
250
200
150
100
50
0
**
**
Antrum
Fundus
Antrum
Fundus
Control siRNA
MRP5 siRNA
Control siRNA
MRP5 siRNA

Figure 33. cGMP efflux by in cells transfecrted with control siRNA. Cultures muscle cells transfected with control siRNA were treated with GSNO for 10 min in the presence of non-specific PDE inhibitor, 100 µM isobutylmethyl xanthine (IBMX). Cyclic cGMP was measured by radioimmuno assay using [^{125}I]cGMP in the cell pellet and supernatant to reflect intracellular and extracellular cGMP levels, respectively. The results are expressed as percent increase above basal level (antrum: basal intracellular 0.34± 0.03 pmol/mg protein; basal extracellular 0.11± 0.01 pmol/mg protein; fundus: basal intracellular 0.28± 0.02 pmol/mg protein; basal extracellular 0.14±0.02 pmol/mg protein). GSNO stimulated both intra- and extracellular cGMP levels in antrum and fundus. The increase in intracellular levels was higher in antrum compared to extracelluar levels. In contrast, increase in extracellular levels was higher in fundus compared to intracelluar levels. Values represent the means ±SEM of 5 separate experiments. *$p<0.05$ significant increase in cGMP levels by GSNO above basal levels; ##$p<0.05$ significant increase in extracellular cGMP in fundus compared to antrum.

Figure 33

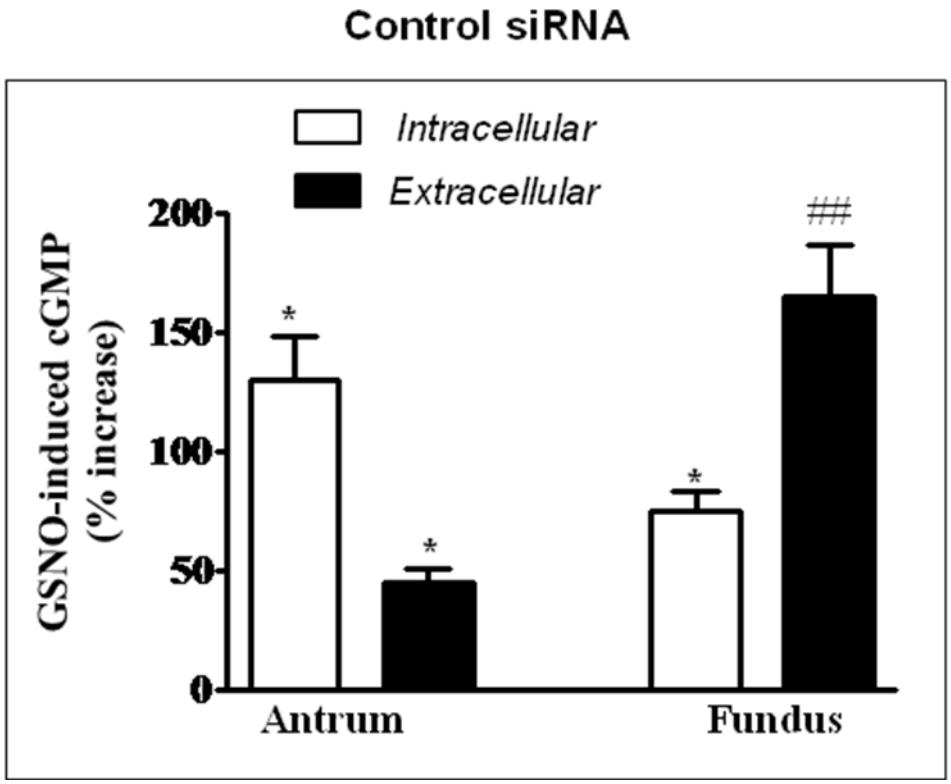
Control siRNA
Intracellular
Extracellular
GSNO-induced cGMP
(% increase)
200
150
100
50
0
*
*
*
##
Antrum
Fundus

Figure 34. GSNO-induced muscle relaxation. Relaxation of dispersed muscle cells from antrum and fundus in response to different concentrations of s-nitrosoglutathione (GSNO) was measured by scanning micrometry as decrease in ACh-induced contraction. Contraction was measured in response to maximal concentrations of ACh (0.1 μm) at 30 s as decrease in muscle control cell length (antrum: control cell length 98±3 μm; fundus: control cell length 91±4 μm). Contraction was similar in muscle cells from antrum (28±3% decrease) and fundus (29±2% decrease). GSNO caused relaxation that was concentration-dependent in both antrum and fundus and the relaxation was greater in antrum compared to fundus. The maximal response to 10 μM GSNO was significantly greater in antrum (73±3% relaxation) compared to muscle cells from fundus (58±4% relaxation). Values represent the means ±SEM of 4 separate experiments. *$p<0.05$ significant increase in relaxation in antrum versus relaxation in fundus.

Figure 34

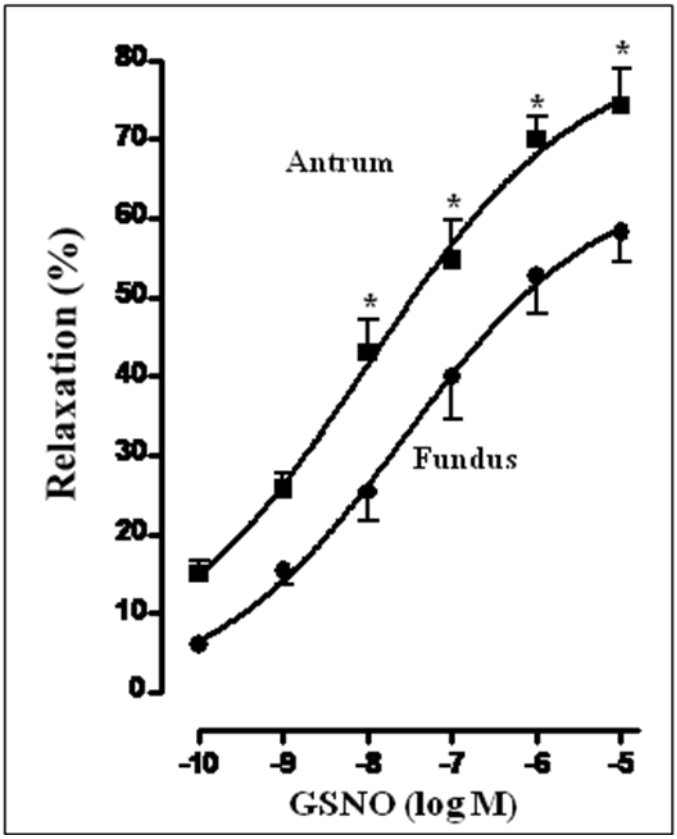
Relaxation (%)
80
70
60
50
40
30
20
10
0
Antrum
Fundus
*
*
*
*
*
-10
-9
-8
-7
-6
-5
GSNO (log M)

CHAPTER 8

DISCUSSION

Smooth muscle cells are the fundamental structural and functional units of the gastrointestinal system and exhibit distinct contractile phenotypes. The underlying features of phasic muscles (e.g., distal stomach and intestine) are the ability to generate rhythmic contractions and relaxations, while tonic muscles (e.g., sphincters and proximal stomach) have sustained tone and relax transiently in response to relaxant transmitters. Contractile agonists increase MLC_{20} phosphorylation by Ca^{2+}/CaM-dependent stimulation of MLCK and RhoA-dependent inhibition of MLCP activity. Relaxant agonists decrease MLC_{20} phosphorylation either by decreasing Ca^{2+} levels or increasing MLCP activity via PKA and PKG-dependent pathways. Although MLC_{20} phosphorylation is a prerequisite of contraction in both muscle types, the biochemical basis of phasic and tonic phenotypes of smooth muscle is not clear and is the major question of inquiry in the present study. *The objective of this project is to determine whether the expression of contractile protein isoforms, the regulation of Ca^{2+}/calmodulin-dependent MLCK and Rho kinase/ZIPK-dependent MLCP activity, and the termination of cGMP signaling are different in phasic and tonic smooth muscle.* Using biochemical, molecular and functional approaches, and antrum (distal stomach) and fundus (proximal stomach) of rabbit stomach as models of phasic and tonic smooth muscle, respectively, the present study

characterized the differences in the signaling pathways that regulate MLCK and MLCP activities and cGMP levels. Expression of contractile proteins is tissue specific with higher levels of caldesmon, calponin, tropomyosin and smoothelin A expression in antrum compared to fundus. In muscle cells from antrum MLCK activity is under feedback negative control by higher expression and activation of CaMKKβ/AMPK pathway, and MLCP is positively regulated by higher expression of telokin, an endogenous MLCP activator. In muscle cells from fundus, in contrast, MLCP activity is suppressed by higher expression and activation of Rho kinase/ZIPK/MYPT1 and PKC/CPI-17 pathways, and cGMP/PKG pathway is attenuated by rapid degradation and efflux of cGMP via higher expression PDE5 and MRP5, respectively (figure 33). These differences in the biochemical pathways highly correlate with the functional phasic phenotype of antrum and tonic phenotype of fundus.

8.1 Differences in the contractile protein content and isoforms and their associated proteins

It is hypothesized that differences in the mechanical behavior between tonic and phasic smooth muscles could be due to differences in the contractile proteins themselves; actin, myosin and their associated proteins such as caldesmon and calponin. Previous studies[110,111] have demonstrated that the tonic muscle myosin has a greater affinity for MgADP at low phosphorylation levels than the phasic myosin, a property that aids in maintaining the developed force in tonic muscles. In this study, we investigated the content and isoform distribution of the main contractile proteins; actin and myosin, and the thin filament associated proteins; tropomyosin, caldesom, calponin, and smoothelin in smooth muscles of the antrum and fundus. The results showed that the expression of contractile proteins is tissue specific with higher levels of caldesmon, calponin, tropomyosin and smoothelin A expression in antrum compared to

fundus. These results are consistent with the results previous studies using different models of phasic and tonic tissues in different species[6,112,113].

8.1.1 Myosin isoforms

Myosin molecule is a hexamer with 2 subunits of smooth muscle-specific myosin heavy chain (MHC), a pair of 17 kDa MLC and a pair 20 kDa MLC (MLC_{20}). Alternative RNA processing of a single gene generates four isoforms of MHC. Alternate splicing of a 21-neoclutide exon at the 5' end of the gene results in the presence (SMB isoform) or absence (SMA isoform) of a seven-amino acid insert at the globular head region of the MHC molecule[114]. In addition, alternate splicing of a 39-neoclutide exon in the non-helical portion of the 3' end of the gene coding for 9 unique amino acids at the COOH terminus and an in-frame stop codon results in a molecule that is 34 amino acids shorter (SM2) than the alternately spliced isoform (SM1)[115].

It has been suggested that differential expression of myosin heavy chain isoforms may influence smooth muscle contractility[116], Chi et al., for example, have found that ablation of smooth muscle myosin heavy chain SM2 increases smooth muscle contraction[117]. Others have found a positive correlation between SM1 myosin content and maximal velocity of muscle shortening (Vmax) in rat uterine smooth muscle[116]. In the present study, we could detect SM1 and SM2 isoforms only in antrum, and that SM1 expression was greater than SM2.

Our results are consistent with this proposed function of these MHC isoforms in smooth muscle. In antrum, higher SM1 expression might be pertinent with the rapid crossbridge cycling and as a result smooth muscle shortening and contraction that is needed in this region of the stomach which is characterized by rapid contraction and relaxation cycles. In addition, greater SM2 expression in this distal part of the stomach might be of importance in preventing the development of any basal tone, and thus leading to rapid fade of the stimulated contraction in the

phasic smooth muscles of the antrum. Eddinger et al.,[75], on the other hand, reported approximately equal amounts of both SM1 and SM2 MHC isoforms in all regions of the rabbit stomach. However, these measurements were made on tissue pieces taken from different locations along the greater curvature of the stomach and this expression pattern might differ at the cellular level.

Regarding MHC isoforms with (SMB) and without (SMA) the seven-amino acid insert at the globular head region of the MHC molecule, Kelley et al. [118] showed that the phasic chicken gizzard, but not the tonic chicken aortic smooth muscle, contains myosin with the seven-amino acid insert and showed that the presence of SMB isoform correlates with a higher velocity of movement of actin filaments over myosin heads in the in vitro motility assay and a higher actin-activated myosin ATPase activity. Moreover, DiSanto et al., [119] howed that the inserted myosin mRNA level increases in more distal muscular arteries that show phasic contractions compared to aorta which primarily possesses tonic activity.

By measuring mRNA expression levels in cultured gastric smooth muscle cells, we demonstrated that antrum contains greater SMB but lower SMA mRNA contents than fundus. This is consistent with the previous reports and with the proposed functional role of these isoforms with actomyosin ATPase activity and maximum shortening velocity, which are greater in phasic smooth muscles than in tonic ones. Further work is needed to examine the correlation between protein expression of each of these different isoforms and RNA expression pattern.

It is important to mention that other myosin II isoforms might add a complexity to the above mentioned differences between phasic and tonic smooth muscles. For example, it is known that non-muscle myosin (NMII A, B, and C) interacts with actin and converts the chemical energy from ATP hydrolysis to force[120]. The expression of non-muscle myosin isoforms, NMIIA and NMIIB, has been well documented to be different between phasic and tonic smooth muscle.

It has been reported that NMIIA isoform is predominating in the phasic mouse bladder muscle, while NMIIB is the major isoform in the tonic aorta[121]. Whether these non-muscle myosins are regionally distributed in the GI tract or have a functional contribution to muscle contractility is not known yet.

8.1.2 Actin isoforms

Of the thin filaments, actin stands as the major constituent and plays an important role, with myosin, in crossbridge formation. Three major actin isoforms are expressed in smooth muscle; α, β, and γ. The β -isoform is a cytoskeletal actin, whereas α and γ isoforms colocalize within the contractile apparatus. We found that the relative content of β-actin is similar in the antrum and fundus. However, muscle cells from fundus contain more α-actin but less γ-actin than antrum. Our results are in agreement with the early data of Fatigati and Murphy [122] who showed that α-actin is mainly found in arterial smooth muscle, whereas γ -actin usually predominates in visceral smooth muscle. Szymanski et al., have also reported about two to three times more α-actin in the lower esophageal sphincter than in the esophageal body, whereas γ -actin was ~43% more in the esophageal body compared to lower esophageal sphincter[100]. Future functional studies might correlate these different regional distributions of the different actin isoforms to smooth muscle contractility.

8.1.3 Caldesmon, calponin, and tropomyosin

Besides actin, it is strongly believed now that the thin-filament-associated proteins regulate actomyosin ATPase activity and thus modulate the rapid cross-bridge cycling formed by actomyosin interaction; the essential event of muscle contraction. In the present study, we show that there is a greater abundance of tropomyosin, calponin, and caldesmon in antrum compared to fundus. It has been shown that caldesmon and calponin exert an inhibitory effect on actin-activated myosin ATPase activity and suppress contraction in a Ca^{2+}-regulated manner[56,59,60].

Phosphorylation of caldesmon by kinases, mainly PKC and MAPK, or binding of Ca^{2+}/CaM to caldesmon, although with low affinity, dissociates caldesmon from F-actin and thus removes the inhibitory effect of caldesmon on actomyosin ATPase by allowing myosin heads to interact with the freed actin filaments and so muscle to contract[123,124].

Consistent with our data, Haeberle et al., [125] have shown that caldesmon content is higher in smooth muscles from rabbit ileum, guinea pig taenia coli, and rat uterus than in muscles isolated from bovine aorta or porcine carotid arteries. In addition, Caldesmon level in the extreme example of phasic muscles, chicken gizzard smooth muscle, was reported to be about twofold higher than in vascular smooth muscle [124,125].

Regarding calponin , the recent report of faster unloaded shortening velocity in smooth muscle of calponin knock-out mice is consistent with the suggested negative regulation of the cross bridge cycle by calponin[126]. Calponin's inhibitory effect on actomyosin ATPase was found to be removed via either phosphorylation by PKC or Ca^{2+}-CaM-dependent kinase II [56] or binding to CaM[127].

Goyal and coworkers reported similar calponin content in both the phasic esophageal body and the tonic lower esophageal sphincter smooth muscles[100]. The discrepancy between this data and our calponin data could be simply a consequence of species and tissue differences, but additional work is needed to demonstrate this possibility.

In parallel with the proposed roles for caldesmon and calponin, it was proposed that tropomyosin might impose an inhibitory effect on myosin ATPase activity by covering and spanning actin monomers. The removal of this inhibitory regulation, upon smooth muscle activation, displaces tropomyosin from myosin-binding sites on actin leading to cooperative actomyosin cross-bridge formation and muscle contraction[48]. Our data, which shows higher contents of caldesmon, calponin and tropomyosin in antrum might fit with the suggested roles for

these thin filament-associated proteins in facilitating the accelerated relaxation and preventing the generation of basal tone in phasic smooth muscle.

8.1.4 Smoothelin

Smoothelin is another α-actin-binding protein and is a constituent of the cytoskeleton which is specific for smooth muscle cells in a broad range of species. It is encoded by a single-copy gene via dual promoter system that generates two major isoforms; A (59 kDa) and B (110 kDa) [128]. Although our knowledge about its function is still incomplete, previous embryological [129] and knock-out [66] studies have revealed that lack of smoothelin leads to a decreased contractile potential of smooth muscle. It was proposed that smoothelin A isoform is predominantly expressed in visceral tissues while B isoform is the vascular isoform of smoothelin, although not all vascular smooth muscle cells in arterial media express smoothelin. For example, in elastic arteries, such as the aorta, the percentage of smoothelin-expressing smooth muscle is lower than in muscular arteries, such as the femoral artery [64]. Consistent with those previous reports, we found that mRNA levels of smoothelin A are greater in antrum while smoothelin B mRNA levels are higher in fundus. More research on other different types of phasic and tonic smooth muscle tissues is needed to flourish literature in this aspect. In addition, better understanding of smoothelin function might be the link to its differential expression in various smooth muscle types.

8.2 Differences in the regulation of MLCK activity

The major mechanism responsible for contraction in smooth muscle is the phosphorylation of MLC_{20} by MLCK. Phosphorylation of MLC_{20} removes its inhibitory effect on actomyosin ATPase and increases cross-bridge cycling that eventually leads to muscle

contraction [23,31,130,131]. It is now well-established that MLCK interacts with Ca^{2+}/CaM with a very high affinity, and then the formed Ca^{2+}/CaM-MLCK complex phosphorylates MLC_{20}.

Our results show that both mRNA and protein expression levels of MLCK are higher in antrum compared to fundus of rabbit stomach. Our results seem to be in parallel with the results of Szymanski et al., who found that MLCK content in esophageal body was approximately threefold higher and phosphorylation of MLC_{20} was approximately fivefold faster than in lower esophageal sphincter[99]. However, in spite of greater MLCK expression in antrum, ACh-stimulated activity of MLCK was similar in both regions. Moreover, contraction of permeabilized muscle in response to 0.5μM Ca^{2+} was similar in cells from the two regions, suggesting that Ca^{2+}-dependent MLCK activity is similar in both regions. These results raise the possibility that MLCK activity may be selectively suppressed in antrum via negative feedback mechanisms involving other kinases such as AMPK.

It is important to note that changes in $[Ca^{2+}]i$ do not always lead to proportional increases in MLCK activation. At longer time after initiation of neural stimulation, there is an apparent desensitization of the kinase to Ca^{2+}. This desensitization occurs when MLCK is phosphorylated at the C terminus of its CaM-binding sequence that would decrease the affinity of the kinase for Ca^{2+}/CaM. This phosphorylation was shown previously to be Ca^{2+}-dependent [131]. Recent evidence indicates that it is mediated by Ca^{2+}-dependent activation of CaM-dependent protein kinase kinase-β, CaMKK-β, via Gq-coupled receptors[104]. CaMKK-β in turn phosphorylates and activates AMPK. Although MLC_{20} is not a direct downstream physiological substrate of AMPK [132] but still it desensitizes smooth muscle by phosphorylating MLCK at Ser^{815} and thus leading to its inhibition[29]. Moreover, if the concentration of AMP increases sufficiently in the contracting muscle, AMP can also directly activate AMPK. So, both Ca^{2+}-dependent and AMP-stimulated feedback mechanisms would thus diminish MLCK activity.

AMP-activated protein kinase (AMPK) is a Ser/Thr kinase heterotrimer consisting of a catalytic α-subunit and two regulatory subunits, β and γ. It acts as an energy sensor at both cellular and systemic levels in mammals[133,134]. Phosphorylation of Thr[172] in the activation loop of the catalytic α-subunit [134] by upstream kinases (e.g., CaMKK-β) activates AMPK which in turn decreases ATP consumption and stimulates ATP-producing processes [133]. AMPK is dephosphorylated and deactivated by protein phosphatase-2C (PP2C) [105].

There are multiple isoforms of AMPK that are encoded by different genes; two isoforms of the catalytic α subunit (α1 and α2), two isoforms of the β subunit (β1 and β2), and three isoforms of the γ subunit (γ1, γ2, γ3), that can lead to the formation of 12 different complexes with differing properties [105].

α1 subunit is ubiquitously expressed and localized predominantly to the cytosol and hence likely to phosphorylate cytosolic and plasma membrane substrates, whereas the α2 subunit is expressed predominantly in skeletal muscle, liver and cardiac muscle, where it is found in both cytosol and nuclei [105]. As the primary AMPK isozyme, α1 is found in pulmonary arterial smooth muscle [135], carotid smooth muscle [136], vascular endothelial cells and mouse aorta[137].

Our results showed that both protein and mRNA expression of AMPKα1 was greater in antrum than in fundus. Functionally, ACh-stimulated AMPK activity was also greater in muscle cells from antrum compared to fundus. AMPK activity was measured using recombinant MLCK as substrate, implying that activation of AMPK might regulate MLCK in a feedback mechanism. To examine such a pathway, we used STO609 compound, an inhibitor of CAMKK-β, the upstream activator of AMPK. Our theory was that if there is a feedback inhibition of MLCK by AMPK, then blockade of AMPK activation by STO609 should reverse this inhibition and further augment the activity of MLCK. ACh-stimulated AMPK was blocked by STO609, which is consistent with the fact of CAMKK-β-dependent activation of AMPK. Most importantly,

blockade of AMPK augmented ACh-stimulated MLCK activity selectively in antrum without changing its activity in fundus. These results imply that in antrum muscle of the stomach, MLCK activity is rapidly terminated via a feedback mechanism involving phosphorylation and activation of the highly expressed AMPK. Furthermore, measurements of muscle cell length via scanning micrometry showed that contraction in response to ACh was enhanced in the presence of STO609 in anrum, but not fundus. This is again consistent with the augmentation of MLCK activity by AMPK inhibition in antrum.

Moreover, our data clearly show that stimulation of AMPK activity is Ca^{2+}/CaM-dependent. Using either the calmodulin antagonist, calmidazolium, to inhibit the calmodulin-regulated activity of CaMKK-β or BAPTA, to chelate intracellular Ca^{2+} abolished both ACh- and KCl-stimulated AMPK activity in antrum without an effect in fundus (as both ACh- and KCl-induced AMPK activity was minimum in fundus). These results suggest that CaMKK-β is main upstream activator of AMPK in smooth muscles of antrum. In addition, both Ca^{2+} influx and Ca^{2+} release from intracellular stores seem to be important for CaMKK-β-mediated AMPK activation as both KCl-induced membrane depolarization and ACh-stimulated m3 receptor activation resulted in a significant increase in AMPK activity in antrum.

In addition, AMPK activation was found to trigger cADPR-dependent SR Ca^{2+} release via RyRs in isolated pulmonary arterial smooth muscle cells by yet unknown mechanism[138-140]. This effect might be of relevance in longitudinal smooth muscles where cADPR-dependent SR Ca^{2+} release via RyRs seems to be important especially in the intestine[26].

Our MLCK activity data looks contradictory to the ones of Gong et al., in which they found that guinea pig ileum and portal vein smooth muscles, which represent phasic muscles, have approximately threefold higher activity of MLCK than rabbit femoral artery smooth muscles, which represents tonic muscles[141]. Knowing that other non-muscle components and

regulators might affect enzyme activity in the whole tissue homogenates, MLCK activity measured in those tissue samples could be different than our measurements in dispersed smooth muscle cells. In addition, differential expression and regional distribution of AMPK isoforms could be different in these various smooth muscle organs.

Other signaling components might add to the above mentioned differences regarding the regulation of MLCK in tonic versus phasic smooth muscles. For example, CaM-dependent kinase II (CAMKII) protein expression was found to be higher in proximal colon, which represents phasic smooth muscles, than in fundus [142]. CAMKII might regulate smooth muscle contraction by phosphorylating several substrates such as MLCK[143] and phospholamban, a negative regulator of sarcoplasmic reticulum Ca^{2+}-ATPase [144]. CAMKII expression profile seems to be in parallel with the results of Goyal and his coworkers who found the total content and concentration of CaM to be higher in the phasic esophageal body compared to the tonic lower esophageal sphincter[99]. These findings might be of more relevance to other CaM-binding proteins such as caldesmon and calponin, which we found to be higher in antrum compared to fundus.

In summary, higher expression of AMPK and greater AMPK-mediated inhibition of MLCK in antrum is correlated with rapid contraction and relaxation cycles in antrum (figure 33). This observation may be applicable to other phasic smooth muscles [23,145]. Future studies should be directed towards identifying the relative and the regional importance of these regulatory pathways in smooth muscle contraction.

8.3 Differences in the regulation of MLCP activity and muscle contraction

Phosphorylation of MLC_{20} by MLCK is counterbalanced by its dephosphorylation by myosin light chain phosphatase (MLCP), an essential step in smooth muscle relaxation[141]. MLCP is a holoenzyme consisting of three subunits: a catalytic subunit that is a 38 kDa-type I-protein

phospatase delta isoform (PP1cδ) and two regulatory subunits consisting of a small 20 kDa subunit and a 110- to 130-kDa subunit (myosin phosphatase target subunit 1, MYPT1). The interactions of the three subunits are required to form the functional enzyme. MYPT1 subunit contains a PP1c-binding motif occuring at the amino acids 35-38, followed by seven NH2-terminal ankyrin repeats. Binding of PP1Cδ with MYPT1 alters substrate specifity and enhances catalytic activity.

MLCP content and activity have been reported to be higher in phasic muscles of ileum, portal vein, and gizzard than in tonic muscles of femoral artery and aorta [141,146]. Others have also reported higher basal levels of MYPT1 in the predominantly phasic rectum smooth muscle compared to the internal anal sphincter [147]. Relatively higher content and activity of MLCP in phasic smooth muscles may contribute to the lack of steady-state MLC_{20} phosphorylation and basal muscle tone. The lack of basal tone in these muscles might be of relevance to the proposed role and behavior of these smooth muscle types where accelerated rate of MLC_{20} dephosphorylation and rapid initiation of relaxation is required [23,141,145].

Phosphorylation of the MYPT1 is thought to regulate the activity of MLCP. The major regulatory phosphorylation sites of MYPT1 are Thr^{696}, Thr^{853}, Ser^{695}. Phosphorylation of Thr^{696} in MYPT1 by Rho kinase dissociates the enzyme from PP1cδ and inhibits the activity of the catalytic subunit of MLCP. Phosphorylation of Thr^{853} by Rho kinase within the myosin-binding domain on MYPT1 dissociates the enzyme from myosin and decreases the efficiency of the enzyme by decreasing availabilty of the substrate. While Rho kinse can phosphorylate both Thr^{696} and Thr^{853}, several other kinases have also been shown to phosphorylate the Thr^{696} site such as ZIPK.

In addition to the inhibitory role of MYPT1 phophorylation at the Thr^{696} and Thr^{853} sites, MLCP inhibition can occur via PKC- or arachidonic acid-mediated pathways. Phorbol ester- or

DAG-mediated activation of PKC, mainly PKC-δ and PKC-ε, [38] results in phosphorylation of the 17 kDa PKC-potentiated inhibitor protein (CPI-17), at Thr[38]. This phosphorylation significantly increases the binding affinity of CPI-17 to the catalytic PP1cδ subunit of MLCP leading to dissociation of the holoenzyme and thus inhibition of the catalytic activity [148]. Arachidonic acid activates both Rho kinase and PKC, and sphingosylphosphorylcholine (SPC) has also been suggested to directly activate Rho kinase[149]. MLCP inhibition by either PKC or Rho kinase is thought to be the general mechanism for G-protein-dependent elevation of MLC_{20} phosphorylation level and thus maintaining contraction at constant $[Ca^{2+}]i$; a process called Ca^{2+} sensitization.

On the other hand, phosphorylation at the Ser[695] site of MYPT1 by PKA or PKG blocks the ability of Rho kinase to phosphorylate the nearby Thr[696] and thus increases MLCP activity. Moreover, PKA and PKG can indirectly augment MLCP activity through phosphorylating and thus enhancing the acivity of telokin. Telokin is an endogenous 17 kDa activator of MLCP. It is a smooth muscle specific protein that is independently and invariably expressed in different smooth muscles from a promoter located within an intron of MLCK gene and is thus identical to the C-terminus of MLCK downstream from the kinase and calmodulin binding domains. The ability of telokin to stimulate MLCP is moderately enhanced upon phosphorylation of Ser[13] by PKA or PKG.

Our results demonstrate characteristically higher levels (both protein and mRNA) of Rho kinase II-the most common isoform of Rho kinase involved in smooth muscle contraction[130,150] and CPI-17, in the smooth muscles of the fundus compared with the antrum. Our results are consistent with the previous studies, which showed higher levels of RhoA/Rho kinase pathway and CPI-17 in the internal anal sphincter, which represents tonic smooth muscles, compared with the predominantly phasic rectal smooth muscle [147]. It is of interest that Woodsome et al. [151] also

reported higher levels of CPI-17 in the tonic smooth muscle of the femoral artery than in the phasic smooth muscle of the vas deferens. In addition, our data showed that both protein and mRNA contents of ZIPK were similar in both stomach regions. However, stimulation of ZIPK activity was greater in antrum compared to fundus reflecting higher expression and activation of upstream kinase, Rho kinase.

To functionally elucidate the singular contribution of CPI-17 in the muscle contraction, we used the PKC activator, PMA. We found that treatment of dispersed muscle cells with PMA caused significantly, 2 to 3 folds, greater contraction in muscle cells from fundus than in muscle cells from antrum. In contrast, the extent of PKC activation by PMA was similar in muscle cells from both antrum and fundus. Knowing that CPI-17 is a downstream target of PKC, these results correlate well with the higher expression of CPI-17 in the fundus compared to the antrum. Future knockout and siRNA studies might further confirm CPI-17 role in MLCP inhibition and thus muscle contraction in response to contractile agonist, which activate both Rho kinase/MYPT1 and PKC/CPI-17 pathways.

Moreover, our results demonstrated that ACh-induced stimulation of both Rho kinase and ZIPK was significantly higher in muscle cells from fundus compared to antrum. Data are also consistent with the concept that RhoA/Rho kinase components (responsible for the inhibition of MLCP and sustained elevated levels of p-MLC_{20}), are higher in tonic than phasic smooth muscles. These results also clarify the relationship between the functional status and the levels of these different signal transduction proteins in the tonic versus phasic smooth muscles in their basal state in support of previous studies demonstrating constitutive activation of Rho kinase pathway in tonic muscle under physiological conditions[152-154].

Low levels of RhoA/Rho kinase may unleash MLCP, causing rapid dephosphorylation of p-MLC_{20}, preventing the development of any basal tone, and causing rapid fade of stimulated contraction in phasic smooth muscles such as the antrum [155]. This data collectively show that fundus is characterized with the molecular apparatus designed to provide sustained levels of MLC_{20} phosphorylation responsible for the basal tone.

Interestingly, upon treating muscle cells with Y27632, a selective blocker of Rho kinase, both Rho kinase and ZIPK activities were inhibited, suggesting that stimulation of ZIPK activity is dependent on and downstream of Rho kinase and this might explain the higher ZIPK activity in fundus in spite of similar contents in both antrum and fundus. Although literature is rich in research favoring the roles of both Rho kinase and ZIPK in myosin and MYPT1 phosphorylation and thus smooth muscle contraction, still few studies haves considered the possibility that these two enzymes may in fact directly interact [43,156,157].

It is now believed that both Rho kinase and ZIPK cause Ca^{2+}-independnet contraction in smooth muscle cells. In addition, ZIPK in smooth muscle phosphorylates many of the same substrates as Rho kinase in vitro, including MYPT1 [43]. Moreover, both kinases show a preference for threonine and target similar phosphorylation site consensus sequences, i.e. 3–4 basic amino acids +1 or +2 N-terminal to the phosphorylation site [156]. Consistent with our data, Borman et al., found that, in smooth muscle, carbachol-induced activation of ZIPK was sensitive to Y27632 even though ZIPK is not directly inhibited by this compound in vitro [43].

However, knowing that Rho kinase is largely membrane-bound upon RhoA activation, a question being raised is how this membrane-bound kinase can directly phosphorylate MYPT1 and myosin[158,159]. Morgan and co-workers have shown in their studies that stimulation of isolated smooth muscle cells by PGF2α induces a marked change in the localization of MLCP, in which MYPT1 is initially phosphorylated in the cytosol and then, MLCP is translocated to the

membrane where the subunits are dissociated. PP1c returns to the core of the cell while MYPT1 remains at the membrane location. The isolated PP1c reduces phosphatase activity towards phosphorylated myosin and thus decreases MLC_{20} dephosphorylation [160].

Endo et al., [157] demonstrated that transfection of HEK293 cells with constutively active RhoA promoted interaction of ZIPK with MYPT1. So, it is suggested that ZIPK is a downstream target of both RhoA and Rho kinase signaling, forming a signal transduction module to ultimately regulate myosin phosphorylation in smooth muscle. Given the location of active Rho kinase at the plasma membrane, mechanisms must exist to translocate ZIPK to the activated Rho kinase. One possible mechanism might involve binding to MYPT1 where Rho kinase directly interacts with ZIPK via translocation of MYPT1 itself from the cytoskeleton to the plasma membrane. In another scenario, ZIPK might act as a soluble Rho kinase target to transduce the signal from the cell membrane to the actomyosin cytoskeletal elements within the cytoplasm.

In summary, our studies identified a strong correlation between higher levels and activities of Rho kinase/ZIPK/MYPT1 and CPI-17/PKC pathways and tonic phenotype of fundus muscle. These studies combined with the previous studies in different sphincteric muscles in several species suggest a pivotal role for MLCP inhibition via Rho kinase/ZIPK/MYPT1 and CPI-17/PKC pathways in the maintenance of MLC_{20} phosphorylation and muscle tone (figure 33).

8.4 Differences in the regulation of MLCP activity and muscle relaxation

On the other side of MLCP regulation, telokin has been shown to activate MLCP and to be important for cGMP-mediated calcium desensitization and thus relaxation of smooth muscle tissues [161]. Our data demonstrating higher expression of telokin in antrum compared to fundus are in agreement with the previous studies showing higher telokin expression in urinary bladder

(phasic) compared to aorta (tonic) [162,163]. Higher expression of telokin and greater activation of MLCP and relaxation in antrum compared to fundus is correlated with phasic phenotype of antrum. This is in contrast to the higher expression of CPI-17, an endogenous inhibitor of MLCP in fundus.

To examine the role of telokin in smooth muscle relaxation, contraction was induced by Ca^{2+} in permeabilized muscle cells and relaxation in response to 8-Br-cGMP was measured. This approach precludes the effect of 8-Br-cGMP on intracellular Ca^{2+} levels and reflects the effect on MLCP probably via phosphorylation of telokin at Ser^{13}. As the response to NO-donor was different in antrum and fundus due to differences in the expression of PDE5 and MRP5, relaxation in response to 8-Br-cGMP, non-hydrolyzable analog of cGMP, was measured. Our results demonstrated that 8-Br-cGMP, caused significantly greater relaxation in muscle cells from antrum compared to fundus. In contrast, the extent of PKG activation by 8-Br-cGMP was similar in muscle cells from antrum and fundus. This relaxation difference between these two muscle types is in parallel with the higher telokin expression in antrum.

These findings were further strengthened by the measurements of MLC_{20} dephosphorylation (i.e., MLCP activity) in cells expressing wild type telokin and phosphorylation-deficient telokin (telokin S13A) under conditions of where the effects of cGMP/PKG on Ca^{2+} levels are precluded as described above. We found that MLC_{20} phosphorylation was decreased by the PKG activator 8-Br-cGMP in antrum and fundus, but with greater inhibition in antrum. In addition, the effect of 8-Br-cGMP was attenuated in cells expressing phosphorylation-deficient telokin (S13A), and again greater attenuation was found in smooth muscle cells from antrum. Similar levels of MLC_{20} phosphorylation and contraction in response to Ca^{2+} support the notion that telokin action is through the increased activity of MLCP rather than inhibition of MLCK activity. It is noteworthy to mention that the functional

contribution of telokin to relaxation of Ca^{2+}-independent contraction and MLC_{20} dephosphorylation has not been determined yet.

Taken together, our results in antrum and fundus, and those of previous studies in phasic visceral and tonic vascular muscle, support the hypothesis that preferential expression telokin and increase in MLCP activity contributes to higher relaxation in telokin-rich smooth muscle and correlate with the phasic phenotype of the muscle. In contrast, lower expression of MLCP activator, telokin, and higher expression of MLCP inhibitor, CPI-17, in tonic muscle facilitate greater sensitivity of contractile proteins to low Ca^{2+} levels, a well recognized, but poorly understood biochemical characteristic of tonic muscle. Both mechanisms of MLCP regulation may operate in parallel in vivo to restrain MLCP activation and to maintain muscle tone (figure 33).

8.5 Differences in the regulation cGMP levels and muscle relaxation.

The main relaxant neurotransmitters of gastrointestinal smooth muscle are nitric oxide (NO), vasoactive intestinal peptide (VIP), and its homologue pituitary adenylate cyclase-activating polypeptide (PACAP). These neurotransmitters induce relaxation through generation of cAMP and cGMP and activation of PKA and PKG, respectively. These kinases, in turn, target different components of MLCK and MLCP signaling pathways that eventually induce and augment myosin light chain dephosphorylation and consequently desensitize the process of contraction. Although generation of both cAMP and cGMP and activation of PKA and PKG are the physiological norm, studies in transgenic mice lacking nNOS, sGC, and PKG-Iα suggest that cGMP/PKG plays a critical role in relaxation of smooth muscle [106-108].

Cyclic GMP levels in gastrointestinal smooth muscle are well-controlled by the balance between the synthetic activities of soluble guanylyl cyclase, and the degradative activities of specific PDE5, the main cGMP-specific PDE5 in smooth muscle. Soluble GC is a heterodimeric

enzyme made up of one α and one β subunit with α1/β1 being the most abundant and the most widely expressed isoform of sGC. This isoform was shown to have the most basal and NO-stimulated activity [164]. PDE5 is a dimer containing two allosteric cGMP-binding sites in its regulatory N-terminal domain and a specific cGMP-binding site in its catalytic C-terminal domain that hydrolyses cGMP. An increase in cGMP levels not only stimulates PKG, but also augments PDE5 activity by allosteric activation via binding to its regulatory domain, and by PKG-mediated phosphorylation of PDE5 at a conserved serine residue in the N-terminal region.

Beside degradation by phosphodiesterases, cyclic nucleotides elimination via MRPs-mediated active export into the extracellular space has been found to be an important pathway in returning cyclic nucleotide levels back to basal state. MRP5 mRNA has been detected in various smooth muscle tissues with high transcript levels and has been shown to be competent in the transport of cGMP. This is supported by the observation that in cerebral cells and platelets, and after stimulation with NO, cGMP accumulation is decreased faster than it could be explained solely by the phosphodiesterase activity [165]. Cyclic GMP secretion via MRP5 has been shown to be unidirectional and energy dependent [72]. Studies, using immunofluorescence microscopy, have shown that MRP5 is co-expressed with PDE5 in smooth muscle cells, providing a strong evidence that these two pathways might complement with each other in keeping cGMP levels within a low range [166]. Thus, the strength and duration of cGMP signaling depends on the activity sGC, PDE5 and MRP5.

Our studies demonstrate higher expression of PDE5 and MRP5 in fundus compared to antrum. As a result, intracellular cGMP levels and relaxation in response to NO-donors were attenuated more in fundus compared to antrum (figure 34). Increased degradation and efflux of cGMP might play an important role in rapid termination of relaxation in fundus. Relaxation of tonic smooth muscle in response to NO is transient and the muscle regains contraction to prevent

continuous distending forces or reflux of materials. At the tissue level, non-muscle elements add more complexity to the above mentioned biochemical differences in cGMP handling between phasic and tonic muscles. For example, it was found that the density of eNOS positive neurons was scarce in fundus part of the human stomach while their density in distal part was intensive [167].Thus it is possible that in addition to increase in the termination of cGMP signaling, the mechanisms responsible for generation of cGMP such as generation of NO and activation of sGC are also constrained in fundus to facilitate tone and optimal organ function.

Figure 35. Differential expression and/or activation of signaling proteins involved in the regulation of MLC_{20} phosphorylation in antrum and fundus of stomach correlate with the phasic and tonic smooth muscle phenotypes, respectively. ***Signaling proteins shown in red are involved in phasic phenotype and those shown in green are involved in tonic phenotype; + and – signify stimulation and inhibition, respectively.***

Antrum: Higher expression of AMPK and selective feedback inhibition of MLCK activity via AMPK-mediated phosphorylation, and higher expression of telokin and activation of MLCP correlate with the rapid cyclical contractile function in phasic muscle.

Fundus: Higher expression and activation of Rho kinase/ZIPK/MYPT1 and PKC/CPI-17 pathways leading to preferential inhibition of MLCP activity and sustained phosphorylation of MLC_{20} correlate with the sustained contraction in tonic muscle. In addition, rapid termination of cGMP signal and thus, muscle relaxation by degradation and efflux of cGMP via higher expression of PDE5 and MRP5, respectively, facilitate rapid restoration of tone.

Figure 35

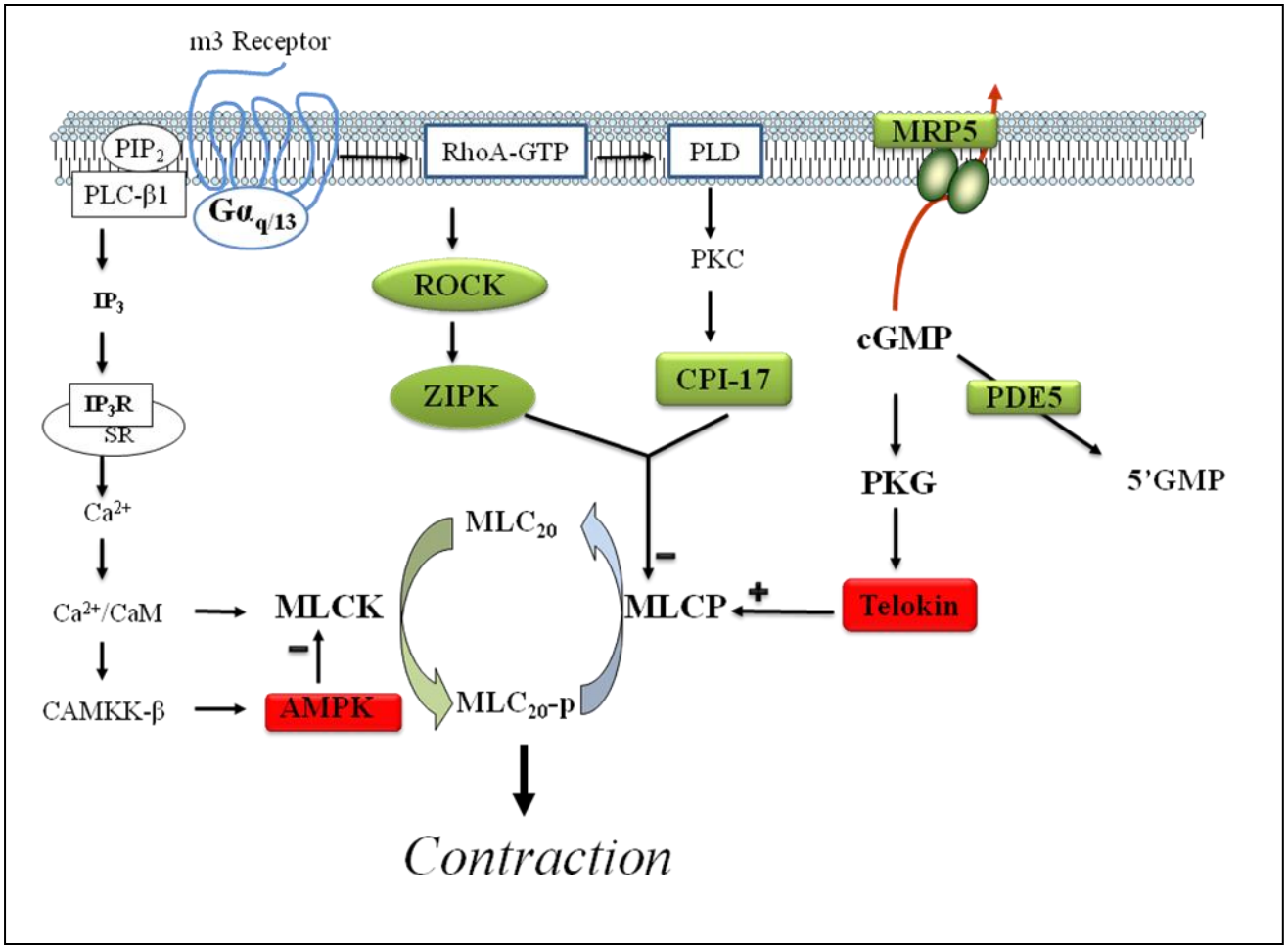
m3 Receptor
PIP2
PLC-β1
Gαq/13
RhoA-GTP
PLD
MRP5
IP3
ROCK
PKC
cGMP
IP3R
SR
ZIPK
CPI-17
PDE5
Ca2+
PKG
5'GMP
MLC20
Ca2+/CaM
MLCK
MLCP
Telokin
CAMKK-β
AMPK
MLC20-p
Contraction

List of References

1 Kunze, W. A. & Furness, J. B. The enteric nervous system and regulation of intestinal motility. *Annu Rev Physiol* **61**, 117-142, (1999).

2 Gabella G. New York: Raven Press. Structure of muscle and nerves in the gastrointestinal tract. *In: Johnson LR (ed.). Physiology of the Gastrointestinal tract, 2d edn. New York: Raven Press* (1987).

3 Somlyo, A. P., Somlyo, A. V., Shuman, H. & Stewart, M. Electron probe analysis of muscle and X-ray mapping of biological specimens with a field emission gun. *Scan Electron Microsc*, 711-722 (1979).

4 Gabriel M. Makhlouf, K. S. M. smooth muscle of the gut. *In: Textbook of Gastroenterology, fifth edition.* (2008).

5 Barany, M. ATPase activity of myosin correlated with speed of muscle shortening. *J Gen Physiol* **50**, Suppl:197-218 (1967).

6 Barany, M., and K. Barany. . Myosin light chains. . *In: Biochemistry of Smooth Muscle Contraction, edited by M. Barany. San Diego, CA: Academic*, p. 21–36 (1996).

7 Bitar, K. N. Function of gastrointestinal smooth muscle: from signaling to contractile proteins. *Am J Med* **115 Suppl 3A**, 15S-23S, (2003).

8 Farness JB, C. M. Identification of gastrointestinal neurotransmitters. *In: Bertaccini G (ed.). Handbook of Experimental Pharmacology: Mediators and Drugs in Gastrointestinal Motility. Berlin: Springer-Verlag*, **59:279.** (1982).

9 Murthy, K. S. Signaling for contraction and relaxation in smooth muscle of the gut. *Annu Rev Physiol* **68**, 345-374, (2006).

10 Murthy, K. S. & Makhlouf, G. M. Differential coupling of muscarinic m2 and m3 receptors to adenylyl cyclases V/VI in smooth muscle. Concurrent M2-mediated inhibition via Galphai3 and m3-mediated stimulation via Gbetagammaq. *J Biol Chem* **272**, 21317-21324 (1997).

11 Murthy, K. S. & Makhlouf, G. M. Phosphoinositide metabolism in intestinal smooth muscle: preferential production of Ins(1,4,5)P3 in circular muscle cells. *Am J Physiol* **261**, G945-951 (1991).

12 Murthy, K. S., Zhang, K. M., Jin, J. G., Grider, J. R. & Makhlouf, G. M. VIP-mediated G protein-coupled Ca2+ influx activates a constitutive NOS in dispersed gastric muscle cells. *Am J Physiol* **265**, G660-671 (1993).

13 Mazzone, A. & Farrugia, G. Evolving concepts in the cellular control of gastrointestinal motility: neurogastroenterology and enteric sciences. *Gastroenterol Clin North Am* **36**, 499-513 vii (2007).

14 L., T. Interstitial cells of Cajal. . *New York: American Physiological Society* **In: Wood JD (ed.). Motility and circulation. Handbook of Physiology.Vol. 1, Sect. 6: The Gastrointestinal system.** (1989).

15 Ward, S. M., Burns, A. J., Torihashi, S. & Sanders, K. M. Mutation of the proto-oncogene c-kit blocks development of interstitial cells and electrical rhythmicity in murine intestine. *J Physiol* **480 (Pt 1)**, 91-97 (1994).

16 Faussone Pellegrini, M. S., Cortesini, C. & Romagnoli, P. [Ultrastructure of the tunica muscularis of the cardial portion of the human esophagus and stomach, with special reference to the so-called Cajal's interstitial cells]. *Arch Ital Anat Embriol* **82**, 157-177 (1977).

17 Sanders, K., Koh, D., Ward, S. . . Organization and electrophysiology of interstitial cells of Cajal and smooth muscle cells in the gastrointestinal tract. *In L. R. Johnson (Ed.). Physiology of the gastrointestinal tract Burlington MA : Elsevier Academic Press.*, (pp. 533-548) (2006).

18 Sanders, K. M., Koh, S. D. & Ward, S. M. Interstitial cells of cajal as pacemakers in the gastrointestinal tract. *Annu Rev Physiol* **68**, 307-343, (2006).

19 Bayliss, W. M. & Starling, E. H. The movements and innervation of the small intestine. *J Physiol* **24**, 99-143 (1899).

20 Foxx-Orenstein, A. E., Kuemmerle, J. F. & Grider, J. R. Distinct 5-HT receptors mediate the peristaltic reflex induced by mucosal stimuli in human and guinea pig intestine. *Gastroenterology* **111**, 1281-1290, (1996).

21 Grider, J. R. & Jin, J. G. Distinct populations of sensory neurons mediate the peristaltic reflex elicited by muscle stretch and mucosal stimulation. *J Neurosci* **14**, 2854-2860 (1994).

22 Grider, J. R. Neurotransmitters mediating the intestinal peristaltic reflex in the mouse. *J Pharmacol Exp Ther* **307**, 460-467, (2003).

23 Somlyo, A. P. & Somlyo, A. V. Signal transduction and regulation in smooth muscle. *Nature* **372**, 231-236, (1994).

24 Rhee, S. G. Regulation of phosphoinositide-specific phospholipase C. *Annu Rev Biochem* **70**, 281-312, (2001).

25 Murthy, K. S., Grider, J. R. & Makhlouf, G. M. InsP3-dependent Ca2+ mobilization in circular but not longitudinal muscle cells of intestine. *Am J Physiol* **261**, G937-944 (1991).

26 Kuemmerle, J. F., Murthy, K. S. & Makhlouf, G. M. Longitudinal smooth muscle of the mammalian intestine. A model for Ca2+ signaling by cADPR. *Cell Biochem Biophys* **28**, 31-44, (1998).

27 Kamm, K. E. & Stull, J. T. Dedicated myosin light chain kinases with diverse cellular functions. *J Biol Chem* **276**, 4527-4530, (2001).

28 Tansey, M. G., Luby-Phelps, K., Kamm, K. E. & Stull, J. T. Ca(2+)-dependent phosphorylation of myosin light chain kinase decreases the Ca2+ sensitivity of light chain phosphorylation within smooth muscle cells. *J Biol Chem* **269**, 9912-9920 (1994).

29 Horman, S. *et al.* AMP-activated protein kinase phosphorylates and desensitizes smooth muscle myosin light chain kinase. *J Biol Chem* **283**, 18505-18512, (2008).

30 Murthy, K. S. *et al.* Differential signalling by muscarinic receptors in smooth muscle: m2-mediated inactivation of myosin light chain kinase via Gi3, Cdc42/Rac1 and p21-activated kinase 1 pathway, and m3-mediated MLC20 (20 kDa regulatory light chain of myosin II) phosphorylation via Rho-associated kinase/myosin phosphatase targeting subunit 1 and protein kinase C/CPI-17 pathway. *Biochem J* **374**, 145-155, (2003).

31 Somlyo, A. P. & Somlyo, A. V. Ca2+ sensitivity of smooth muscle and nonmuscle myosin II: modulated by G proteins, kinases, and myosin phosphatase. *Physiol Rev* **83**, 1325-1358, (2003).

32 Murthy, K. S., Zhou, H., Grider, J. R. & Makhlouf, G. M. Sequential activation of heterotrimeric and monomeric G proteins mediates PLD activity in smooth muscle. *Am J Physiol Gastrointest Liver Physiol* **280**, G381-388 (2001).

33 Huang, J. *et al.* Signaling pathways mediating gastrointestinal smooth muscle contraction and MLC20 phosphorylation by motilin receptors. *Am J Physiol Gastrointest Liver Physiol* **288**, G23-31, (2005).

34 Zhou, H. & Murthy, K. S. Distinctive G protein-dependent signaling in smooth muscle by sphingosine 1-phosphate receptors S1P1 and S1P2. *Am J Physiol Cell Physiol* **286**, C1130-1138, (2004).

35 Hartshorne, D. J., Ito, M. & Erdodi, F. Myosin light chain phosphatase: subunit composition, interactions and regulation. *J Muscle Res Cell Motil* **19**, 325-341 (1998).

36 Fukata, Y., Amano, M. & Kaibuchi, K. Rho-Rho-kinase pathway in smooth muscle contraction and cytoskeletal reorganization of non-muscle cells. *Trends Pharmacol Sci* **22**, 32-39, (2001).

37 Wooldridge, A. A. *et al.* Smooth muscle phosphatase is regulated in vivo by exclusion of phosphorylation of threonine 696 of MYPT1 by phosphorylation of Serine 695 in response to cyclic nucleotides. *J Biol Chem* **279**, 34496-34504, (2004).

38 Murthy, K. S., Grider, J. R., Kuemmerle, J. F. & Makhlouf, G. M. Sustained muscle contraction induced by agonists, growth factors, and Ca(2+) mediated by distinct PKC isozymes. *Am J Physiol Gastrointest Liver Physiol* **279**, G201-210 (2000).

39 Hersch, E., Huang, J., Grider, J. R. & Murthy, K. S. Gq/G13 signaling by ET-1 in smooth muscle: MYPT1 phosphorylation via ETA and CPI-17 dephosphorylation via ETB. *Am J Physiol Cell Physiol* **287**, C1209-1218, (2004).

40 Zhou H, H. J., Murthy KS. Lysophosphatidic acid (LPA) interacts with LPA3 receptors to activate selectivelyGαq and induce initial and sustained MLC20 phosphorylation and contraction. *Gastroenterology 126:A278* (2004).

41 Shani, G. *et al.* Death-associated protein kinase phosphorylates ZIP kinase, forming a unique kinase hierarchy to activate its cell death functions. *Mol Cell Biol* **24**, 8611-8626, (2004).

42 MacDonald, J. A. *et al.* Identification of the endogenous smooth muscle myosin phosphatase-associated kinase. *Proc Natl Acad Sci U S A* **98**, 2419-2424, (2001).

43 Borman, M. A., MacDonald, J. A., Muranyi, A., Hartshorne, D. J. & Haystead, T. A. Smooth muscle myosin phosphatase-associated kinase induces Ca2+ sensitization via myosin phosphatase inhibition. *J Biol Chem* **277**, 23441-23446, (2002).

44 Niiro, N. & Ikebe, M. Zipper-interacting protein kinase induces Ca(2+)-free smooth muscle contraction via myosin light chain phosphorylation. *J Biol Chem* **276**, 29567-29574, (2001).

45 Murthy KS, H. J., Zhou H, Kuemmerle JF, Makhlouf GM. Receptors coupled to inhibitory G proteins induce MLC20 phosphorylation and muscle contraction via PI3-kinase-dependent activation of integrin-linked kinase (ILK). *Gastroenterology 126:A413* (2004).

46 Somlyo, A. Ultrastructure of vascular smooth muscle. *In: Handbook of Physiology. The Cardiovascular System. Vascular Smooth Muscle. Bethesda, MD: Am. Physiol. Soc,* **sect. 2, vol. II, chapt. 2**, p. 33-67 (1980).

47 Hitchcock-DeGregori, S. E. & Varnell, T. A. Tropomyosin has discrete actin-binding sites with sevenfold and fourteenfold periodicities. *J Mol Biol* **214**, 885-896, (1990).

48 Vibert, P. J., Haselgrove, J. C., Lowy, J. & Poulsen, F. R. Structural changes in actin-containing filaments of muscle. *J Mol Biol* **71**, 757-767 (1972).

49 Graceffa, P. Movement of smooth muscle tropomyosin by myosin heads. *Biochemistry* **38**, 11984-11992, (1999).

50 Smith, C. W., Pritchard, K. & Marston, S. B. The mechanism of Ca2+ regulation of vascular smooth muscle thin filaments by caldesmon and calmodulin. *J Biol Chem* **262**, 116-122 (1987).

51 Somara, S., Pang, H. & Bitar, K. N. Agonist-induced association of tropomyosin with protein kinase Calpha in colonic smooth muscle. *Am J Physiol Gastrointest Liver Physiol* **288**, G268-276, (2005).

52 Takahashi, K., Hiwada, K. & Kokubu, T. Vascular smooth muscle calponin. A novel troponin T-like protein. *Hypertension* **11**, 620-626 (1988).

53 Jin, J. P., Zhang, Z. & Bautista, J. A. Isoform diversity, regulation, and functional adaptation of troponin and calponin. *Crit Rev Eukaryot Gene Expr* **18**, 93-124, (2008).

54 Hossain, M. M., Hwang, D. Y., Huang, Q. Q., Sasaki, Y. & Jin, J. P. Developmentally regulated expression of calponin isoforms and the effect of h2-calponin on cell proliferation. *Am J Physiol Cell Physiol* **284**, C156-167, (2003).

55 Gerthoffer, W. T. & Pohl, J. Caldesmon and calponin phosphorylation in regulation of smooth muscle contraction. *Can J Physiol Pharmacol* **72**, 1410-1414 (1994).

56 Winder, S. J. & Walsh, M. P. Smooth muscle calponin. Inhibition of actomyosin MgATPase and regulation by phosphorylation. *J Biol Chem* **265**, 10148-10155 (1990).

57 Obara, K., Szymanski, P. T., Tao, T. & Paul, R. J. Effects of calponin on isometric force and shortening velocity in permeabilized taenia coli smooth muscle. *Am J Physiol* **270**, C481-487 (1996).

58 Sobue, K., Hayashi, K. & Nishida, W. Expressional regulation of smooth muscle cell-specific genes in association with phenotypic modulation. *Mol Cell Biochem* **190**, 105-118 (1999).

59 Sen, A., Chen, Y. D., Yan, B. & Chalovich, J. M. Caldesmon reduces the apparent rate of binding of myosin S1 to actin-tropomyosin. *Biochemistry* **40**, 5757-5764, (2001).

60 Marston, S. *et al.* Structural interactions between actin, tropomyosin, caldesmon and calcium binding protein and the regulation of smooth muscle thin filaments. *Acta Physiol Scand* **164**, 401-414 (1998).

61 Szpacenko, A., Wagner, J., Dabrowska, R. & Ruegg, J. C. Caldesmon-induced inhibition of ATPase activity of actomyosin and contraction of skinned fibres of chicken gizzard smooth muscle. *FEBS Lett* **192**, 9-12 (1985).

62 Foster, D. B. *et al.* Modes of caldesmon binding to actin: sites of caldesmon contact and modulation of interactions by phosphorylation. *J Biol Chem* **279**, 53387-53394, (2004).

63 North, A. J., Gimona, M., Lando, Z. & Small, J. V. Actin isoform compartments in chicken gizzard smooth muscle cells. *J Cell Sci* **107 (Pt 3)**, 445-455 (1994).

64 van der Loop, F. T., Gabbiani, G., Kohnen, G., Ramaekers, F. C. & van Eys, G. J. Differentiation of smooth muscle cells in human blood vessels as defined by smoothelin, a novel marker for the contractile phenotype. *Arterioscler Thromb Vasc Biol* **17**, 665-671 (1997).

65 Quensel, C., Kramer, J., Cardoso, M. C. & Leonhardt, H. Smoothelin contains a novel actin cytoskeleton localization sequence with similarity to troponin T. *J Cell Biochem* **85**, 403-409, (2002).

66 Niessen, P. *et al.* Smoothelin-a is essential for functional intestinal smooth muscle contractility in mice. *Gastroenterology* **129**, 1592-1601, (2005).

67 Francis, S. H., Turko, I. V. & Corbin, J. D. Cyclic nucleotide phosphodiesterases: relating structure and function. *Prog Nucleic Acid Res Mol Biol* **65**, 1-52 (2001).

68 Murthy, K. S. Activation of phosphodiesterase 5 and inhibition of guanylate cyclase by cGMP-dependent protein kinase in smooth muscle. *Biochem J* **360**, 199-208 (2001).

69 Murthy, K. S., Zhou, H. & Makhlouf, G. M. PKA-dependent activation of PDE3A and PDE4 and inhibition of adenylyl cyclase V/VI in smooth muscle. *Am J Physiol Cell Physiol* **282**, C508-517, (2002).

70 Murthy, K. S. & Makhlouf, G. M. Interaction of cA-kinase and cG-kinase in mediating relaxation of dispersed smooth muscle cells. *Am J Physiol* **268**, C171-180 (1995).

71 Murthy, K. S. cAMP inhibits IP(3)-dependent Ca(2+) release by preferential activation of cGMP-primed PKG. *Am J Physiol Gastrointest Liver Physiol* **281**, G1238-1245 (2001).

72 Ritter, C. A. *et al.* Cellular export of drugs and signaling molecules by the ATP-binding cassette transporters MRP4 (ABCC4) and MRP5 (ABCC5). *Drug Metab Rev* **37**, 253-278, (2005).

73 Murthy, K. S., Zhou, H., Grider, J. R. & Makhlouf, G. M. Inhibition of sustained smooth muscle contraction by PKA and PKG preferentially mediated by phosphorylation of RhoA. *Am J Physiol Gastrointest Liver Physiol* **284**, G1006-1016, (2003).

74 MacDonald, J. A. *et al.* Phosphorylation of telokin by cyclic nucleotide kinases and the identification of in vivo phosphorylation sites in smooth muscle. *FEBS Lett* **479**, 83-88, (2000).

75 Eddinger, T. J. & Meer, D. P. Single rabbit stomach smooth muscle cell myosin heavy chain SMB expression and shortening velocity. *Am J Physiol Cell Physiol* **280**, C309-316 (2001).

76 Eddinger, T. J. & Meer, D. P. Myosin II isoforms in smooth muscle: heterogeneity and function. *Am J Physiol Cell Physiol* **293**, C493-508, (2007).

77 Hansen, M. B. Neurohumoral control of gastrointestinal motility. *Physiol Res* **52**, 1-30 (2003).

78 Lacy, B. E. & Weiser, K. Gastric motility, gastroparesis, and gastric stimulation. *Surg Clin North Am* **85**, 967-987, vi-vii, (2005).

79 Hunt, J. N. Mechanisms and disorders of gastric emptying. *Annu Rev Med* **34**, 219-229, (1983).

80 Hashitani, H., Garcia-Londono, A. P., Hirst, G. D. & Edwards, F. R. Atypical slow waves generated in gastric corpus provide dominant pacemaker activity in guinea pig stomach. *J Physiol* **569**, 459-465, (2005).

81 Patrick, A. & Epstein, O. Review article: gastroparesis. *Aliment Pharmacol Ther* **27**, 724-740, (2008).

82 Burns, A. J., Herbert, T. M., Ward, S. M. & Sanders, K. M. Interstitial cells of Cajal in the guinea-pig gastrointestinal tract as revealed by c-Kit immunohistochemistry. *Cell Tissue Res* **290**, 11-20 (1997).

83 Hirst, G. D. & Edwards, F. R. Role of interstitial cells of Cajal in the control of gastric motility. *J Pharmacol Sci* **96**, 1-10, (2004).

84 Tack, J. Gastric motor disorders. *Best Pract Res Clin Gastroenterol* **21**, 633-644, (2007).

85 Bitar, K. N. & Makhlouf, G. M. Relaxation of isolated gastric smooth muscle cells by vasoactive intestinal peptide. *Science* **216**, 531-533 (1982).

86 Bitar, K. N. & Makhlouf, G. M. Specific opiate receptors on isolated mammalian gastric smooth muscle cells. *Nature* **297**, 72-74 (1982).

87 Bitar, K. N. & Makhlouf, G. M. Selective presence of opiate receptors on intestinal circular muscle cells. *Life Sci* **37**, 1545-1550 (1985).

88 Teng, B. *et al.* Expression of endothelial nitric oxide synthase in human and rabbit gastrointestinal smooth muscle cells. *Am J Physiol* **275**, G342-351 (1998).

89 Pfaffl, M., Hageleit, M. Validities of mRNA quantification using recombinant RNA and recombinant DNA external calibration curves in real-time RT-PCR. *Biotechn Lett.*, 23:275-282. (2001).

90 Livak, K., Schmittgen, T. . Analysis of relative gene expression data using real-time quantitative PCR and the 2(-Delta Delta C(T)) Method. *Methods.*, 25:402-408. (2001).

91 Pfaffl, M. Relative quantification. *In T Dorak (Ed.), Real-time PCR, New York, USA:Taylor & Francis.* , (pp 63-82) (2006).

92 Schmittgen, T. D. & Zakrajsek, B. A. Effect of experimental treatment on housekeeping gene expression: validation by real-time, quantitative RT-PCR. *J Biochem Biophys Methods* **46**, 69-81, (2000).

93 Huang, J., Mahavadi, S., Sriwai, W., Grider, J. R. & Murthy, K. S. Cross-regulation of VPAC(2) receptor desensitization by M(3) receptors via PKC-mediated phosphorylation of RKIP and inhibition of GRK2. *Am J Physiol Gastrointest Liver Physiol* **292**, G867-874, (2007).

94 Hu, W., Mahavadi, S., Huang, J., Li, F. & Murthy, K. S. Characterization of S1P1 and S1P2 receptor function in smooth muscle by receptor silencing and receptor protection. *Am J Physiol Gastrointest Liver Physiol* **291**, G605-610, (2006).

95 Kuemmerle, J. F. & Murthy, K. S. Coupling of the insulin-like growth factor-I receptor tyrosine kinase to Gi2 in human intestinal smooth muscle: Gbetagamma -dependent mitogen-activated protein kinase activation and growth. *J Biol Chem* **276**, 7187-7194, (2001).

96 Murthy, K. S. & Makhlouf, G. M. Differential regulation of phospholipase A2 (PLA2)-dependent Ca2+ signaling in smooth muscle by cAMP- and cGMP-dependent protein kinases. Inhibitory phosphorylation of PLA2 by cyclic nucleotide-dependent protein kinases. *J Biol Chem* **273**, 34519-34526 (1998).

97 Jiang, H., Colbran, J. L., Francis, S. H. & Corbin, J. D. Direct evidence for cross-activation of cGMP-dependent protein kinase by cAMP in pig coronary arteries. *J Biol Chem* **267**, 1015-1019 (1992).

98 Wyatt, T. A., Naftilan, A. J., Francis, S. H. & Corbin, J. D. ANF elicits phosphorylation of the cGMP phosphodiesterase in vascular smooth muscle cells. *Am J Physiol* **274**, H448-455 (1998).

99 Szymanski, P. T., Szymanska, G. & Goyal, R. K. Differences in calmodulin and calmodulin-binding proteins in phasic and tonic smooth muscles. *Am J Physiol Cell Physiol* **282**, C94-C104, (2002).

100 Szymanski, P. T., Chacko, T. K., Rovner, A. S. & Goyal, R. K. Differences in contractile protein content and isoforms in phasic and tonic smooth muscles. *Am J Physiol* **275**, C684-692 (1998).

101 Teng, B. Q., Grider, J. R. & Murthy, K. S. Identification of a VIP-specific receptor in guinea pig tenia coli. *Am J Physiol Gastrointest Liver Physiol* **281**, G718-725 (2001).

102 Helfman, D. M., Cheley, S., Kuismanen, E., Finn, L. A. & Yamawaki-Kataoka, Y. Nonmuscle and muscle tropomyosin isoforms are expressed from a single gene by alternative RNA splicing and polyadenylation. *Mol Cell Biol* **6**, 3582-3595 (1986).

103 Rensen, S. S. *et al.* Expression of the smoothelin gene is mediated by alternative promoters. *Cardiovasc Res* **55**, 850-863, (2002).

104 Stahmann, N., Woods, A., Carling, D. & Heller, R. Thrombin activates AMP-activated protein kinase in endothelial cells via a pathway involving Ca2+/calmodulin-dependent protein kinase kinase beta. *Mol Cell Biol* **26**, 5933-5945, (2006).

105 Hutchinson, D. S., Summers, R. J. & Bengtsson, T. Regulation of AMP-activated protein kinase activity by G-protein coupled receptors: potential utility in treatment of diabetes and heart disease. *Pharmacol Ther* **119**, 291-310, (2008).

106 Groneberg, D. *et al.* Smooth muscle-specific deletion of nitric oxide-sensitive guanylyl cyclase is sufficient to induce hypertension in mice. *Circulation* **121**, 401-409, (2010).

107 Friebe, A., Mergia, E., Dangel, O., Lange, A. & Koesling, D. Fatal gastrointestinal obstruction and hypertension in mice lacking nitric oxide-sensitive guanylyl cyclase. *Proc Natl Acad Sci U S A* **104**, 7699-7704, (2007).

108 Friebe, A. & Koesling, D. The function of NO-sensitive guanylyl cyclase: what we can learn from genetic mouse models. *Nitric Oxide* **21**, 149-156, (2009).

109 Lin, C. S., Lau, A., Tu, R. & Lue, T. F. Expression of three isoforms of cGMP-binding cGMP-specific phosphodiesterase (PDE5) in human penile cavernosum. *Biochem Biophys Res Commun* **268**, 628-635, (2000).

110 Fuglsang, A., Khromov, A., Torok, K., Somlyo, A. V. & Somlyo, A. P. Flash photolysis studies of relaxation and cross-bridge detachment: higher sensitivity of tonic than phasic smooth muscle to MgADP. *J Muscle Res Cell Motil* **14**, 666-677 (1993).

111 Leguillette, R., Zitouni, N. B., Govindaraju, K., Fong, L. M. & Lauzon, A. M. Affinity for MgADP and force of unbinding from actin of myosin purified from tonic and phasic smooth muscle. *Am J Physiol Cell Physiol* **295**, C653-660, (2008).

112 Adelstein, R. S., and J. R. Sellers. . Myosin structure and function. *In: Biochemistry of Smooth Muscle Contraction, edited by M. Barany. San Diego, CA: Academic*, p, 3–20 (1996).

113 Hartshorne, D. J. Biochemistry of the contractile process in smooth muscle. *In: Physiology of the Gastrointestinal Tract, edited by L. R. Johnson, New York: Raven*, p. 423–482 (1987).

114 Hamada, Y. *et al.* Distinct vascular and intestinal smooth muscle myosin heavy chain mRNAs are encoded by a single-copy gene in the chicken. *Biochem Biophys Res Commun*

170, 53-58, (1990).

115 Nagai, R., Kuro-o, M., Babij, P. & Periasamy, M. Identification of two types of smooth muscle myosin heavy chain isoforms by cDNA cloning and immunoblot analysis. *J Biol Chem* **264**, 9734-9737 (1989).

116 Hewett, T. E., Martin, A. F. & Paul, R. J. Correlations between myosin heavy chain isoforms and mechanical parameters in rat myometrium. *J Physiol* **460**, 351-364 (1993).

117 Chi, M., Zhou, Y., Vedamoorthyrao, S., Babu, G. J. & Periasamy, M. Ablation of smooth muscle myosin heavy chain SM2 increases smooth muscle contraction and results in postnatal death in mice. *Proc Natl Acad Sci U S A* **105**, 18614-18618, (2008).

118 Kelley, C. A., Takahashi, M., Yu, J. H. & Adelstein, R. S. An insert of seven amino acids confers functional differences between smooth muscle myosins from the intestines and vasculature. *J Biol Chem* **268**, 12848-12854 (1993).

119 DiSanto, M. E., Cox, R. H., Wang, Z. & Chacko, S. NH2-terminal-inserted myosin II heavy chain is expressed in smooth muscle of small muscular arteries. *Am J Physiol* **272**, C1532-1542 (1997).

120 Kovacs, M., Wang, F., Hu, A., Zhang, Y. & Sellers, J. R. Functional divergence of human cytoplasmic myosin II: kinetic characterization of the non-muscle IIA isoform. *J Biol Chem* **278**, 38132-38140, (2003).

121 Kawamoto, S. & Adelstein, R. S. Chicken nonmuscle myosin heavy chains: differential expression of two mRNAs and evidence for two different polypeptides. *J Cell Biol* **112**, 915-924 (1991).

122 Fatigati, V. & Murphy, R. A. Actin and tropomyosin variants in smooth muscles. Dependence on tissue type. *J Biol Chem* **259**, 14383-14388 (1984).

123 Chalovich, J. M. Actin mediated regulation of muscle contraction. *Pharmacol Ther* **55**, 95-148, (1992).

124 Marston, S. B., and P. A. J. Huber. Caldesmon. *In: Biochemistry of Smooth Muscle Contraction, edited by M. Barany. San Diego, CA: Academic*, p. 77–90 (1996).

125 Haeberle, J. R., Hathaway, D. R. & Smith, C. L. Caldesmon content of mammalian smooth muscles. *J Muscle Res Cell Motil* **13**, 81-89 (1992).

126 Matthew, J. D. *et al.* Contractile properties and proteins of smooth muscles of a calponin knockout mouse. *J Physiol* **529 Pt 3**, 811-824, (2000).

127 Wills, F. L., McCubbin, W. D. & Kay, C. M. Characterization of the smooth muscle calponin and calmodulin complex. *Biochemistry* **32**, 2321-2328 (1993).

128 Kramer, J. *et al.* A novel isoform of the smooth muscle cell differentiation marker smoothelin. *J Mol Med* **77**, 294-298 (1999).

129 Deruiter, M. C. *et al.* Smoothelin expression during chicken embryogenesis: detection of an embryonic isoform. *Dev Dyn* **221**, 460-463, (2001).

130 Somlyo, A. P. & Somlyo, A. V. Signal transduction by G-proteins, rho-kinase and protein phosphatase to smooth muscle and non-muscle myosin II. *J Physiol* **522 Pt 2**, 177-185, (2000).

131 Stull, J. T., Hsu, L. C., Tansey, M. G. & Kamm, K. E. Myosin light chain kinase phosphorylation in tracheal smooth muscle. *J Biol Chem* **265**, 16683-16690 (1990).

132 Bultot, L. *et al.* Myosin light chains are not a physiological substrate of AMPK in the control of cell structure changes. *FEBS Lett* **583**, 25-28, (2009).

133 Hardie, D. G., Carling, D. & Carlson, M. The AMP-activated/SNF1 protein kinase subfamily: metabolic sensors of the eukaryotic cell? *Annu Rev Biochem* **67**, 821-855, (1998).

134 Kahn, B. B., Alquier, T., Carling, D. & Hardie, D. G. AMP-activated protein kinase: ancient energy gauge provides clues to modern understanding of metabolism. *Cell Metab* **1**, 15-25, (2005).

135 Evans, A. M. *et al.* AMP-activated protein kinase couples mitochondrial inhibition by hypoxia to cell-specific Ca2+ signalling mechanisms in oxygen-sensing cells. *Novartis Found Symp* **272**, 234-252; discussion 252-238, 274-239 (2006).

136 Rubin, L. J., Magliola, L., Feng, X., Jones, A. W. & Hale, C. C. Metabolic activation of AMP kinase in vascular smooth muscle. *J Appl Physiol* **98**, 296-306, (2005).

137 Davis, B. J., Xie, Z., Viollet, B. & Zou, M. H. Activation of the AMP-activated kinase by antidiabetes drug metformin stimulates nitric oxide synthesis in vivo by promoting the association of heat shock protein 90 and endothelial nitric oxide synthase. *Diabetes* **55**, 496-505, (2006).

138 Dipp, M. & Evans, A. M. Cyclic ADP-ribose is the primary trigger for hypoxic pulmonary vasoconstriction in the rat lung in situ. *Circ Res* **89**, 77-83 (2001).

139 Dipp, M., Nye, P. C. & Evans, A. M. Hypoxic release of calcium from the sarcoplasmic reticulum of pulmonary artery smooth muscle. *Am J Physiol Lung Cell Mol Physiol* **281**, L318-325 (2001).

140 Wilson, H. L. *et al.* Adp-ribosyl cyclase and cyclic ADP-ribose hydrolase act as a redox sensor. a primary role for cyclic ADP-ribose in hypoxic pulmonary vasoconstriction. *J Biol Chem* **276**, 11180-11188, (2001).

141 Gong, M. C. *et al.* Myosin light chain phosphatase activities and the effects of phosphatase inhibitors in tonic and phasic smooth muscle. *J Biol Chem* **267**, 14662-14668 (1992).

142 Lorenz, J. M., Riddervold, M. H., Beckett, E. A., Baker, S. A. & Perrino, B. A. Differential autophosphorylation of CaM kinase II from phasic and tonic smooth muscle tissues. *Am J Physiol Cell Physiol* **283**, C1399-1413, (2002).

143 Ikebe, M. & Reardon, S. Phosphorylation of smooth myosin light chain kinase by smooth muscle Ca2+/calmodulin-dependent multifunctional protein kinase. *J Biol Chem* **265**, 8975-8978 (1990).

144 Chen, W., Lah, M., Robinson, P. J. & Kemp, B. E. Phosphorylation of phospholamban in aortic smooth muscle cells and heart by calcium/calmodulin-dependent protein kinase II. *Cell Signal* **6**, 617-630 (1994).

145 Horiuti, K., Somlyo, A. V., Goldman, Y. E. & Somlyo, A. P. Kinetics of contraction initiated by flash photolysis of caged adenosine triphosphate in tonic and phasic smooth muscles. *J Gen Physiol* **94**, 769-781 (1989).

146 Guerriero, V., Jr., Rowley, D. R. & Means, A. R. Production and characterization of an antibody to myosin light chain kinase and intracellular localization of the enzyme. *Cell* **27**, 449-458, (1981).

147 Patel, C. A. & Rattan, S. Spontaneously tonic smooth muscle has characteristically higher levels of RhoA/ROK compared with the phasic smooth muscle. *Am J Physiol Gastrointest Liver Physiol* **291**, G830-837, (2006).

148 Kitazawa, T., Takizawa, N., Ikebe, M. & Eto, M. Reconstitution of protein kinase C-induced contractile Ca2+ sensitization in triton X-100-demembranated rabbit arterial smooth muscle. *J Physiol* **520 Pt 1**, 139-152, (1999).

149 Shirao, S. *et al.* Sphingosylphosphorylcholine is a novel messenger for Rho-kinase-mediated Ca2+ sensitization in the bovine cerebral artery: unimportant role for protein kinase C. *Circ Res* **91**, 112-119 (2002).

150 Feng, J. *et al.* Rho-associated kinase of chicken gizzard smooth muscle. *J Biol Chem* **274**, 3744-3752 (1999).

151 Woodsome, T. P., Eto, M., Everett, A., Brautigan, D. L. & Kitazawa, T. Expression of CPI-17 and myosin phosphatase correlates with Ca(2+) sensitivity of protein kinase C-induced contraction in rabbit smooth muscle. *J Physiol* **535**, 553-564, (2001).

152 Dhaliwal, J. S. *et al.* Rho kinase and Ca2+ entry mediate increased pulmonary and systemic vascular resistance in L-NAME-treated rats. *Am J Physiol Lung Cell Mol Physiol* **293**, L1306-1313, (2007).

153 Rattan, S. The internal anal sphincter: regulation of smooth muscle tone and relaxation. *Neurogastroenterol Motil* **17 Suppl 1**, 50-59, (2005).

154 Rattan, S. & Singh, J. Basal internal anal sphincter tone, inhibitory neurotransmission, and other factors contributing to the maintenance of high pressures in the anal canal. *Neurogastroenterol Motil* **23**, 3-7 (2011).

155 De Godoy, M. A. & Rattan, S. Autocrine regulation of internal anal sphincter tone by renin-angiotensin system: comparison with phasic smooth muscle. *Am J Physiol Gastrointest Liver Physiol* **289**, G1164-1175, (2005).

156 Hagerty, L. *et al.* ROCK1 phosphorylates and activates zipper-interacting protein kinase. *J Biol Chem* **282**, 4884-4893, (2007).

157 Endo, A., Surks, H. K., Mochizuki, S., Mochizuki, N. & Mendelsohn, M. E. Identification and characterization of zipper-interacting protein kinase as the unique vascular smooth muscle myosin phosphatase-associated kinase. *J Biol Chem* **279**, 42055-42061, (2004).

158 Miyazaki, K. *et al.* Rho-dependent agonist-induced spatio-temporal change in myosin phosphorylation in smooth muscle cells. *J Biol Chem* **277**, 725-734, (2002).

159 Gong, M. C., Fujihara, H., Somlyo, A. V. & Somlyo, A. P. Translocation of rhoA associated with Ca2+ sensitization of smooth muscle. *J Biol Chem* **272**, 10704-10709 (1997).

160 Shin, H. M. *et al.* Differential association and localization of myosin phosphatase subunits during agonist-induced signal transduction in smooth muscle. *Circ Res* **90**, 546-553 (2002).

161 Khromov, A. S. *et al.* Smooth muscle of telokin-deficient mice exhibits increased sensitivity to Ca2+ and decreased cGMP-induced relaxation. *Proc Natl Acad Sci U S A* **103**, 2440-2445, (2006).

162 Choudhury, N., Khromov, A. S., Somlyo, A. P. & Somlyo, A. V. Telokin mediates Ca2+-desensitization through activation of myosin phosphatase in phasic and tonic smooth muscle. *J Muscle Res Cell Motil* **25**, 657-665, (2004).

163 Herring, B. P., Lyons, G. E., Hoggatt, A. M. & Gallagher, P. J. Telokin expression is restricted to smooth muscle tissues during mouse development. *Am J Physiol Cell Physiol* **280**, C12-21 (2001).

164 Nakane, M. & Murad, F. Cloning of guanylyl cyclase isoforms. *Adv Pharmacol* **26**, 7-18 (1994).

165 Bellamy, T. C., Wood, J., Goodwin, D. A. & Garthwaite, J. Rapid desensitization of the nitric oxide receptor, soluble guanylyl cyclase, underlies diversity of cellular cGMP responses. *Proc Natl Acad Sci U S A* **97**, 2928-2933, (2000).

166 Nies, A. T., Spring, H., Thon, W. F., Keppler, D. & Jedlitschky, G. Immunolocalization of multidrug resistance protein 5 in the human genitourinary system. *J Urol* **167**, 2271-2275, (2002).

167 Peng, X., Feng, J. B., Yan, H., Zhao, Y. & Wang, S. L. Distribution of nitric oxide synthase in stomach myenteric plexus of rats. *World J Gastroenterol* **7**, 852-854 (2001).

VITA

CONTACT INFORMATION:

Othman A Al-Shboul

Jordan University of Science and Technology
B.O Box: 3030
Irbid 22110
Jordan
Tel: 00962-2-7201000 Ext. 23676
Othman_shboul@yahoo.com

EDUCATION:

B.S. in Dentistry, Jordan University of Science and Technology (2004)

HONORS AND AWARDS:

- **Ramsey Award (2008)**, first year student in the PhD program with highest academic standing, department of physiology and biophysics-VCU.
- **Charles C. Clayton Award (2009)**, outstanding rising second year graduate student in the biomedical sciences, school of medicine-VCU.
- **Member of the Honor Society of Phi Kappa Phi**.
- **Member of Golden Key International Honor Society**.
- **Member of American Physiology Society (APS).**

TEACHING EXPERIENCE:

- Anatomy Lab Teaching Assistant, Jordan University of Science and Technology (2005-2007)
- PHIS501 Teaching Assistant, Virginia Commonwealth University (2008)
- M1 Lab Teaching Assistant, Virginia Commonwealth University (2008)

POSTERS AND PRESENTATIONS FROM THIS WORK

1. Expression of AMP-Activated Kinase (AMP Kinase) and Inactivation of Myosin Light Chain (MLC) Kinase By AMP Kinase Determines the Magnitude of Smooth Muscle Contraction in Different Regions of the Stomach. **(DDW 2009, Oral Presentation)**

2. Expression of PDE5 and its stimulation by cGMP-dependent protein kinase (PKG) determine the magnitude of smooth muscle relaxation in different regions of the stomach. **(EB 2010, Poster)**

3. Agonist-induced Rho kinase and zip kinase activity levels in different regions of the stomach. **(EB 2011, Poster)**

4. Differences in the expression of multi-drug resistant protein 5 and regulation of cGMP levels in phasic and tonic smooth muscles. **(EB 2011, Poster)**

5. Differences in the expression of VPAC2 receptors and adenylyl cyclase V/VI and VIP-induced cAMP generation in phasic and tonic smooth muscles. **(EB 2011, Poster)**